New Biocatalytic Approaches for Lactonization and Lactamization

Vom Promotionsausschuss der
Technischen Universität Hamburg
zur Erlangung des akademischen Grades

Doktor der Naturwissenschaften (Dr. rer. nat.)

genehmigte Dissertation

von

Lei Huang

aus
Jiangxi (China)

2018

i

"Enzymes are proteins, things of beauty and a joy forever."

Richard Nelson Perham (1937–2015)

LIST OF PUBLICATIONS

Part of this work has already been published or submitted for publication in the form of scientific papers (I – II):

I.   **Lei Huang**, Giovanni Vallian Sayoga, Frank Hollmann, Selin Kara. Horse liver alcohol dehydrogenase-catalyzed oxidative lactamization of amino alcohols. *ACS Catalysis,* **2018**, 8, 8680−8684. (ACS Editors' Choice Article)

II.   **Lei Huang**, Elvira Romero, Anna K. Ressmann, Florian Rudroff, Frank Hollmann, Marco W. Fraaije, Selin Kara. Nicotinamide adenine dinucleotide-dependent redox-neutral convergent cascade for lactonizations with new type II Flavin-containing monooxygenase. *Advanced Synthesis & Catalysis*, **2017**, 359, 2142-2148.

Related papers by the author, but not included in this work (III – IV):

III. **Lei Huang**, Pablo Domínguez de María, Selin Kara. The 'water challenge': Opportunities and challenges of using oxidoreductases in non-conventional media. *Chimica Oggi-Chemistry Today*, **2018**, 36, 48-56.

IV.   **Lei Huang**, Friso S. Aalbers, Wei Tang, Robert Röllig, Marco W. Fraaije, Selin Kara. Fusion enzyme of type II Flavin-containing monooxygenase and alcohol dehydrogenase for convergent cascade in non-conventional media. In preparation, **2018**

LIST OF ORAL PRESENTATION

08.06.2017   Workshop des FSP "Integrated Biotechnology and Process Engineering" (2017), Hamburg, Germany
Lei Huang, Elvira Romero, Anna K. Ressmann, Florian Rudroff, Frank Hollmann, Marco W. Fraaije, Selin Kara
NADH-dependent redox-neutral convergent cascade for lactonizations

LIST OF POSTER PRESENTATIONS

26.08.2018-   9th International Congress on Biocatalysis (Biocat2018), Hamburg, Germany
30.08.2018   **Lei Huang**, Friso S. Aalbers, Wei Tang, Robert Röllig, Marco W. Fraaije, Selin Kara
Fusion enzyme of FMO-E and HLADH for a convergent cascade reaction in

non-conventional media

02.07.2017- 06.07.2017	The 19th International Symposium on Flavins and Flavoproteins, Groningen, The Netherlands **Lei Huang**, Elvira Romero, Anna K. Ressmann, Florian Rudroff, Frank Hollmann, Marco W. Fraaije, Selin Kara Nicotinamide adenine dinucleotide (NADH)-dependent convergent cascade for lactonizations
28.08.2016- 01.09.2016	8th International Congress on Biocatalysis (Biocat2016), Hamburg, Germany **Lei Huang**, Elvira Romero Guzman, Frank Hollmann, Marco W. Fraaije, Selin Kara NADH-dependent redox-neutral convergent cascades for lactonizations
17.02.2016	Workshop des FSP "Integrated Biotechnology and Process Engineering" (2016), Hamburg, Germany **Lei Huang**, Marco W. Fraaije, Selin Kara Expanding the substrate scope of the multi-enzymatic convergent cascade for lactonizations
21.09.2015- 22.09.2015	Workshop-New Reactions with Enzymes and Microorganisms, Stuttgart, Germany **Lei Huang**, Till Augustin, Bodo Fiedler, Andreas Liese Design immobilized enzymes on carbon nanostructures for applications in biocatalysis
15.12.2014	Workshop des FSP "Integrated Biotechnology and Process Engineering" (2014), Hamburg, Germany **Lei Huang**, Lorenzo Pesci, Jian-He Xu, Andreas Liese Investigations on enzyme immobilization on carbon nanostructures and their applications

Acknowledgement

I would like to express my sincerest gratitude and thanks to my supervisor Prof. Andreas Liese for giving me the chance to pursue my PhD in the Institute of Technical Biocatalysis. Thank you for your support, inspiration, encouragement and giving me a great degree of freedom with my research. Your positive attitude towards life, profound professional knowledge, care of institute members, managerial skills, excellent teaching level have inspired me a lot. You are a great, friendly, easy going and young-minder supervisor.

A special acknowledgement goes to Assoc. Prof. Selin Kara. You are a charming and open-minder supervisor. Without your daily guidance, faith, advice and gentle prodding, I cannot image I could finish my PhD in time with both fruitful scientific achievements and a lot of good memory. I am especially honored and lucky to meet you in Hamburg. I appreciate the easiness of approaching you and the efficient way that you would address any problems. Your enthusiasm, professional knowledge and skills, as well as your open mind, experiences of life have inspired me a lot and will stay with me in the future. You motivated me in a natural way and I could constantly keep passion in my work. I had a wonderful period of time working with you and also have big confidence on our future cooperation.

I would like to thank my second examiner, Prof. Dr.-Ing. Ralf Pörtner from the Institute of Bioprocess and Biosystems Engineering at Hamburg University of Technology for reviewing my thesis. I also want to thank Prof. Dr. Dr. h.c. Garo Antranikian from the Institute of Technical Microbiology at Hamburg University of Technology for being the chairman of my PhD defense committee.

I owe my deepest gratitude to Prof. Marco W. Fraaije, Dr. Elvira Romero from University of Groningen for the enzyme plasmid and great contribution to our publication. Thanks to Dr. Florian Rudroff and Dr. Anna K. Ressmann from TU Wien for the synthesis of some important compounds in my topics. Thanks to Assoc. Prof. Dirk J. Opperman from University of the Free State in South Africa and Prof. Wolfgang Kroutil from University of Graz in Austria for their enzyme plasmids. Very special thanks to our "idea machine" Assoc. Prof. Frank Hollmann from Delft University of Technology for his ideas, comments, suggestions and improvement regarding our topics and publications.

This thesis could not be finished without the members of the reading committee: Jennifer Engel, Miriam Aßmann, Dr. Christian Scherkus. Thanks for going through part of this thesis and helpful suggestions.

My sincere thanks to Dr. Alexander Himmelspach, Steffen Kühn, Lorenzo Pesci, Miriam

Chengwei Ma, Lifu Song, Jin Guo, Lin Chen, Yujun Zhang, Ying Dong, Ying Liu, Kai Lyu, Li Huo, Minliang Chen for the great food and fun we had together. Special thanks to Yunlong Jia for helping me prepare my PhD defense ceremony and being the audience of my trial presentation.

My heartfelt appreciation goes to my family for their support to pursue my PhD in Germany and their endurance during this period. My deepest thanks to my mother, who teacher me how to be a human and kindness, for her endless and unconditional love and faith forever. Special thanks to my parents in law, for their understanding and unconditional support. It is my honour and my lucky to have you in my life.

I owe a very special thanks to Yahui Xing, my beloved wife. Thank you for your unconditional love, company, understanding and support. It is the biggest harvest to have a family with you during my PhD period. Thank you for teaching me a lot of good habits and making me much better than before. Whenever and wherever we are, I know you are an absolutely reliable person in my life.

Hamburg 18.11.2018

Abstract

Lactones and lactams are cyclic esters and amides, respectively. They are the monomers of polyesters and polyamides, such as polycaprolactone and polycaprolactam, which are the commonly used polymer materials in our daily life and in industry. Apart from that, lactones and lactams are also widely used as raw materials in the pharmaceutical industry and as flavors and fragrances or laundry detergents for bleaching. Up to date, the industrial synthesis of most of the lactones and lactams applies chemical synthesis methods established decades ago that need expensive metal catalysts, aggressive chemicals, high temperature, and depend on non-renewable resources. Thus, there is a necessity to develop more sustainable methods for the synthesis of lactones and lactams. In general, enzymatic reactions show high selectivity and can be conducted in mild conditions leading to environmentally benign approaches compared to chemical methods.

In the first part of the PhD study, a nicotinamide adenine dinucleotide (NADH)-dependent redox-neutral convergent cascade for lactonizations was developed. The redox-neutral convergent cascade is composed of a recently discovered type II flavin-containing monooxygenase from *Rhodococcus jostii* RHA1 (FMO-E) and the well-known horse liver alcohol dehydrogenase (HLADH). Two molar equivalents of ketone substrate converted by FMO-E and one molar equivalent of diol substrate converted by HLADH were converted into three molar equivalents of the single lactone product with high atom efficiency and self-sufficient cofactor regeneration. Two model cascade reactions were demonstrated for the synthesis of γ-butyrolactone and chiral bicyclic lactones. Biochemical characterization of FMO-E and HLADH was firstly done using the individual substrates of the enzymes in the evaluated cascades in order to find the optimal reaction conditions. Having identified the optimized conditions for the enzymatic cascade, achiral and chiral lactone products could be synthesized in high analytical yields (87%) and moderate to high enantioselectivities (up to 99%).

In the second part of the PhD study, a direct synthesis of lactams (5-, 6- and 7-membered) starting from amino alcohols in a parallel cascade was developed. HLADH together with the H_2O forming NADH oxidase variant from *Streptococcus mutans* (*Sm*NOX) made up the parallel cascade. First, crucial reaction parameters for the efficiency of this novel cascade reaction were elucidated. pH of the buffer, concentrations of HLADH and NAD^+ were identified as the key parameters for the lactamization reaction. Under the optimized conditions, up to 95% analytical yields could be achieved in this newly developed cascade reaction in the case of γ-butyrolactam, whereby the yield decreased with increasing ring-size, as also known

from the literature for ring-closure reactions.

Overall this PhD study dealt with new biocatalytic approaches for the synthesis of lactones and lactams. For lactone synthesis, NADH-dependent redox-neutral convergent cascade consisting of FMO-E and HLADH was developed for the synthesis of γ-butyrolactone and chiral bicyclic lactones with high atom efficiency in a self-sufficient cofactor regeneration fashion. For lactam synthesis, it was the first report on the direct synthesis of lactams from amino alcohols catalyzed by an alcohol dehydrogenase. The NAD^+ regeneration was also achieved by coupling the SmNOX forming H_2O as the sole by-product.

Zusammenfassung

Lactone und Lactame sind cyclische Ester bzw. Amide. Sie werden als Monomere für die Synthese von Polyestern und Polyamiden wie Polycaprolacton und Polycaprolactam eingesetzt und finden als vielseitig einsetzbare Polymere Anwendungen im täglichen Leben sowie in der Industrie. Weiterhin werden Lactone und Lactame als Rohstoffe in der pharmazeutischen Industrie, als Aromen und Duftstoffe oder zum Bleichen verwendet. Bei der industriellen Synthese der meisten Lactone und Lactame werden seit langem chemische Synthesemethoden angewendet, die vor Jahrzehnten auf teure Metallkatalysatoren, aggressive Chemikalien, hohe Temperaturen und auf nicht erneuerbare Ressourcen angewiesen sind. Daher besteht die Notwendigkeit, nachhaltigere Methoden für die Synthese von Lactonen und Lactamen zu entwickeln. Im Allgemeinen zeigen enzymatische Reaktionen eine hohe Selektivität und können unter milden Bedingungen durchgeführt werden, was im Vergleich zu chemischen Methoden zu umweltfreundlicheren Verfahren führt.

Im ersten Teil der Dissertation wurde eine Nicotinamidadenindinucleotid (NADH)-abhängige redoxneutrale und konvergente Kaskade für Lactonisierungen entwickelt. Die redoxneutrale, konvergente Kaskade besteht aus einer kürzlich entdeckten Flavin-haltigen Typ-II-Monooxygenase aus *Rhodococcus jostii* RHA1 (FMO-E) und der bekannten Pferdeleber-Alkoholdehydrogenase (HLADH). Zwei Moläquivalente Keton-Substrat, umgesetzt durch FMO-E und ein Moläquivalent Diol-Substrat, umgesetzt durch HLADH, reagierten zu drei Moläquivalenten eines einzelnen Lactons als Produkt mit hoher Atomeffizienz und autarker Cofaktorregeneration. Hierzu wurden zwei Modellreaktionskaskaden für die Synthese von γ-Butyrolacton und chiralen, bicyclischen Lactonen gezeigt. Die biochemische Charakterisierung von FMO-E und HLADH wurde zunächst anhand der jeweiligen Substrate der einzelnen Enzyme in den evaluierten Kaskaden durchgeführt, um die optimalen Reaktionsbedingungen zu ermitteln. Nachdem diese für die enzymatische Kaskade festgelegt werden konnten, war es möglich, sowohl achirale als auch chirale Lactonprodukte in hohen analytischen Ausbeuten (87%) und moderaten bis hohen Enantioselektivitäten (bis zu 99%) zu synthetisiert.

Im zweiten Teil wurde eine direkte Synthese von Lactamen (5-, 6- und 7-gliedrig) ausgehend von Aminoalkoholen in einer parallelen Kaskade durchgeführt. Dazu bildete die HLADH zusammen mit der wassererzeugenden NADH-Oxidase-Variante aus *Streptococcus mutans* (*Sm*NOX) die parallele Kaskade. Zunächst wurden die entscheidenden Reaktionsparameter für die Effizienz dieser neuen Kaskadenreaktion untersucht. Der pH-Wert des Puffers, die Konzentrationen von HLADH und NAD$^+$ wurden als die Schlüsselparameter für die Lactambildungsreaktion identifiziert. Unter den optimierten Bedingungen konnte bei dieser

neu entwickelten Kaskadenreaktion, bzgl. der Synthese von γ-Butyrolactam, eine analytische Ausbeute von bis zu 95% erzielt werden, wobei die Ausbeute mit zunehmender Ringgröße abnahm, wie es auch aus der Literatur für Ringschlussreaktionen bekannt ist.

Insgesamt befasste sich diese Arbeit mit neuen biokatalytischen Ansätzen zur Synthese von Lactonen und Lactamen. Für die Lactonsynthese wurde eine NADH-abhängige redoxneutrale, konvergente Kaskade, bestehend aus FMO-E und HLADH, für die Synthese von γ-Butyrolacton und chiralen, bicyclischen Lactonen mit hoher Atomeffizienz in eigenständiger Cofaktorregeneration entwickelt. Über die Lactamsynthese wurde hiermit erstmals von der direkten Synthese von Lactamen aus Aminoalkoholen berichtet, welche durch eine Alkoholdehydrogenase realisiert werden konnte. Die NAD^+-Regeneration wurde hierbei ebenfalls durch die Kupplung von *Sm*NOX erreicht, wobei Wasser das einzige Nebenprodukt darstellte.

Contents

List of Abbreviations

ABN	Abnormal
ADH	Alcohol dehydrogenase
a_w	Water activity
BCA	Bicinchoninic acid assay
BVMO	Baeyer-Villiger monooxygenase
CalB	*Candida antarctica* lipase B
CFE	Cell-free extract
CHES	N-Cyclohexyl-2-aminoethanesulfonic acid (buffer)
CHMO	Cyclohexane monooxygenase
CV	Column volume
DMSO	Dimethyl sulfoxide
DoE	Design of Experiment
DTT	Dithiothreitol
E	Enzyme
EC	Enzyme class
E. coli	*Escherichia coli*
EDTA	Ethylenediaminetetraacetic acid
e.g.	*Exempli gratia*
ee	Enantiomeric excess
et al.	*Et alia*
FAD	Flavin adenine dinucleotide
FID	Flame ionization detector
FMN	Flavin mononucleotide
FMO-E	Flavin-containing monooxygenase E
GC	Gas chromatography
His	Histidine
HLADH	Horse liver alcohol dehydrogenase
HPLC	High pressure liquid chromatography
IPTG	Isopropyl β-D-1-thio-galacto-pyranoside
LB	Lysogeny broth (*medium*)
mM	mmol/L
MTBE	Methyl tert-butyl ether
N	Normal
NAD^+	Oxidized nicotine amide dinucleotide
NADH	Reduced nicotine amide dinucleotide
$NADP^+$	Oxidized nicotinamide adenine dinucleotide phosphate
NADPH	Reduced nicotinamide adenine dinucleotide phosphate
Ni	Nickel
OD	Optical density
pH	Negative logarithm of molar concentration of dissolved hydronium ions
Pefabloc® SC	4-(2-Aminoethyl)-benzene-sulfonyl fluoride
(*R*)-	One of two enantiomers having a chiral center and being mirror images

	of each other and non-superposable, *R* (*rectus*) – IUPAC nomenclature
rac-	Racemic mixture
rpm	Revolutions per minute
(*S*)-	One of two enantiomers having a chiral center and being mirror images of each other and non-superposable, *S* (*sinister*) – IUPAC nomenclature
SDS-PAGE	Sodium dodecyl sulfate polyacrylamide gel electrophoresis
*Sm*NOX	NADH oxidase from *Streptococcus mutans*
SOC	Super optimal broth with catabolite repression (*medium*)
TB	Terrific Broth (*medium*)
TEA	Triethanolamine
TON	Turnover number
U	Unit; unit of enzyme activity [μmol/min]
UF	Ultrafiltration
v/v	volume/volume

List of Symbols

λ	Lambda: Symbol of wavelength [nm]
Δ	Delta: Symbol for difference
C	Concentration [mM]
Da	Dalton: Molecular weight of protein [g/mol]
k	Reaction rate constant [s^{-1}]
k_{cat}	Turnover number [s^{-1}]
k_{cat}/K_M	Catalytic efficiency [mM^{-1}·s^{-1}]
k_d	Deactivation constant
K	Equilibrium constant
K_i	Inhibition constant [mM]
K_M	Michaelis-Menten constant [mM]
$\tau_{1/2}$	Half-life time [h]
U	Unit; enzymatic activity [μmol/min]
U/mg	Mass specific enzyme activity
V	Volume [mL]
v	Reaction rate [U/mg]
v_{max}	Maximum reaction rate [U/mg]

1 INTRODUCTION

1.1 Target products: lactones and lactams

1.1.1 Application

Lactones are cyclic esters of hydroxycarboxylic acids. They are an important class of compounds with versatile application in organic, bioorganic, and natural product chemistry (**Figure 1.1**). Lactones are widely used for the production of polyesters *via* ring-opening polymerization (ROP) reaction. An excellent example is ε-caprolactone (ECL), the important precursor for the production of thermoplastic, biodegradable, and elastomeric polymers: poly-ε-caprolactone (PCL)[1-2]. PCL is an important polymer material owing to its special mechanical, thermal and physical properties. Owing to its biodegradability and biocompatibility, PCL has been used in medical devices, such as scaffolds[3-6] in tissue engineering, long-term drug delivery systems[7-8], packaging[9], and as adhesives[10]. Another important lactone is γ-valerolactone (GVL), which can be produced from lignocellulosic biomass[11]. GVL is renewable, easy and safe to store and transport globally in large quantities. It has low melting point (–31℃), high boiling-(207℃) and open cup flash points (96℃), a definitive but acceptable smell, and is miscible with water and biodegradable. These important characteristics of an ideal sustainable liquid makes GVL to be used for the production of polymers, fuel additives, solvent and jet fuel[12-13]. Lactones contribute significantly to the flavor of fruit, and of unfermented and fermented dairy products, and are therefore used as flavors and fragrances[14]. The γ- and δ-lactones of less than 12 carbons make up a group of compounds of great interest to the flavors and fragrances industry[15]. Some examples are γ-decalactone with a characteristic peach flavor and δ-decalactone with a creamy peach flavor[16].
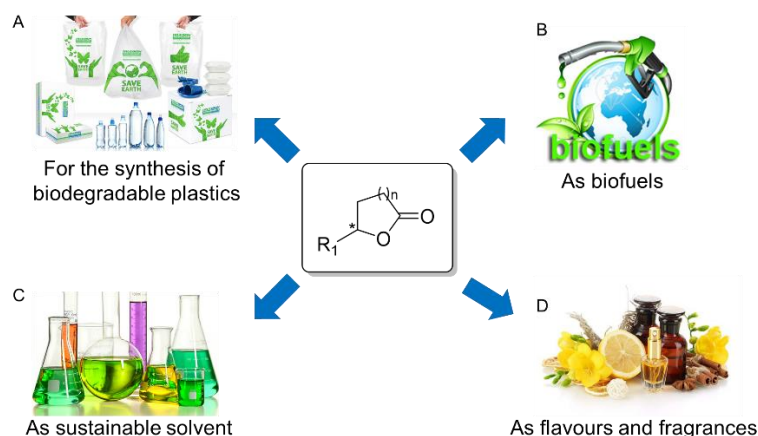
Figure 1.1. Applications of lactones (pictures: A[17], B[18], C[19] and D[20]).

Lactams are cyclic amides whose names are the portmanteau of lactone and amide. Lactams are monomers of polyamides, which are commonly used polymer materials known as Nylons in our daily life and industry[21]. Polyamides are the first engineering plastics and still represent by far the biggest and most important class of these types of material[21]. Polycaprolactam (Nylon 6) is the most popular nylon material and synthesized by ring-opening polymerization of ε-caprolactam (CPL) in industry[22]. Apart from that, lactams are also used as raw materials in the pharmaceutical industry[23] and as laundry detergents for bleaching[24] (**Figure 1.2**). γ-Butyrolactam (2-pyrrolidone) is a valuable bulk chemical which is used as precursor for the production of N-vinylpyrrolidone, a building block for active pharmaceutical ingredients (APIs)[23]. γ-Butyrolactam can also be used as a solvent and the precursor for the production of Nylon 4 (polybutyrolactam). Another important lactam is β-lactam, because it is the core structure of several antibiotic families. These antibiotics containing β-lactam structure, including penicillins, cephalosporins, carbapenems, and monobactams, are called β-lactam antibiotics[25]. More than half of the commercial antibiotics used in the world were β-lactam antibiotics compared by sales until 2012[26].
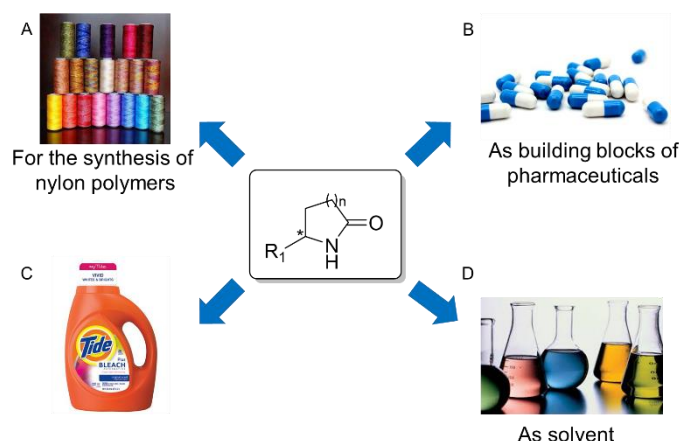
Figure 1.2. Applications of lactams (pictures: A[27], B[28], C[29] and D[30]).

1.1.2 Synthesis routes

1.1.2.1 Chemical methods

Lactones

Since lactones and lactams are cyclic esters and amides, many methods in ester and amide synthesis can also be applied to that of lactones and lactams. Up to date, most of lactones and lactams are manufactured with conventional chemical methods. ε-Caprolactone, the most important lactone, is produced almost through the reaction of cyclohexanone (CHO) with

peracetic acid known as Baeyer-Villiger (BV) oxidation reported more than 100 years ago (**Scheme 1.1**)[31]. However, this method possesses some intrinsic disadvantages: (i) The reagent peracetic acid is considered as a problematic chemical in terms of toxicity, safety, and ecology; (ii) The treatment of the by-product acetic acid is a time-, resource- and energy consuming process, which increases the cost of the production; (iii) The chemical BV oxidation lacks high chemo-, regio-, and enantioselectivity, which is required for some high valued chemicals.
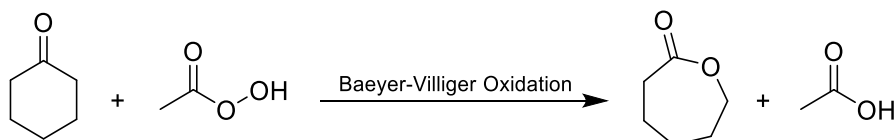
Scheme 1.1. Industrial synthesis of ε-caprolactone (ECL) from cyclohexanone (CHO) by Baeyer-Villiger oxidation.

Other two common methods for the synthesis of lactones include intramolecular esterification of hydroxy acids (**Scheme 1.2**) and intramolecular hydroacyloxylation of olefinic acids[32]. Both γ- and δ-hydroxy acids are easily converted to lactones by treatment with acids, but larger or smaller lactone rings cannot be made in this manner, because polyester formation occurs more readily[33]. Normally these intramolecular esterification takes place in organic solvent since aqueous medium would lead to the product hydrolysis. Common (n = 5–7) and medium (n = 8–11) ring-sized unsaturated lactones can be efficiently synthesized through the ring-closing metathesis (RCM) approach[34].
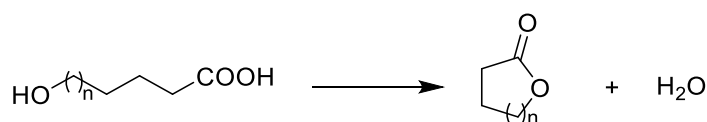
Scheme 1.2. Synthesis of lactones through intramolecular esterification of hydroxy acids.

Direct lactonization of diols is an important approach for the production of lactones (**Scheme 1.3**). A number of oxidative lactonization of diols systems have been reported using environmentally acceptable oxidants, such as oxygen[35-36], acetone[37-39], and hydrogen peroxide[40] (**Scheme 1.3A**). Dehydrogenative lactonization of diols is also developing fast and has attracted much attention[41-43]. It enables the lactonization of diols without any oxidants with H_2 as the by-product, which minimizes the potential waste and maximizes the atom efficiency of these reactions (**Scheme 1.3B**). Most of these diol lactonization reactions were catalyzed by ruthenium catalyst, but there was one case of dehydrogenative lactonization catalyzed by iridium catalyst[44] and one case catalyzed by iron(II) catalyst[45]. Most of these catalytic reactions had to be conducted in toxic organic solvents (e.g. toluene) or at high temperatures (> 200°C).

A. Catalytic oxidative lactonization of diols
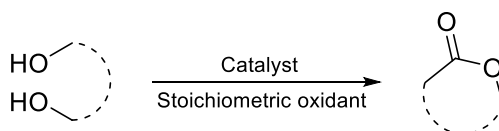
B. Catalytic dehydrogenative lactonization of diols

Scheme 1.3. Two kinds of direct lactonization of diols methods. A) Oxidative lactonization of diols with oxidant, and B) dehydrogenative lactonization of diols.

Lactams

More than 98% of the ε-caprolactam is produced from CHO *via* the intermediate cyclohexanone oxime (**Scheme 1.4**)[46]. CHO is first converted to its oxime, which is then under Beckmann rearrangement induced by fuming sulfuric acid to give ε-caprolactam. However, this method will produce large amount of the by-product ammonium sulfate. The profitability of this process is dependent on the relative prices of sulfuric acid and ammonia *versus* ammonium sulfate. Thus, in the industrial process, much attention is put on minimizing the production of ammonium sulfate. Approximate 2% of ε-caprolactam is produced by photonitrosation of cyclohexane[46]. Photonitrosation converts cyclohexane to cyclohexanone oxime dihydrochloride followed by Beckmann rearrangement. Cyclohexane is converted into cyclohexanone oxime dihydrochloride through photonitrosation followed by Beckmann rearrangement.
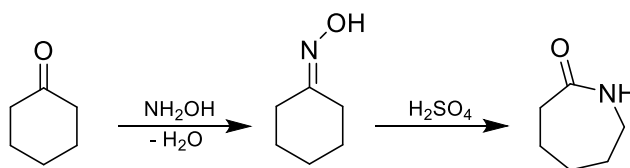
Scheme 1.4. Industrial synthesis of ε-caprolactam (CPL) from cyclohexanone (CHO) *via* cyclohexanone oxime.

Like the synthesis of lactones through intramolecular esterification of hydroxy acids, lactams can also be produced through intramolecular amidation of ω-aminocarboxylic acids (**Scheme 1.5**). However, the synthesis of lactams through intramolecular ring closure reaction of ω-aminocarboxylic acids is entropically unfavored[47]. Laurolactam was synthesized from the ring closure reaction of 12-aminododecanoic acid with higher yield with *N*-hexadecyl-2-chloropyridinium iodide (c16Pycl, I) as an activating agent[47]. The disadvantages of this method

were the utilization of toxic chemicals, stoichiometric amount of c16Pycl, I, and undesired intermolecular dimerization or polymerization reactions. Medium ring lactams (n = 7-12) could be synthesized from their corresponding ω-aminocarboxylic acids using polymer-supported hydroxybenzotriazole (HOBT) as the catalyst[48]. However, the toxic solvents and protection groups required in this process rendered it environmentally unfriendly and laborious.

Scheme 1.5. Synthesis of medium ring lactams from ω-aminocarboxylic acids (n = 3–10).

The oxidative or dehydrogenative direct lactamization of amino alcohols represents an attractive alternative approach to produce lactams (**Scheme 1.6**). Transition metal-catalyzed methods have been reported for decades[49-53]. Iron catalyst was also reported to catalyze the dehydrogenative synthesis of lactams from amino alcohols recently[45, 52]. The transition metal (mainly ruthenium catalyst)-catalyzed oxidative and dehydrogenative lactonization from amino alcohols, despite its conceptual beauty and versatility, is plagued by a poor selectivity.

A. Catalytic oxidative lactamization of amino alcohols
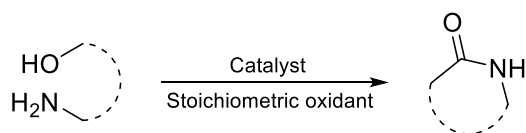
B. Catalytic dehydrogenative lactamization of amino alcohols
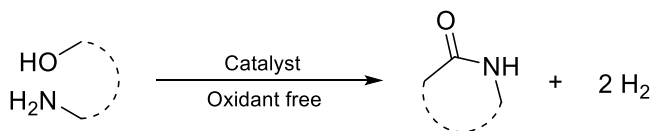
Scheme 1.6. Two kinds of direct lactamization of amino alcohols methods. A) Oxidative lactamization of amino alcohols with oxidant, and B) dehydrogenative lactamization of amino alcohols.

1.1.2.2 Enzymatic methods

Lactones

Baeyer-Villiger monooxygenases (BVMOs, E.C. 1.14.13.xx) are the alternatives to the chemical catalysts of Baeyer-Villiger oxidation. Compared to the chemical catalysts, the main advantages of BVMOs lie on their high chemo-, regio-, and enantioselectivity and broad substrate specificity[54]. BVMOs also have the advantage of using oxygen as the oxidant and

forming water as the by-product. These features can be illustrated by the prototype BVMO, cyclohexanone monooxygenase from *Acinetobacter calcoaceticus* NCIMB 9871 (CHMO[Acineto]; EC 1.14.13.22), which has been shown to convert hundreds of different substrates[55]. Apart from performing Baeyer-Villiger oxidation, BVMOs can also be able to catalyze many other oxidations, such as sulfoxidations, oxidations of selenium and boron-containing compounds, epoxidations, and N-oxidations[56]. Most of BVMOs-catalyzed reactions were performed in whole cell systems due to the issues of enzyme stability and cofactor regeneration. One of the few practical processes is the recombinant whole cell catalyzed oxidation of bicyclo[3.2.0]hept-2-en-6-one (**Scheme 1.7**)[57]. This process employed recombinant *E. coli* TOP10 [pQR239] expressing CHMO[Acineto] to catalyze bicyclo[3.2.0]hept-2-en-6-one to its corresponding regioisomeric lactones in 1.5 L and 55 L fed-batch reactors using a substrate feeding strategy to overcome substrate inhibition. In this way, the final product concentration could reach 3.5 g/L with a yield of 85% on the substrate. Afterwards, this process was successfully scaled up to pilot-plant (200 L) scale with the yield of 495 g final lactone product from 900 g substrate[58]. In that study, issues for fermentation, biotransformation and product recovery were discussed for the scale up of a whole-cell biocatalytic Baeyer-Villiger oxidation process.
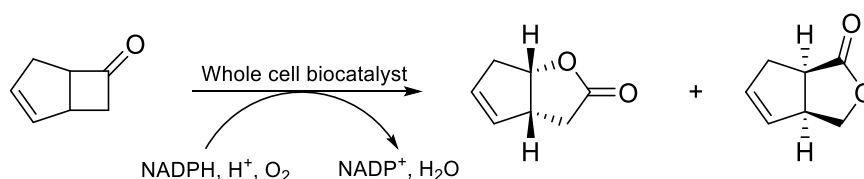
Scheme 1.7. Whole cell Baeyer-Villiger catalyzed regiodivergent oxidation of bicyclo[3.2.0]hept-2-en-6-one yielding (–)-(*1S, 5R*)-2-oxabicyclo[3.3.0]oct-6-en-3-one and (–)-(*1R, 5S*)-3-oxabicyclo[3.3.0]oct-6-en-2-one[57].

Lipase catalyzed intramolecular lactonization of hydroxy acids or esters has been extensively studied[59-62]. Gatfield was the first one to synthesize pentadecanolide through the intramolecular esterification of 15-hydroxypentadecanoic acid catalyzed by the lipase from *Mucor miehei*[63]. Later, the lipase-catalyzed intramolecular lactonization of 16-hydroxyhexadecanoic acids was investigated systemically and many factors, such as substrate concentration, choice of organic solvent and water content in the system were found to be able to affect the final lactone yield[64-65]. (*S*)-γ-valerolactone ((*S*)-GVL) could be obtained with excellent enantiomeric excess from the intramolecular esterification of (*S*)-ethyl-4-hydroxypentanoate (4HPOEt) catalyzed by lipase B from *Candida antarctica* (CalB) in methyl-*tert*-butylether (MtBE) combined in a chemo-enzymatic route starting from levulinic acid[66].
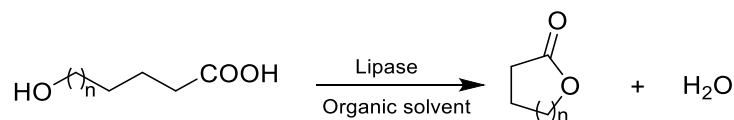
Scheme 1.8. Synthesis of lactones through intramolecular esterification of hydroxy acids catalyzed by lipase in an organic solvent.

Enzymatic oxidative lactonization of diols is an alternative route to synthesize lactones and has been already known for a long time (**Scheme 1.9**). Jones and his co-workers initiated the investigation of synthesis of chiral lactones *via* horse liver alcohol dehydrogenase (HLADH)-catalyzed oxidation of substituted pentane-l,5-diol[67], hydroxycyclopentanes[68], monocyclic meso diols[69], and meso diols[70]. Similarly, a number of other diol substrates had been converted into lactones by HLADH with moderate to excellent enantioselectivity[71-75]. In the HLADH-catalyzed systems, the oxidant, NAD^+, was regenerated *via* flavin mononucleotide (FMN), electrochemical method, photocatalytic method or laccase-mediator system to enable these reactions performed economically. The laccase/2,2,6,6-tetramethylpiperidinoxyl radical (TEMPO) system has been shown to oxidize aliphatic diols quantitatively to their corresponding lactones with complete regio- and/or monoselectivity in aqueous and biphasic media[76-77].
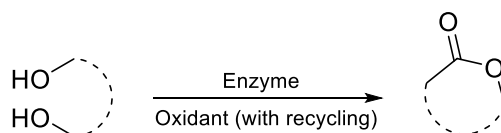
Scheme 1.9 Enzyme catalyzed lactonization of diols with oxidant (NAD^+ or TEMPO) regeneration.

Lactams

Lactams can be synthesized through the intramolecular amide bond formation of ω-aminocarboxylic acids or esters (**Scheme 1.10**). Porcine liver esterase could catalyze the aminolysis of γ-amino esters to give the corresponding γ-lactam in aqueous buffer[78]. However, the lactam formation *via* intramolecular ring closure reaction of ω-aminocarboxylic acids is thermodynamically unfavored in aqueous media. Laurolactam could be synthesized *via* ω-laurolactam hydrolase catalyzed intramolecular amide bond formation of 12-aminododecanoic acid methyl ester, as an activated form of 12-aminododecanoic acid with a maximum yield of 13%[79]. Furthermore, these kinds of reactions were also carried out in organic solvents. Porcine liver esterase could catalyze the formation of small ring lactams by intramolecular aminolysis of aminoesters in tertiary amyl alcohol[80]. Similarly, 4-, 5-, 6- and 8-aminocaproic acids were converted into corresponding lactams by CalB with different conversion in toluene[81]. In these

reactions, the anhydrous reaction conditions played a crucial role for obtaining high yields of lactams.
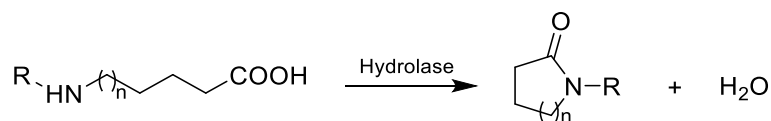
Scheme 1.10. Synthesis of lactams from ω-aminocarboxylic acids (R = H) or ω-aminocarboxylic esters.

Turner and coworkers recently reported biocatalytic lactamization of linear aliphatic amino alcohols[82]. These amino alcohols were first oxidized by a galactose oxidase variant (GOase) to the intermediate amino aldehydes, which were then converted into lactams by a molybdenum-dependent xanthine dehydrogenase (XDH) (**Scheme 1.11**)[82]. The results also showed that pH played an important role in the cyclization of these amino aldehydes intermediates as the lactam yield increased with pH from 7.0 to 8.5. Then whole cell monoamine oxidase (MAO) was utilized to convert cyclic amine to lactam coupled with a Cu-based oxidative system (CuI/H_2O_2) in the same group[83]. Zheng et al. has demonstrated the lactam formation through the biocatalytic α-oxidation of cyclic amines catalyzed by the whole cell of *Pseudomonas plecoglossicida* ZMU-T04 in buffer[84].
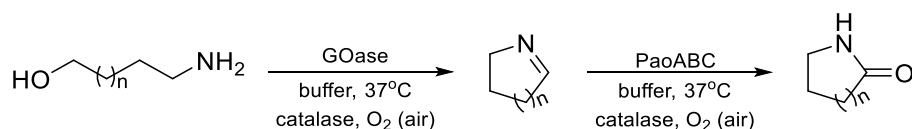
Scheme 1.11. Synthesis of lactams from amino alcohols through one galactose oxidase (GOase) and one aldehyde oxidase (PaoABC).

1.2 Enzymes of interest

Oxidation is a central transformation in modern organic chemistry[85]. Over the decades, enormous development has been achieved in the transition metal-catalyzed oxidation[86]. In general, transition metal-based catalysts are very robust and stable in organic solvents over a board range of temperature and pressure. However, the commonly used toxic organic solvents or additives and the lack of chemo-, regio-, and/or enantioselectivity make them not in line with the principles of "Green Chemistry"[87]. Enzymes are emerging as alternative catalysts for environmentally benign oxidation from simple alcohol oxidation to stereoselective Baeyer-Villiger oxidation as they have been evolved to work under mild conditions (e.g. neutral pH, low temperature and atmospheric pressure). The biggest advantage of enzyme-catalyzed

oxidation over chemocatalysts lies in its good selectivity. Many enzymes have been involved in the bio-oxidation chemistry. Among these enzymes, Baeyer-Villiger monooxygenases (BVMOs) and alcohol dehydrogenases (ADHs) have been extensively studied and widely applied for the enzymatic oxidation.

1.2.1   Baeyer-Villiger monooxygenases (BVMOs)

In 1899 Adolf von Baeyer and his student Victor Villiger published an oxidation reaction in which ketones were converted into corresponding esters or lactones[31]. Hence, this kind of reaction has been named as Baeyer–Villiger (BV) oxidation. Nowadays, BV oxidation has been one of the most frequently used reactions in the synthetic organic chemistry. However, due to the lack of selectivity of chemical catalyst and the harsh conditions (such as intrinsically unstable oxidant peracids) used, the biological BV oxidation has become more and more attractive. In 1948, Turfitt found the first biological BV oxidation reaction in a series of microbiological degradation of steroids[88]. The first potent Baeyer-Villiger monooxygenase (BVMO) is cyclohexanone monooxygenase (CHMO$_{Acineto}$) from *Acinetobacter sp.* strain NCIB 9781 and it is still used nowadays as the prototypical BVMO[89]. CHMO$_{Acineto}$ has been proved to accept hundreds of different carbonylic compounds displaying board substrate scope as well as high regio- and/or enantioselectivity[90]. A large number of studies showed that various oxidation reactions could be catalyzed by CHMO$_{Acineto}$ and other BVMOs[91-92]. These features render BVMOs as attractive oxidative biocatalysts.

BVMOs belong to class B flavoprotein monooxygenases (MOs) which contain four distinct subclasses[93]. The most extensively studied subclass is type I BVMO, which can catalyze the oxidation of carbonyl substrates and heteroatom strictly with NADPH as the cofactor[56]. Three other subclasses of class B flavoprotein MOs are type I flavin-containing monooxygenase (type I FMO), *N*-hydroxylating MOs (NMOs) and type II flavin-containing monooxygenase (type II FMO). Type I FMOs are also strictly NADPH dependent and have been studied for their roles in human metabolism[94]. NMOs are able to hydroxylate primary amines. Type II FMOs can also catalyze Baeyer–Villiger and heteroatom oxidations, but using NADPH and NADH as the cofactors. Jensen reported the first type II FMO from *Stenotrophomonas maltophilia*[95] followed by the identification of seven type II FMOs derived from the genome of *Rhodococcus jostii* RHA1 by Riebel *et al.*[96].

The catalytic circle of flavoprotein monooxygenase could be divided into reductive half reaction and oxidative half reaction[97]. In the reductive half reaction (5 → 1) (**Figure 1.3**), the flavin is reduced by the cofactor NAD(P)H. In the oxidative half reaction, the substrate is

oxidized and the oxidized flavin is generated again for next reductive half reaction. At the beginning, the reduced flavin reacts with oxygen to generate a reactive intermediate by forming a covalent bond between the oxygen and the C4a position of flavin (1 → 2)[98]. Then this intermediate will stay in equilibrium with its protonated style the C4a-hydroperoxyflavin (2 → 3)[99]. Though the two intermediates are stabilized within the enzyme[100], they will decay to oxidized flavin in two possible ways. In the absence of substrate case, the intermediate will directly decay to oxidized flavin yielding hydrogen peroxide (2 → 5, uncoupling). Alternatively, the monooxygenation of substrate leads to the formation of C4a-hydroxyflavin (2/3 → 4), which will decay to the oxidized flavin by the release of water (4 → 5)[101].
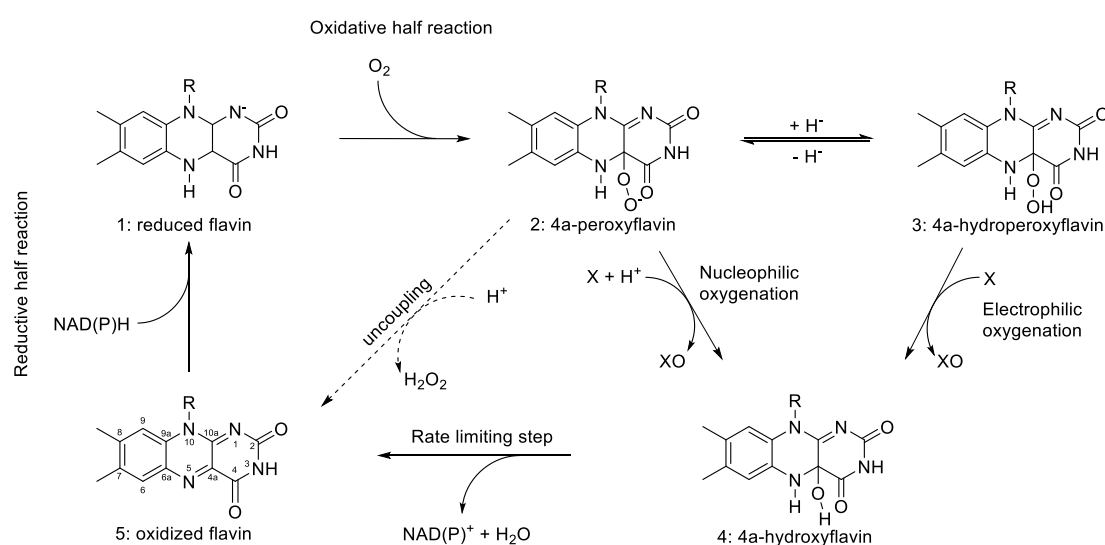
Figure 1.3. General catalytic circle of oxygenation catalyzed by flavoprotein monooxygenases[97].

BVMOs are able to catalyze various oxygenation reactions, such as the BV oxidation of a ketone to an ester, the oxidation of prochiral sulphide to a chiral sulfoxide and the oxidation of an amine to a chiral *N*-oxide[102]. The most interested and studied reaction catalyzed by BVMOs is the BV oxidation of cyclic ketone forming corresponding lactone. The most valuable applications of BVMOs are the desymmetrization of prochiral substrates and the (dynamic) kinetic resolution of chiral ones[85]. Desymmetrizations of various p-substituted cyclobutanones and cyclohexanones had been catalyzed by BVMOs and gave corresponding lactones in excellent yields and optical purities[103]. Especially, many chiral butyrolactones are valuable building blocks of pharmaceuticals. By careful choice of biocatalysts, the stereocomplementary kinetic resolution can be obtained. An interesting case of kinetic resolution is the BV oxidation of fused cyclobutanones (**Scheme 1.12**)[104-105]. This regiodivergent oxidation shows an elegant access to chiral building blocks as exemplified with bicyclo[3.2.0]hept-2-ene-6-one[104].
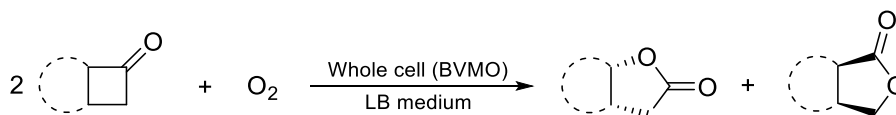
Scheme 1.12. Regiodivergent bio-oxidation of racemic cyclobutanones catalyzed by a BVMO[104].

1.2.2   Alcohol dehydrogenases (ADHs)

ADHs are by far the most popular biocatalyst for the oxidation of alcohols. These enzymes catalyze the reversible conversion of alcohols to aldehydes/ketones using oxidized nicotinamide cofactors $(NAD(P)^+)$ as actual electron acceptors. Compared to many practical applications of ADHs in the reductive direction (forming chiral centres), their oxidative direction applications (destroying chiral centres) have been exploited to a much less extent[106]. Nevertheless, ADHs have been shown a great potential application for oxidation chemistry, such as the kinetic resolution of racemic mixtures to produce enantiopure alcohols[107], synthesis of carboxylic acids[108] and oxidative lactonization of diols (**Figure 1.4**)[67, 75]. Moreover, the number of identified and characterized ADHs has been growing fast over the past decades.
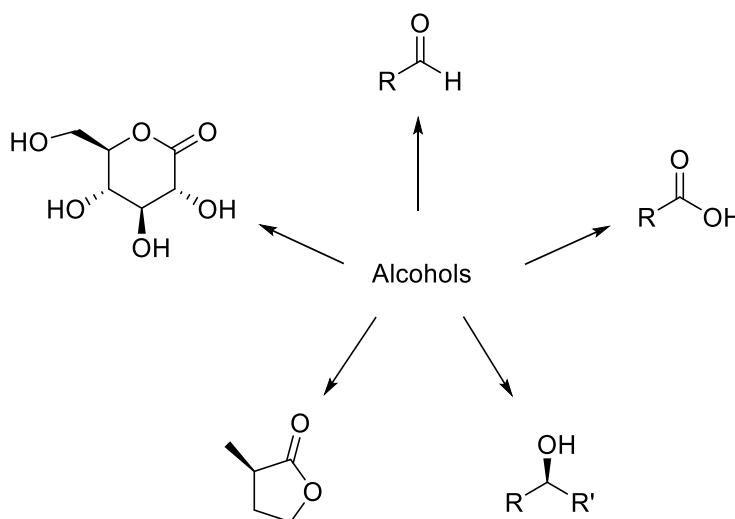
Figure 1.4. ADH-catalyzed oxidation reaction starting from alcohols[109].

One of the earliest and best characterized ADHs is ADH isolated from horse liver (HLADH). HLADH belongs to the medium chain dehydrogenases/reductases (MDR-ADHs) and is a zinc-dependent enzyme. HLADH shows a broad substrate scope towards primary and secondary alcohols with (*S*)-stereoselectivity in most cases, which makes it a highly predictable and very useful tool in the stereoselective oxidation. HLADH has also been widely studied for its application in non-conventional media[110].

For decades, the high cost of the nicotinamide cofactors has been seen as the major hinder to the economical application of many oxidoreductases including ADHs. As a consequence, a

large number of *in situ* regeneration approaches have been developed for the use of NAD(P)$^+$ in catalytic amounts[111]. In general, the turnover number (TON) of NAD(P)$^+$ should exceed 1000[85]. The two kinds of oxidized nicotinamide cofactors, phosphorylated (NADP$^+$) and non-phosphorylated (NAD$^+$) differ with respect to a phosphate group linked to the 2' position of the adenosine ribose[112]. From the point of view of biocatalytic application, NAD$^+$-dependent ADH is definitely prior to the NADP$^+$-dependent ADHs due to their big difference on the cost (**Table 1.1**).

Table 1.1 General cost of nicotinamide cofactors (data from Sigma Aldrich, 2018).

Nicotinamide cofactors	Price (Euro/per gram)
NAD$^+$	58 (Sigma N7004)
NADH	189 (Sigma N8129)
NADP$^+$	766 (Sigma N5755)
NADPH	3280 (Sigma N5130)

1.3 Redox-neutral cascade reactions

Nature uses synthetic strategy to build complex molecules from simple starting materials with astonishing efficiency mainly by the combination of several enzymatic reactions in cascading sequences [113]. This synthetic strategy has inspired chemists for centuries. In recent years, there is more and more attention putting on the use of multi-enzyme cascades in organic synthesis. Multi-enzymatic cascade reactions running in one-pot without isolation of intermediates offer considerable advantages: time and cost needed for the recovery of product is reduced, reversible reactions can be driven to completion and the harmful or unstable compounds can be kept at the minimum level[114-115].

Especially, in redox biocatalysis, multi-enzymatic cascade reactions are attractive since with the so-called redox-neutral cascades (also referred as "self-sufficient" or "closed loop") expensive cofactors, i.e. nicotinamide cofactors most cases, can be recycled *in situ* without an external cofactor regeneration system[111, 116]. The challenge is how to design the reactions in one-pot, either performing these reactions simultaneously, or in a stepwise fashion[117].

Up to date, redox-neutral cascade reactions can be classified into three categories (**Figure 1.5**)[111, 117]. A) Linear cascade: Reactions in this cascade share one common intermediate, which is formed in the first reaction and consumed in the second reaction, giving only one final product. B) Parallel cascade: The two reactions are connected *via* the cofactor recycling and the cascade produces two (or more) different products from two substrates. C) Convergent cascade: two reactions are combined by the cofactor recycling and a single product is produced from the two reactions without intermediate formation[118-119].
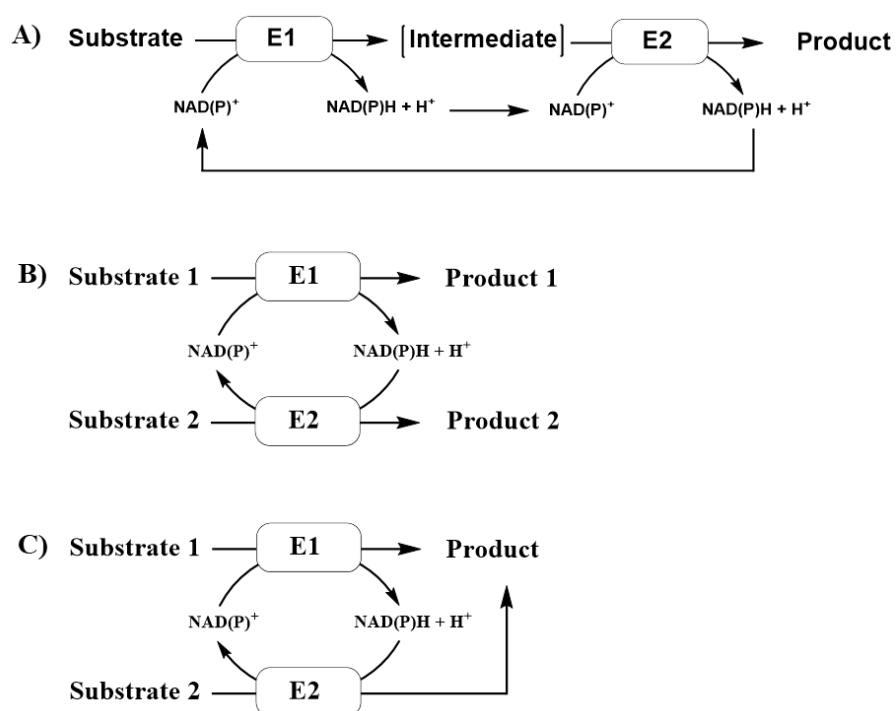
Figure 1.5. Redox-neutral cascade reactions: A. Linear cascade, B. Parallel cascade, C. Convergent cascade

The most straightforward design is a linear cascade, which converts one substrate into one product *via* one or more intermediates. More than 30 years ago, an early example of a redox-neutral linear cascade was reported[120]. Racemic lactate was converted into L-alanine catalyzed by D-, L-lactate dehydrogenase (LDHs) and L-alanine dehydrogenase (AlaDH) in a linear sequence via the intermediate pyruvate. Recently, Francesco G. Mutti, Nicholas J. Turner and their collaborators developed a new linear cascade system to synthesize α-chiral amines from racemic or enantiomerically pure alcohols[121]. This linear cascade system was composed of one ADH and one appropriate amine dehydrogenase (AmDH). In the first step, the ADH catalyzed the oxidation of alcohols to ketones, which were then under reductive amination by AmDH forming α-chiral amines (**Scheme 1.13**).
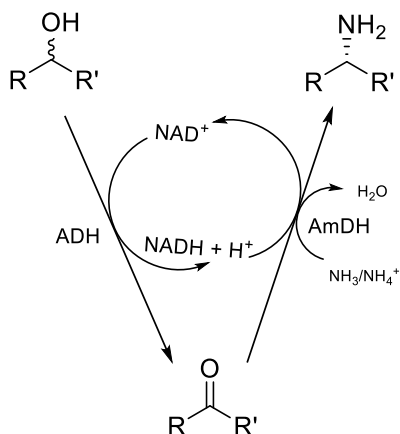
Scheme 1.13. Amination of racemic alcohols for α-chiral amines *via* an ADH-AmDH cascade as an example of linear redox-neutral cascade reaction[121].

Many examples of redox-neutral parallel cascades have been reported[117, 122]. Applying a second enzyme and a second substrate for the regeneration of nicotinamide cofactors in redox biocatalytic reactions can be considered as the traditional redox-neutral parallel cascade reactions. This cascade is of particularly advantage if the second combined reaction is (nearly) irreversible. One well known example is the formate dehydrogenase (FDH)-promoted NADH regeneration for the industrial production of *tert*-leucine (2-amino-3,3-dimethylbutanoic acid) by reductive amination of trimethylpyruvic acid catalyzed by leucine dehydrogenase (LeuDH) with high yield and excellent optical purity (**Scheme 1.14**)[123]. In this case, the only by-product CO_2 avoids the tedious product isolation process.
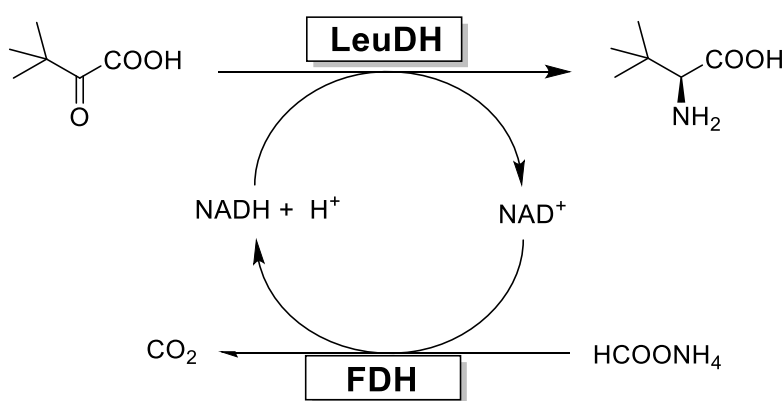
Scheme 1.14. LeuDH-catalyzed synthesis of L-tert-Leucine as an example of parallel redox-neutral cascade reaction.

Recently, Kara and workers reported a new enzymatic cascade system for the synthesis of ECL running in a convergent fashion (**Scheme 1.15**)[118]. This convergent system could convert two equivalents of CHO and one equivalent of 1,6-hexanediol (1,6-HD) to, in theory, three equivalents of ECL. This convergent cascade consisted of a CHMO for the oxidation of CHO and an ADH for the oxidation of 1,6-HD and simultaneous NADPH regeneration. In a following

study, this CHMO-ADH cascade reaction was optimized through Design of Experiment (DoE) and a biphasic system[124]. Under the optimized conditions, the TON values of NADPH and ADH could reach 980 and 392000, respectively.
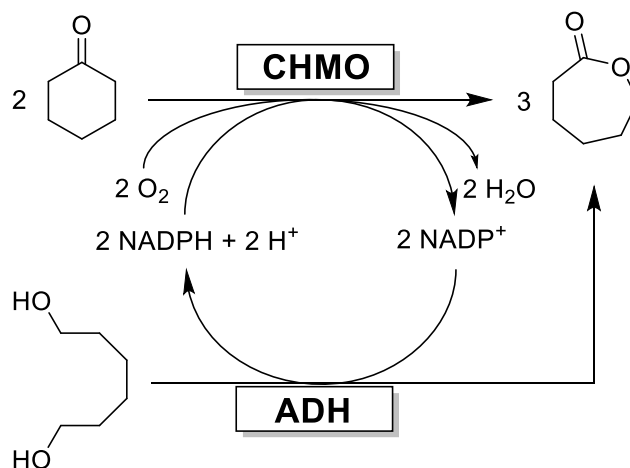
Scheme 1.15. Synthesis of ε-caprolactone (ECL) *via* a CHMO-ADH cascade as an example of convergent redox-neutral cascade reaction.

Overall, lactones and lactams are important chemicals with extensive applications in industry. They can be synthesized by a variety of methods. Among the different approaches, biocatalytic methods have attracted much attention owing to their high selectivity and benign reaction conditions. BVMOs and ADHs are important enzymes that can catalyze bio-oxidation reaction and have been extensively studied and widely applied for the enzymatic oxidation. Redox-neutral cascade reactions are quite attractive since they can achieve internal cofactor regeneration.

2   MOTIVATION AND OBJECTIVES

Lactones and lactams are versatile chemicals used in various fields, such as polymer and pharmaceutical industries. However, the industrial synthesis of most lactones and lactams applies conventional chemical synthesis methods, which need expensive metal catalysts, aggressive chemicals, high temperature and non-renewable resources. Driven by the economic and environmental sustainability issues and the demand for highly chemo-, regio- and stereoselective transformation, the aim of this thesis is to develop more efficient, cleaner, safer and selective enzymatical approaches for the synthesis of lactones and lactams.

Nowadays, biocatalytic synthesis has been recognized as a promising alternative way to traditional chemical reaction due to their resource efficient, energy saving, economical and environmentally benign properties. Especially, biocatalytic cascades have attracted a significant interest due to their several advantages: (i) minimized isolation and purification steps, (ii) high productivities by the shift of equilibrium through cooperative effect of multiple reactions, and (iii) selective transformations of various biocatalysts. Redox enzymes that usually require expensive cofactors are mostly coupled in cascade reactions to make the systems perform more efficiently and economically.

Thus, this PhD thesis has been carried out with focus on two projects, i.e. lactonization and lactamization, and their specific goals are described in the following:

1. Convergent biocatalytic cascade reactions for lactonization

- Elucidation of biocatalytic characterization of type II flavin-containing monooxygenase FMO-E to identify its intrinsic limitations;
- Establish NADH-dependent convergent cascade reaction consisting of FMO-E and HLADH for the synthesis of achiral lactone;
- Establish NADH-dependent convergent cascade reaction consisting of FMO-E and HLADH for the synthesis of chiral lactones.

2. Parallel biocatalytic cascade reactions for lactamization

- Screening of ADHs using a model reaction to identify the suitable ADH candidate for the oxidation of amino alcohols;
- Evaluation of HLADH-catalyzed oxidation of amino alcohols using a model system with stoichiometric cofactor in terms of pH and ionic strength of buffer to identify optimal reaction conditions for lactamization;
- Elucidation of biocatalytic characterization of NADH oxidase from *Streptococcus mutans* (*Sm*NOX) to identify its intrinsic limitations;

- Combine *Sm*NOX with HLADH forming parallel cascade reaction to achieve cofactor regeneration and push the equilibrium of HLADH-catalyzed oxidation of amino alcohols to the lactam formation direction.

3   RESULTS

3.1   Convergent cascade reactions for lactonization

This part of the PhD thesis deals with new biocatalytic approaches for the synthesis of lactones. Since the discovery of cyclohexanone monooxygenase (CHMO) from *Acinetobacter sp.* in 1976[89], synthesis of lactones *via* the Baeyer-Villiger oxidation of ketones catalyzed by BVMO has been a fundamental and useful reaction in organic synthesis. On the other hand, oxidative lactonization of diols has also been an important method for the synthesis of lactones. For both of the two enzymes, cofactor regeneration is a crucial issue for economic synthesis of lactones.

Recently, Kara and coworkers reported a new redox-neutral bi-enzymatic cascade concept in a convergent fashion[118, 124], which intrinsically has the advantages of higher efficiency in terms of the starting materials and reaction steps required. This convergent cascade reaction consisting of a cyclohexanone monooxygenase (CHMO) and an alcohol dehydrogenase (ADH) utilizes two molar equivalents of cyclohexanone and one molar equivalent of 1,6-hexanediol to synthesize three molar equivalents of ε-caprolactone, theoretically, with water as sole by-product (**Scheme 3.1**). The cofactor regeneration of this cascade was achieved *via* the oxidation of cyclohexanone catalyzed by CHMO and the oxidation of "smart co-substrate" 1,6-hexanediol catalyzed by the ADH. In a 50 mL scale level, >99 % conversion of cyclohexanone could be achieved after 18 h and 84% ECL (19 mM) and 16% 1,6-HD (3.7 mM) were detected after 24 h. After the optimization by a two-step Design of Experiment (DoE) and the introduction of two-liquid-phase system (2LPS), the productivity of this system for the synthesis of ε-caprolactone was significantly enhanced yielding 53 mM of the product[124].
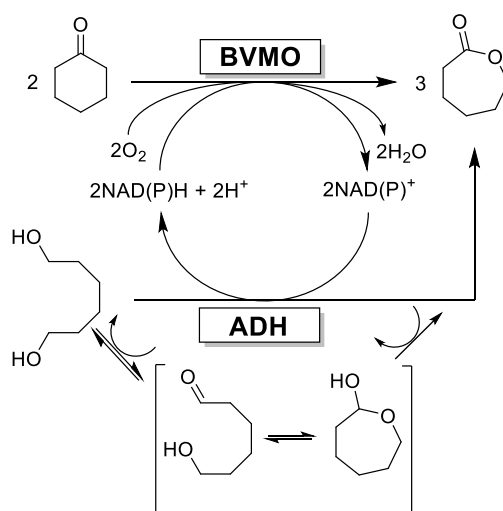
Scheme 3.1. Synthesis of ε-caprolactone through a convergent cascade system by coupling a cyclohexanone monooxygenase (CHMO) and an alcohol dehydrogenase (ADH).

However, this convergent cascade system has been limited to NADPH due to the strict cofactor recognition of CHMO from *Acinetobacter sp.* NCIMB 9871 (CHMO$_{Acineto}$)[54, 125-128]. CHMO$_{Acineto}$ is the most studied type I Baeyer-Villiger monooxygenase, which uses flavin adenine dinucleotide (FAD) as the cofactor and NADPH as electron source[125]. From an industrial point of view, NADH is the preferred cofactor since it is much cheaper (more than 10 times) and more stable than NADPH[112, 129]. Even for the whole-cell conversion using recombinant *Escherichia coli*, NADH is also beneficial as the NADH level in *E. coli* is higher than that of NADPH[130]. Moreover, it is well recognized that the recycling of NAD$^+$ is easier to be performed than that of NADP$^+$[85, 131-133].

Most of the studied BVMOs including CHMO$_{Acineto}$ belong to NADPH-dependent type I BVMOs, which are classified into the subclass B flavoprotein monooxygenase[97]. Although there are some successful examples that switch the cofactor specificity for other enzymes, the process for BVMO is limited. Kamerbeek et al. identified three reserved basic residues (Arg339, Lys439 and Arg440) concerning the cofactor specificity by employing sequence alignment for 4-hydroxyacetophenone monooxygenase (HAPMO) with other known NADPH-dependent BVMOs[134]. Introduction of mutations into these residues revealed that Arg339 and Lys439 were indeed involved in the cofactor recognition while Arg440 was not involved. In the same group, phenylacetone monooxygenase (PAMO) from *Thermobifida fusca* was also investigated for its cofactor specificity using the same method after its crystal structure was resolved[135-136]. They found Arg217 was crucial for binding the adenine moiety of the nicotinamide cofactor and the recognition of NADPH. The best of these mutants could only increase the NADH efficiency by 3-fold while the efficiency for NADPH was hardly affected. One recent reported work by the group of Bornscheuer described the switch of the cofactor specificity of CHMO$_{Acineto}$[137]. They designed variants with three or four mutations showing significantly enhanced activity ratio (NADH/NADPH) up to 4,200-fold with the aid of structure analysis, sequence alignments and literature data. However, the catalytic efficiency (k_{cat}/K_M) of the best variant towards NADH was 670-fold lower than that of wild type CHMO towards NADPH. Up to date, no type I BVMO could be engineered yet to be able to use NADH efficiently as cofactor. Hence, these research indicates that the function of NADPH in type I BVMO cannot be easily replaced by NADH[136].

Recently, Fraaije and coworkers identified a new subclass of class B flavoprotein monooxygenases, namely type II flavin-containing monooxygenases (FMOs) from *Rhodococcus jostii* RHA1[93, 138]. These type II FMOs could perform effective Baeyer–Villiger oxidations using both NADPH and NADH as the cofactor. Such relaxed cofactor specificity is a novel and attractive feature among the Baeyer–Villiger oxidation catalyzing enzymes. One of

these type II FMOs, FMO-E, could be purified in good yield without FAD loss using affinity chromatography purification method[93]. Being inspired by the fascinating feature of FMO-E, we focus on employing FMO-E to establish NADH-dependent convergent cascade reactions by coupling with NADH-dependent ADHs for lactonizations (**Scheme 3.2**).
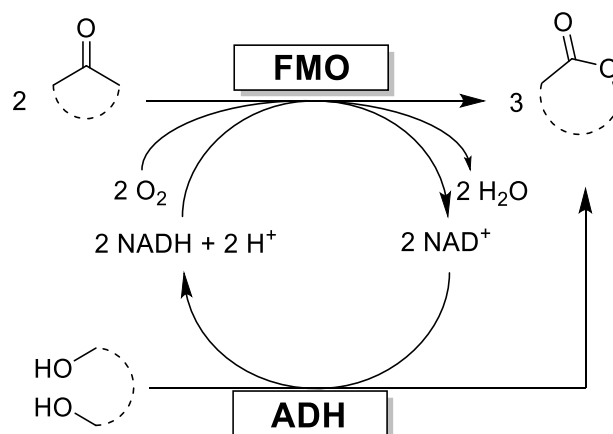
Scheme 3.2. Convergent cascade reactions coupling the flavin-containing monooxygenase (FMO) with alcohol dehydrogenase (ADH) for lactonizations. Two molar equivalents of ketone are coupled with one equivalent of diol to synthesize three molar equivalents of lactone.

3.1.1 Biocatalytic characterization of type II flavin-containing monooxygenase FMO-E

3.1.1.1 Purification of FMO-E

The FMO-E was available as an *N*-terminal strep tag (WSHPQFEK) fusion protein (in pBAD*NS*). Thus, the purification of FMO-E from cell free extract (CFE) could be easily done via affinity chromatography using Strep-Tactin® Sepharose (IBA GmbH, Germany) by following the manufacture introduction. As a minor modification, FAD (10 µM), DTT (1.0 mM) and glycerol (10%, v/v) were added in the buffers. The purification procedure can be seen in **A2.1.6** section. During the whole PhD topic, FMO-E was purified several times and one typical purification was shown in **Figure 3.1**.
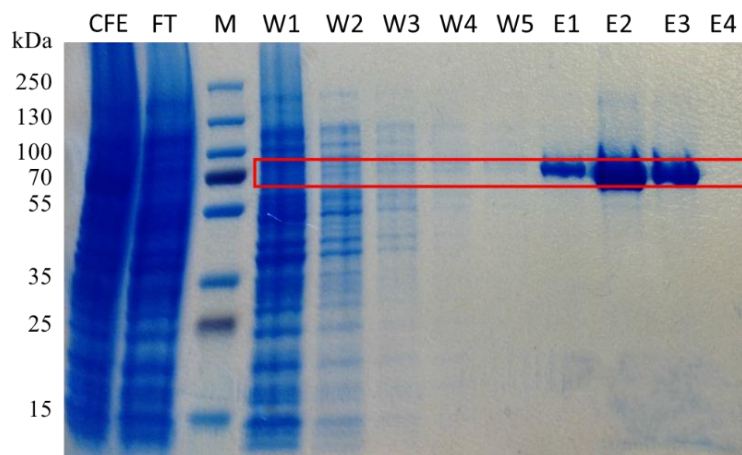
Figure 3.1. SDS-PAGE analysis of different fractions taken during the purification of FMO-E. CFE: cell free extract; FT: flow through; M: PageRuler Prestained Protein Ladder (Thermo Fisher); W: washing fraction; E: elution fraction.

The obtained purified enzyme was diluted with desalting buffer (10 mM phosphate buffer, pH 6.5, 1.0 mM DTT, 10 μM FAD, 25% glycerol (v/v)) to remove the additives (such as NaCl, EDTA, biotin) in the buffer. The obtained concentrated purified enzyme was stored at –80°C by aliquoting in micro-reaction tubes (each 100 μL). The concentration of the protein and activity of the enzyme were measured for each step and a typical purification was summarized in **Table 3.1**. The purified FMO-E was yellow like other BVMOs because of the presence of FAD in the enzyme. Approximately 50 mg pure FMO-E protein could be obtained from 1 L culture. Using purified FMO-E, the biocatalytic characterization of FMO-E was carried out.

Table 3.1. Summary of the FMO-E purification steps.

Purification Steps[a]	V [mL]	Protein [mg]	Specificity activity[b] [U/mg]	Total activity [U]	Purification factor [-]	Yield [%]
CFE	10	63.5	0.237	15.5	1	100
UF	1.9	13.5	0.696	9.4	3	61

[a] CFE: Cell free extract, UF: Ultrafiltration

[b] FMO-E activity assay with 2 mM bicyclo[3.2.0]hept-2-en-6-one as substrate and NADH.

3.1.1.2 Analysis of cofactor specificity of FMO-E

Using purified FMO-E, its cofactor specificity was verified with the BVMO standard substrate bicyclo[3.2.0]hept-2-en-6-one. The steady-state kinetic parameters of FMO-E using NADPH and NADH as cofactors were measured. As previously described[93], FMO-E could accept both nicotinamide cofactors and show typical Michaelis-Menten behavior (**Figure 3.2**). The catalytic rate (k_{cat}) and Michaelis constant (K_M) were obtained by simulation based on Michaelis-Menten double-substrate equation (**Equation 3.1**).

$$v = \frac{v_{max} \cdot c_{sub} \cdot c_{NAD(P)H}}{\left(K_{M_{Sub}} + c_{sub}\right) \cdot \left(K_{M\_NAD(P)H} + c_{NAD(P)H}\right)}$$ **(Equation 3.1)**

Even though FMO-E shows relaxed cofactor specificity, the enzyme still has higher affinity towards NADPH (K_M = 3 μM) than NADH (K_M = 10 μM) and both values are in the micromolar range (**Table 3.2**). Nevertheless, k_{cat} for NADPH is only a little higher than that of NADH (2.8 s^{-1} vs 2.0 s^{-1}), which indicates that FMO-E is an efficient biocatalyst with NADH as its cofactor. It is worth mentioning that the k_{cat} value of FMO-E for NADH is approximately two orders of magnitude higher than that of another reported type II FMO from *Stenotrophomonas maltophilia* (0.029 s^{-1})[95]. The catalytic rate of FMO-E with NADH is in the same range of 1–20 s^{-1} with that of many other class B flavoprotein MOs[139-140]. Therefore, it seemed interesting to combine FMO-E with other redox enzymes in enzymatic cascade reactions and to perform a deep study of its biocatalytic features.
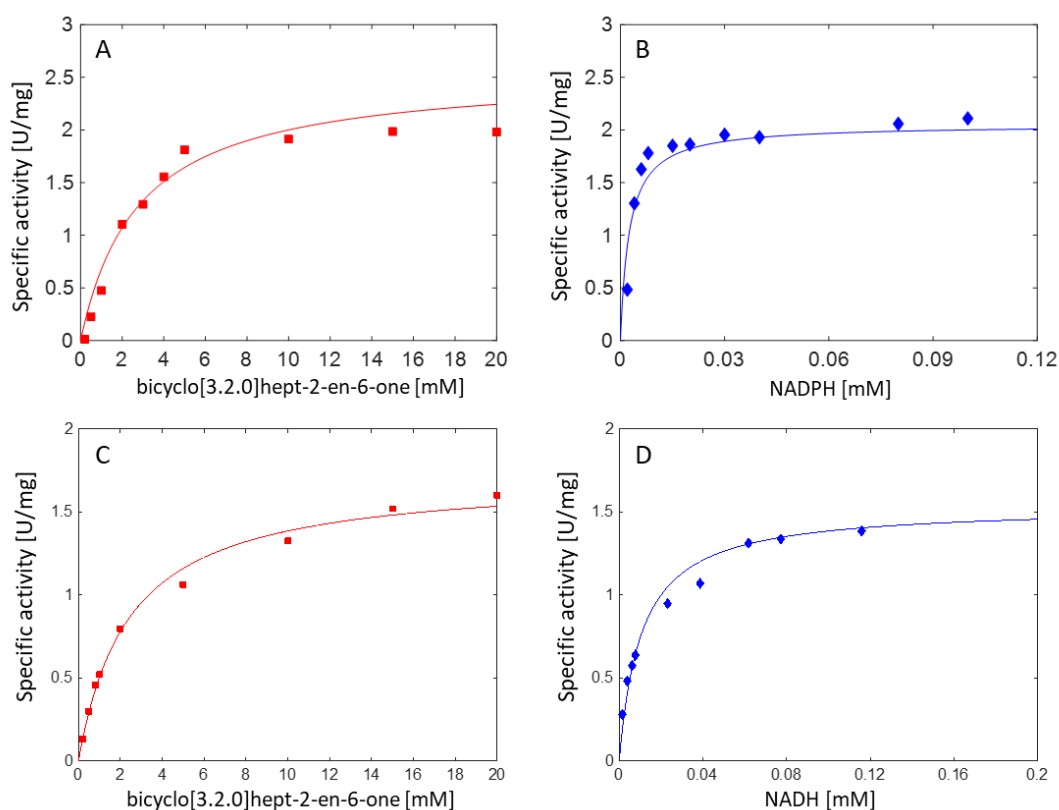
Figure 3.2. The kinetic assay of FMO-E towards model substrate bicyclo[3.2.0]hept-2-en-6-one using NADPH (A and B) and NADH (C and D) as cofactor based on Michaelis-Menten double substrate equation. Reaction conditions: (A and C): c(bicyclo[3.2.0]hept-2-en-6-one) = 0–20 mM, c(NAD(P)H) = 0.1 mM, c(FMO-E) = 0.08 μM, 50 mM pH 7 Tris-HCl; (B and D): c(NAD(P)H) = 0–0.1 mM, c(bicyclo[3.2.0]hept-2-en-6-one) = 10 mM, c(FMO-E) = 0.08 μM, 50 mM pH 7 Tris-HCl. 25°C.

22

Table 3.2. Kinetic parameters of FMO-E for the model substrate bicyclo[3.2.0]hept-2-en-6-one with NADPH and NADH based on Michaelis-Menten double-substrate equation.

Cofactor	v_{max} [U/mg]	K_M [μM]	k_{cat} [s^{-1}]
NADPH	2.6 ± 0.4	3 ± 1	2.8
NADH	1.9 ± 0.2	10 ± 4	2.0

3.1.1.3 Effect of pH on activity and stability of FMO-E

Enzyme activity is highly dependent from the pH value, especially in an assay mixture. Most of the enzyme activities show a bell-shaped curve on the pH-enzyme activity diagram. The activity starts to increase from zero at strong acidic region until reaching a maximum at a specific pH value and starts to decrease to zero again at strong alkaline region[141]. The pH value at which the enzyme shows its highest activity (v_{max}) is the optimal pH, which is it is the compromise between activity and stability, and normally ranging between pH 7–8 (not in all cases). The optimal pH (the compromise between activity and stability) is excellent for storage (not for all enzymes) or to test the enzymes because the enzymes are stable within the range of its optimal pH and the deactivation rate is low[142].

The effect of pH on the activity of purified FMO-W was investigated by measuring the oxidation of NADH with BVMO model substrate bicyclo[3.2.0]hept-2-en-6-one at various pH range from pH 5 to 9. Sodium acetate buffer (5.0, 5.5), PBS buffer (6.0, 6.5, 7.0, 7.5) and Tris-HCl buffer (7.5, 8.0, 8.5, 9.0) were selected based on their pK_a values. To display the effect of pH on the activity of HLADH, pH values are plotted against their corresponding relative activities and the result is shown in **Figure 3.3**. The maximum enzyme activity is characterized as 100% relative activity which corresponds to pH 7.5, 50 mM PBS buffer. The enzyme activity increased with the pH from pH 5 to pH 7.5, which indicates that the FMO-E enzyme favors the acidic environment. The activity decreased drastically from pH 7.5 and there was almost no activity shown at pH 9.0. FMO-E is active over a narrow range of pH with more than 50% relative activity between pH 6.5 and pH 8.0. This corresponds well to the optimum pH of some characterized BVMOs[54], including cyclohexanone monooxygenase from *Rhocococcus sp.* TK6 (CHMO$_{RhodoTK6}$)[143], pH 7.5; cyclopentanone monooxygenase from *Comamonas sp.* NCIMB 9872 (CPMO)[144], pH 7.7; phenylacetone monooxygenase from *Thermobifida fusca* YX (PAMO)[139], pH 8.0, and cyclohexanone monooxygenase from *Acinetobacter sp.* NCIMB 9871 (CHMO$_{acinet}$)[89], pH 9.0.
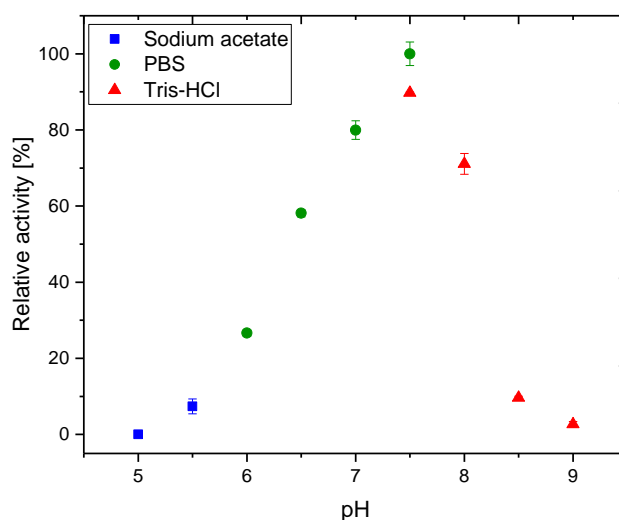
Figure 3.3. Effect of pH on the FMO-E activity. Reaction conditions: reaction system (1.0 mL) contained 50 mM buffers with different pH values, 0.1 mM NADH, 10 mM bicyclo[3.2.0]hept-2-en-6-one, and 0.08 μM FMO-E solution at 25°C, duplicate measurements. The maximum relative activity of 100% was set to the value obtained at pH 7.5 (PBS buffer).

To study the effect of pH on the stability of FMO-E, 50 μL of 1 mg/mL (16 μM) of the purified enzyme was incubated at 4°C in different pH (5.0–9.0) and the residual activity was detected after 24 h. The results are depicted in **Figure 3.4**. FMO-E inside pH 6.5 (50 mM PBS) had the highest residual activity with 94% activity left. That is the reason pH 6.5 PBS buffer was used as the desalting buffer to store purified FMO-E. The residual activity of FMO-E increased from pH 5.0 to pH 6.5 and then decreased constantly to pH 9.0, which corresponds to the effect of pH on FMO-E activity.
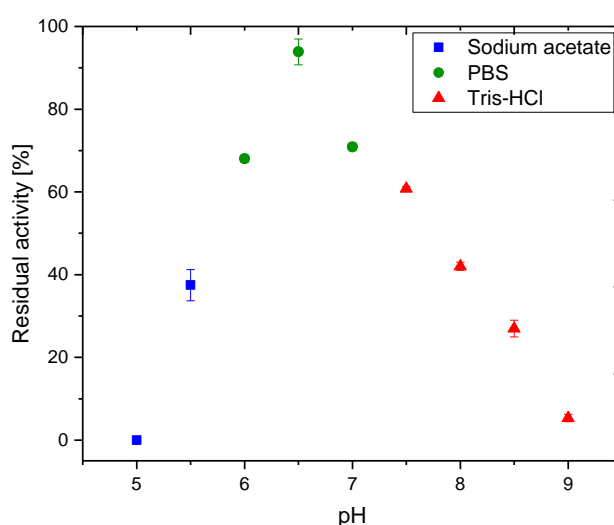
Figure 3.4. Effect of pH on the FMO-E stability. 500 μL of 1.0 mg/mL (16 μM) enzyme solution in 50 mM buffer with different pH values was incubated at 45°C and the residual activity was measured after 24 h, duplicate measurements. The maximum residual activity of 100% was determined for each individual reaction before the

24

incubation.

3.1.1.4 Effect of temperature on activity and stability of FMO-E

Temperature affects the enzyme activity the same as the pH and enzymes are exceedingly delicate to temperature changes. The enzymatic reactions follow the same rule as the chemical reactions, that their reaction rates increase with increasing temperature by two to three times every 10°C according to Van't Hoff's rule[141]. The enzyme activity dependency towards temperature is somehow resembling the bell-shaped curve of pH dependency, with the activity increasing with temperature to a maximum and then decreasing (maximum enzyme activity does not necessarily mean optimal temperature). The three-dimensional structure of the enzyme denatures at high temperature and decelerates the reaction velocity. The inactivation rate depends on the actual temperature and time (higher temperature, faster denaturation)[142].

The effect of temperature on the activity of purified FMO-E was investigated by measuring the oxidation of NADH with BVMO model substrate bicyclo[3.2.0]hept-2-en-6-one at various temperature from 20 to 45°C. **Figure 3.5** depicts the effect of temperature on the enzyme activity in 50 mM pH 7.5 Tris-HCl buffer. FMO-E kept more than 50% activity between 20°C and 35°C, with the highest activity at 25°C. A constant decrease was observed after 25°C and FMO-E was almost fully inactivated at 45°C. FMO-E was a thermally unstable enzyme as its optimal temperature was only 25°C. It is not surprised since most discovered BVMOs are thermally unstable, such as $CHMO_{acinet}$, its optimal temperature is 30°C[145].
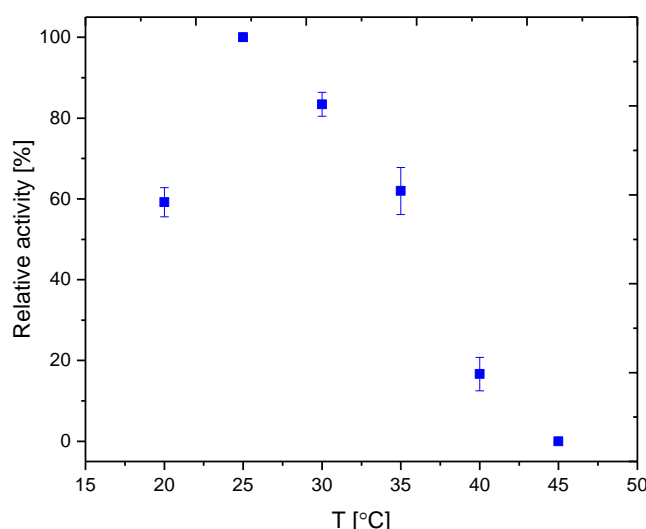
Figure 3.5. Effect of temperature on the FMO-E activity. Reaction conditions: reaction system (1.0 mL) contained 50 mM Tris-HCl buffer (pH 7.5), 0.1 mM NADH, 10 mM bicyclo[3.2.0]hept-2-en-6-one, and 0.08 μM FMO-E solution at different temperature from 20 to 45°C, duplicate measurements. The maximum relative activity of 100% was set to the value obtained at 25°C.

To study the effect of temperature on the short-term stability of FMO-E, a set of 50 μL of the purified enzyme (1.0 mg/mL, 16 μM) was incubated at various temperatures from 20–45°C (20, 25, 30, 35, 40, and 45°C) for 10 min in 50 mM pH 7.5 Tris-HCl buffer. The residual activity of enzyme incubated at 20°C was only 90%, indicating that FMO-E was unstable even at that temperature. Then the residual activity saw a sharp decrease from 30°C and there was only 10% activity left after incubating at 35°C for 10 min (**Figure 3.6**). FMO-E was almost inactivated after incubating at 45°C for 10 min.
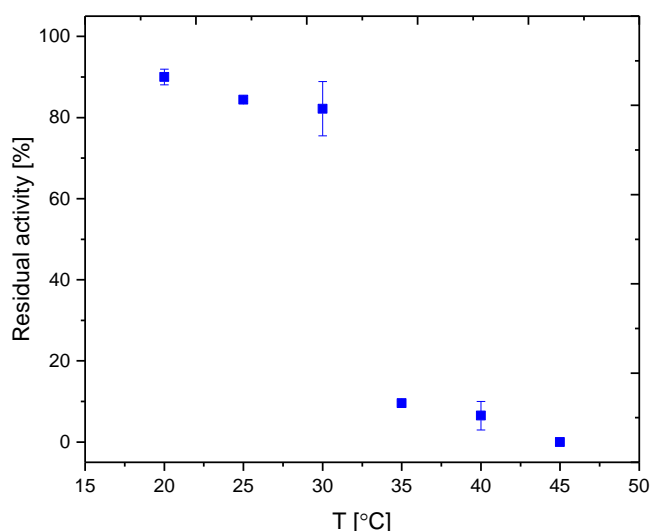
Figure 3.6. Effect of temperature on the FMO-E stability. 50 μL of 1.0 mg/mL (16 μM) enzyme solution in 50 mM pH 7.5 Tris-HCl buffer at different temperature and the residual activity was measured after 10 min, duplicate measurements. The maximum residual activity of 100% was set to the activity value before the incubation.

3.1.1.5   Effect of co-solvent on activity of FMO-E

FMO-E readily accepted small cyclic ketones and exhibited excellent and unique regio- and enantioselectivities compared with other typical type I BVMOs and type I FMOs[93]. However, most of these cyclic ketones are water-insoluble compounds and their low solubility in aqueous buffer is one of the hinders for the application of FMO-E for synthetic purposes. One strategy to circumvent this limitation is adding cosolvent, such as water miscible organic solvent to increase the solubility of hydrophobic in the aqueous system. However, organic solvents have some effect on the activity, stability and selectivity of enzymes[146-147]. Therefore, the investigation of effect of organic solvent on FMO-E can contribute to the selection of cosolvent for FMO-E.

Here, one concept of C_{50} is introduced to describe the effect of co-solvent on enzyme activity, which means the concentration (v/v) of cosolvent at which half of activity is left (**Table 3.3**). The higher value of C_{50} means the higher tolerance of FMO-E towards the organic solvent, and

vice versa. Acetone and acetonitrile had low C_{50} values which means they are toxic to the enzyme (**Figure 3.7**). Methanol, DMSO, ethanol and 1,4-dioxane had a similar C_{50} value towards the enzyme activity. Considering FMO-E will be combined with ADH in the cascade reactions, methanol and ethanol are not the suitable co-solvents. 1,4-dioxane is a potential cancerogenic substance. Therefore, DMSO was selected as the co-solvent for the future study.
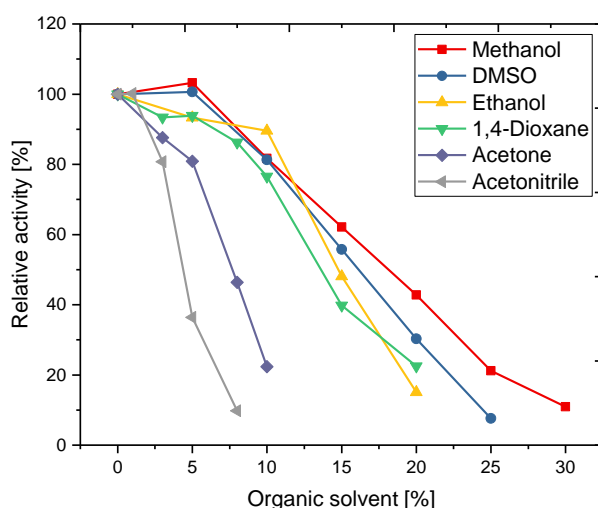
Figure 3.7. Effect of co-solvent on the FMO-E activity. The enzyme activity was determined by performing the standard FMO-E activity assay in 50 mM pH 7.5 Tris-HCl buffer with different contents of organic solvents from 0% to 30% (v/v). The maximum residual activity of 100% was set to the activity value without any organic solvent. Lines are only for visual guidance.

Table 3.3. C_{50} values of different co-solvents.

Cosolvent	Methanol	DMSO	Ethanol	1,4-Dioxane	Acetone	Acetonitrile
C_{50} (% v/v)	18	16	15	13	8	4

3.1.1.6   Effect of cofactor on long-term stability of FMO-E

Recently, Goncalves et al., have systematically evaluated the effect of cofactors on the stability of class B flavin monooxygenases (FMOs)[148]. Three unrelated class B FMOs were all significantly stabilized by adding cofactors NADPH and FAD, and superoxide dismutase and catalase with up to 10^3-10^4-fold increase of the half-life time ($\tau_{1/2}$). It was also documented that the coenzyme binding with enzyme could lead to dramatic increase of stability of NADPH-dependent dimeric flavoenzyme 4-hydroxyacetophenone monooxygenase (HAPMO)[149]. Inspired by these findings, some factors, such as NADPH, FAD and NADH were studied for their effects on the stability of FMO-E.

Four kinds of formulation of cofactor additives (10 μM FAD, 10 μM FAD + 0.1 mM NADH, 10 μM FAD + 0.1 mM NADPH, 10 μM FAD + 2.5 mM NADH) were investigated for their

effects on the half-life time of FMO-E at 30°C (**Figure 3.8**). Not to our surprise, both FAD and NADPH could enhance the stability of FMO-E, which is consistent with the finding of Goncalves et al.[148]. The half-life time of FMO-E with 10 μM FAD + 0.1 mM NADPH was 2.6-fold longer than that without these cofactors (**Table 3.4**). On the other hand, NADH didn't show any beneficial effect on the stability of FMO-E with even much higher concentration to 2.5 mM (**Table 3.4**).
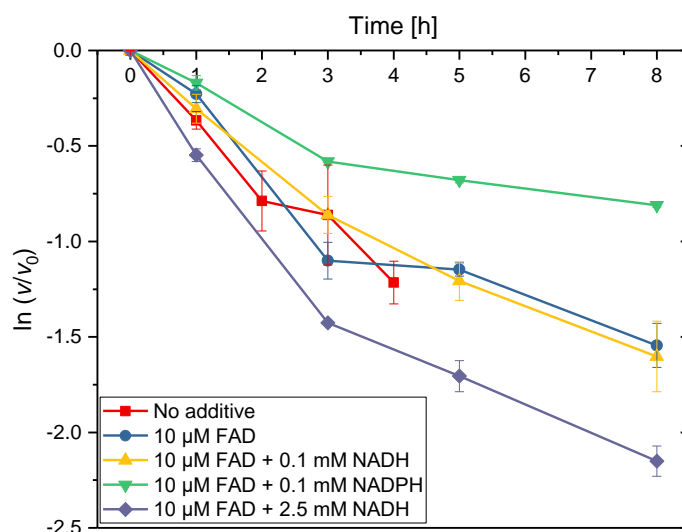
Figure 3.8. Effect of cofactor on FMO-E long-term stability at 30°C. 1.0 mg/mL (16 μM) enzyme solutions in 50 mM pH 7.5 Tris-HCl buffer with different cofactors formulations were incubated at 30°C and the residual activities were measured at different time points (0, 1, 3, 5, and 8 h) with duplicate measurements. Lines are only for visual guidance.

Table 3.4. Half-life times of FMO-E at 30 °C with different cofactor components. Experiments were performed in duplicates.

Cofactor	k_d[a] [h^{-1}]	$\tau_{1/2}$[b] [30°C, h]	Stabilization factor [-]
No additive	0.313 ± 0.020	2.21 ± 0.14	1.0
10 μM FAD	0.218 ± 0.004	3.17 ± 0.06	1.5
10 μM FAD + 0.1 mM NADH	0.220 ± 0.022	3.17 ± 0.32	1.5
10 μM FAD + 0.1 mM NADPH	0.119 ± 0.001	5.82 ± 0.04	2.6
10 μM FAD + 2.5 mM NADH	0.309 ± 0.002	2.25 ± 0.02	1.0
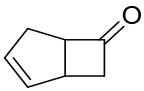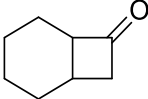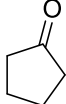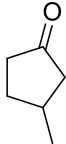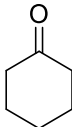
[a] k_d [h^{-1}] = Deactivation constant; [b] $\tau_{1/2}$ [h] = Half-life time.

3.1.1.7   Substrate scope of FMO-E

A range of ketones, including three (fused) cyclobutanones, two cyclopentanones and one cyclohexanone were tested as the substrates of FMO-E with UV-Vis spectrophotometer . FMO-E showed significant Baeyer-Villiger oxidation activity towards cyclobutanone (**1**, **2**) and fused cyclobutanone (**3**), whereas cyclopentanones (**4**, **5**) and cyclohexanone (**6**) were poorly accepted or not at all (**Table 3.5**). This was partly demonstrated by Riebel et al[93]. These results

indicate that the substrate scope of FMO-E is restricted to cyclobutanones. This biocatalytic feature is similar to another type II FMO from *Stenotrophomonas maltophilia*[95], which could only convert the BVMO standard substrate **1** with NADH as cofactor.

Table 3.5. Ketone substrates investigated for FMO-E.

No.	Ketone		Specific activity[a] (U mg^{-1})
1	bicyclo[3.2.0]hept-2-en-6-one		1.35 ± 0.05
2	cyclobutanone		0.92 ± 0.01
3	bicyclo[4.2.0]octan-7-one		1.51 ± 0.02
4	cyclopentanone		n.d.[b]
5	3-methylcyclopentanone		n.d.
6	cyclohexanone		n.d.

[a] Activity assay conditions: c(ketone) = 10 mM, c(NADH) = 0.1 mM, c(FMO-E) = 0.08 μM, 50 mM pH 7.0 Tris-HCl, 25°C. [b] n.d.: Not detected.

3.1.1.8   Interim summary

- FMO-E could be purified with high yield of 61% via affinity chromatography using Strep-Tactin® Sepharose.

- FMO-E exhibited similar kinetic parameters towards NADPH and NADH. It is a potent biocatalyst using NADH as cofactor.

- FMO-E showed the highest activity at pH 7.5 while maintaining the highest stability at pH 6.5.

- The half-life time of FMO-E at 30°C was 2.21 h, but addition of 0.1 mM NADPH and 10 μM FAD could improve its half-life time by 2.6-fold.

- FMO-E only showed Baeyer-Villiger oxidation activity towards cyclobutanones and fused cyclobutanones, indicating its narrow substrate range.

3.1.2 NADH-dependent convergent cascade reaction for the synthesis of achiral lactone

To accomplish the above designed NADH-dependent convergent cascade, a NADH-dependent ADH is required. Horse liver alcohol dehydrogenase (HLADH) is a well-known and widely studied zinc- and NADH-dependent ADH[150-153], whose study is still ongoing[154]. HLADH has been found to be a versatile biocatalyst for the synthesis of γ-, δ- or ε-lactones from diols *via* two-step one-pot oxidation[69, 75, 155-156]. Remarkably, HLADH has been reported to promote NAD(P)H-dependent redox biocatalysis by using 1,4-butanediol as the "smart co-substrate"[157]. The thermodynamically stable and kinetically inert co-product γ-lactone makes the cofactor regeneration reaction irreversible, thus leading to dramatically reduced molar surplus of co-substrate and faster reaction rates. Therefore, HLADH was selected as the target ADH to perform the NADH-dependent convergent cascade coupling with FMO-E.

3.1.2.1 Proof-of-concept study

At the beginning, cyclobutanone and the corresponding 1,4-butanediol were selected as the substrates of FMO-E and HLADH for the proof-of-concept study of the NADH-dependent convergent cascade (**Scheme 3.3**). It is worth mentioning that 1,4-butanediol can be produced from renewable feedstocks at industrial scale which has been developed by Genomatica Inc (San Diego, USA)[158-159]. The fermentative synthesis of 1,4-butanediol process has been licensed by BASF SE (Ludwigshafen, Germany).
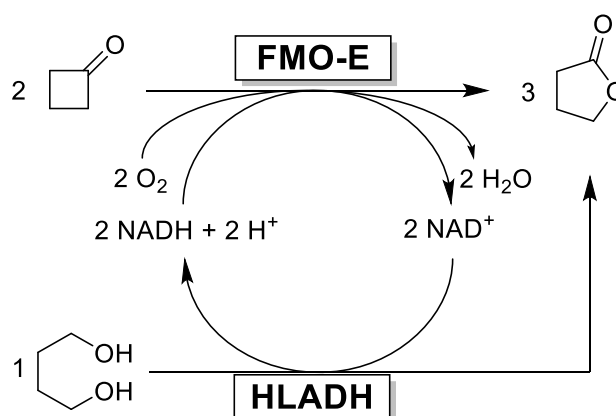
Scheme 3.3. NADH-dependent convergent cascade employing FMO-E and HLADH with cyclobutanone and 1,4-butanediol as substrates to synthesize γ-butyrolactone. Two molar equivalents of cyclobutanone are coupled with one equivalent of 1,4-butanediol to synthesize three molar equivalents of γ-butyrolactone.

Firstly, the steady-state kinetic parameters of FMO-E towards cyclobutanone and HLADH

towards 1,4-butanediol were determined using NADH and NAD$^+$ as their cofactors, respectively. The catalytic rate (k_{cat}), Michaelis constant (K_M) and inhibition constant (K_i) were obtained by simulation based on Michaelis-Menten equation without inhibition (**Equation 3.2, FMO-E**) or Michaelis-Menten uncompetitive substrate inhibition equation (**Equation 3.3, HLADH**). The NADH concentration was fixed at 0.1 mM, which is 10-fold higher than the K_M value of FMO-E towards NADH (**Table 3.2**), to make sure FMO-E was saturated with NADH. Similarly, NAD$^+$ concentration was fixed at 1.0 mM.

$$v = \frac{v_{max} \cdot c_{sub}}{K_{M\_Sub} + c_{Sub}}$$
(**Equation 3.2**)

$$v = \frac{v_{max} \cdot c_{sub}}{K_M + c_{Sub} \cdot (1 + \frac{c_{sub}}{K_{i,sub}})}$$
(**Equation 3.3**)

Both FMO-E and HLADH showed typical Michaelis-Menten behaviors towards their substrates (**Figure 3.9**). The K_M and k_{cat} values of FMO-E towards cyclobutanone (2.1 mM and 1.3 s^{-1}) were found to be in the same range with the BVMO standard substrate bicyclo[3.2.0]hept-2-en-6-one (2.4 mM and 2.0 s^{-1}). These data also confirm the substrate specificity of FMO-E towards cyclobutanones. HLADH showed similar range of K_M and k_{cat} values (3.5 mM and 3.5 s^{-1}) towards 1,4-butanediol with that of FMO-E towards cyclobutanone (**Table 3.6**). The difference is that HLADH also showed some extent of substrate inhibition towards 1,4-butanediol with a relatively high K_i value of 1810 mM. However, it is worth mentioning that the kinetic assay of HLADH towards 1,4-butanediol might only represent the first step of lactonization, i.e. the oxidation of diol to hydroxy aldehyde *via* an UV assay method.
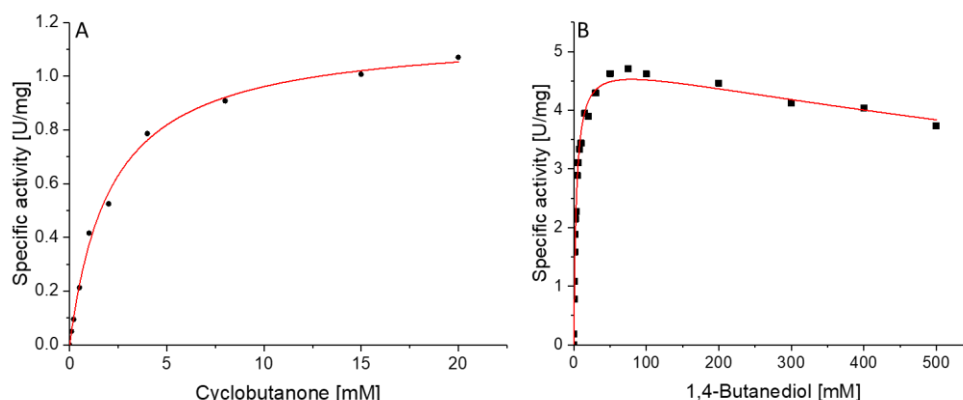
Figure 3.9. The kinetic assay of FMO-E towards cyclobutanone (**A**) and HLADH towards 1,4-butanediol (**B**) according to the Michaelis-Menten equation and Michaelis-Menten uncompetitive substrate inhibition equation. Reaction conditions: (A) c(cyclobutanone) = 0–20 mM, c(NADH) = 0.1 mM, c(FMO-E) = 0.08 μM, 50 mM pH 7 Tris-HCl, 25°C, duplicate measurements; (B) c(1,4-butanediol) = 0–500 mM, c(NAD$^+$) = 1.0 mM, c(HLADH) = 0.19 μM, 100 mM pH 8 Tris-HCl, 25°C, duplicate measurements. The fixed NADH and NAD$^+$ concentration ($\geq$ 5 times of K_M) was chosen based on the preliminary kinetic assay to determine the K_M value of NADH and NAD$^+$.

Table 3.6. Kinetic parameters of FMO-E towards cyclobutanone and HLADH towards 1,4-butanediol.

Substrate	v_{max} [U/mg]	K_M [mM]	k_{cat} [s^{-1}]	K_i [mM]
cyclobutanone	1.2 ± 0.02	2.1 ± 0.2	1.3	-
1,4-butanediol	5.2 ± 0.01	3.5 ± 0.4	3.5	1810 ± 533

Next, a set of experiments including one positive reaction and four negative control reactions by eliminating one or two components in the positive reaction were performed with 20 mM cyclobutanone and 10 mM 1,4-butanediol. The concentration of product γ-butyrolactone increased to approximate 25 mM (analytical yield of 83%) after 24 h and no substrate cyclobutanone could be detected at that time point in the positive reaction (**Figure 3.10**). However, there was still small amount of 1,4-butanediol detected after 72 h, which could be attributed to the evaporation of cyclobutanone ($T_{boiling\ point}$ = 99.7°C) leading to inefficient cofactor regeneration of the whole cascade. The reaction was carried out in a 30 mL reactor (1 mL total reaction volume), which could be the reason for the substrate evaporation as there was relatively large head space in the system. The increase of 1,4-butanediol after 48 h might be attributed to reduced reaction volume resulting from evaporation. In addition, it could also be partly the result of analytical errors.

Figure 3.10. NADH-dependent convergent cascade employing FMO-E and HLADH with cyclobutanone and 1,4-butanediol as substrates to synthesize γ-butyrolactone. Reaction conditions: c(cyclobutanone) = 20 mM, c(1,4-butanediol) = 10 mM, $c(NAD^+)$ = 1 mM, c(FMO-E) = 1 U (16.6 µM), c(HLADH) = 1 U (7.3 µM), buffer: Tris-HCl (100 mM, pH 8.0), 180 rpm, T = 20ºC. Reactions (1 mL in total) run in 30 mL glass-vial, single experiment. Lines are only for visual guidance.

On the other hand, the continuous decrease in the concentration of γ-butyrolactone after 24 h could mainly result from its hydrolysis to the corresponding acid, which was previously documented in the literature[75, 124] and is also demonstrated here experimentally (**Figure 3.11**). When 20 mM γ-butyrolactone solution in pH 8.0, 100 mM Tris-HCl buffer was incubated in the reaction conditions (180 rpm shaking and T = 20°C), the autohydrolysis rate was 90 µM/h. The autohydrolysis rate at pH 9.0 buffer was even doubled compared with that at pH 8.0 buffer. This indicates that the hydrolysis of lactones in the buffer is one of the main, if not the most important, issues for the lactonization.
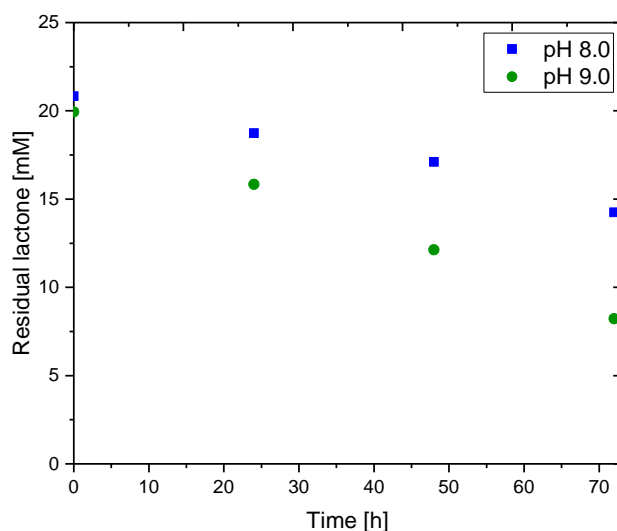
Figure 3.11. Hydrolysis of 20 mM γ-butyrolactone in aqueous solution. Conditions: 100 mM Tris-HCl pH 8.0 or pH 9.0, 180 rpm, T = 20°C, single experiment.

No target lactone product was detected in all negative control reactions except the one in the absence of FMO-E (**Figure 3.12B**). This observation can be attributed to the present HLADH that can use the oxidized NAD^+ to synthesize lactone from 1,4-butanediol. The concentrations of cyclobutanone in four reactions saw different levels of decrease, which could also be attributed to its evaporation in the big vials, as previously mentioned.
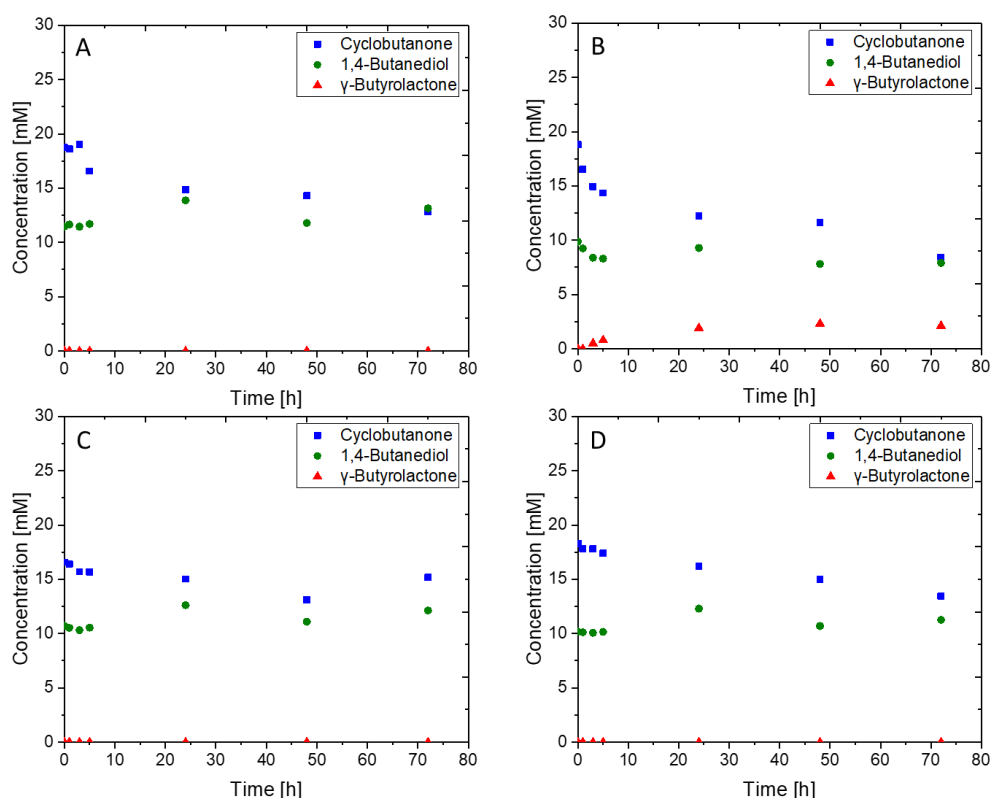
Figure 3.12. Results of negative control reactions of NADH-dependent convergent cascade employing FMO-E and HLADH with cyclobutanone and 1,4-butanediol as substrates to synthesize γ-butyrolactone. Reaction conditions: c(cyclobutanone) = 20 mM, c(1,4-butanediol) = 10 mM, c(NAD$^+$) = 1 mM, c(FMO-E) = 1 U (16.6 μM), c(HLADH) = 1 U (7.3 μM), buffer: Tris-HCl (100 mM, pH 8.0), 180 rpm, T = 20°C. Based on the above conditions, **A**: without NAD$^+$, **B**: without FMO-E, **C**: without HLADH, **D**: without FMO-E and HLADH. Reactions (1 mL in total) run in 30 mL glass-vial, single experiment. Lines are only for visual guidance.

The newly established reaction system showed about 18% depletion in the mass balance after 72 h (**Figure 3.10**). As mentioned above, this can be attributed to a large extent to the evaporation of the substrate cyclobutanone and the undesired autohydrolysis of the product γ-butyrolactone. Furthermore, the lactonization of 1,4-butanediol to γ-butyrolactone catalyzed by HLADH consists of three subsequent steps: i. oxidation of 1,4-butanediol to the hydroxy aldehyde, ii. spontaneous cyclization of the hydroxy aldehyde intermediate to lactol followed by iii. the final oxidation of lactol to γ-butyrolactone (**Scheme 3.4**). It could be possible that not all the 1,4-butanediol was converted by HLADH to the final product γ-butyrolactone, and some amounts were remained as intermediates, which could not be detected by the analytical method used in this study.
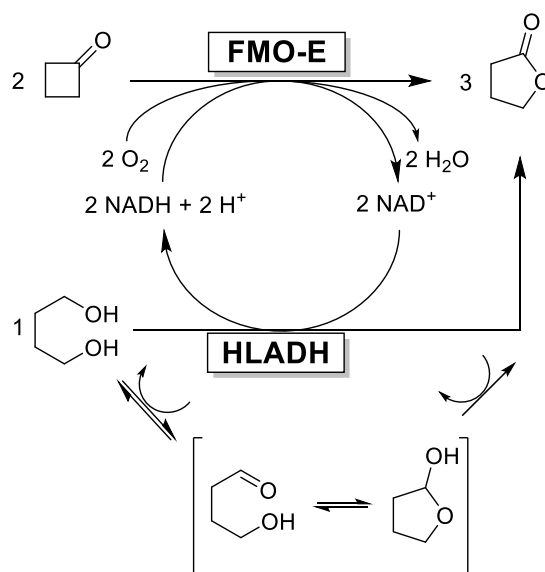
Scheme 3.4. NADH-dependent convergent cascade employing FMO-E and HLADH with cyclobutanone and 1,4-butanediol as substrates to synthesize γ-butyrolactone. The lactonization of 1,4-butanediol to γ-butyrolactone catalyzed by HLADH consists of three subsequent steps.

3.1.2.2 Semi-preparative synthesis of γ-butyrolactone

Encouraged by the successful proof-of-concept, we aimed to enhance the productivity of this FMO-E-HLADH coupled system. For this purpose, higher concentration of substrates was used in the system. When the concentration of cyclobutanone and 1,4-butanediol was increased to 100 mM and 50 mM, both substrates were still remained after 72 h using one unit of each enzyme (**Figure 3.13A**). However, turnover number (TON) of the enzymes ($mol_{lactone}/mol_{FMO-E\ and\ HLADH}$) significantly increased from 904 to 5163 compared with 20:10 mM (ketone:diol) substrates concentration. By using two-fold amounts of each enzyme, none of the two substrates could be detected after 48 h (**Figure 3.13B**) and the concentration of γ-butyrolactone could reach 134 mM (89% analytical yield) at 72 h (**Table 3.7**). However, the TON value decreased from 5163 to 2811.

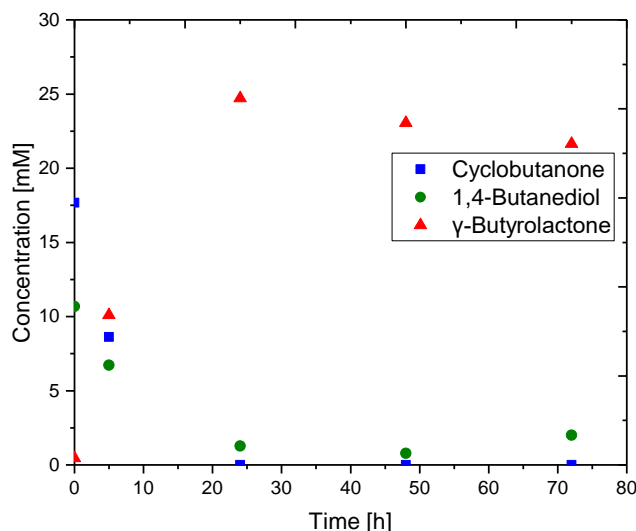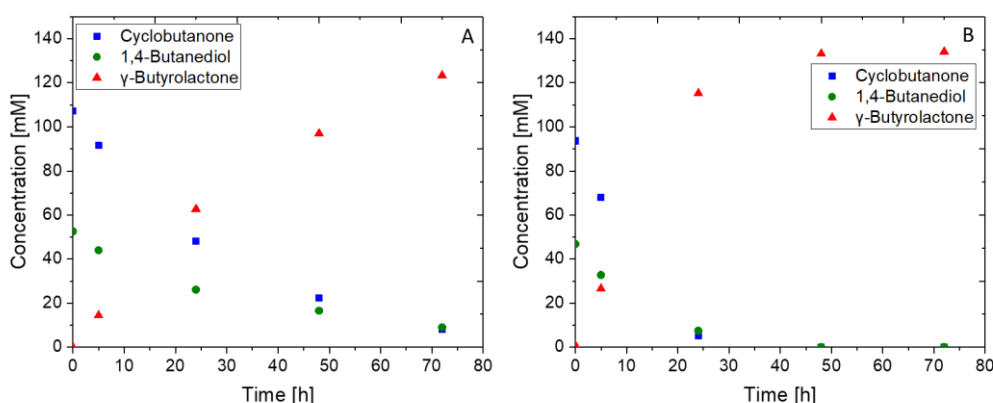**Figure 3.13**. Results of NADH-dependent convergent cascade employing FMO-E and HLADH with cyclobutanone and 1,4-butanediol as substrates to synthesize γ-butyrolactone with high concentration of substrates. Reaction conditions: c(cyclobutanone) = 100 mM, c(1,4-butanediol) = 50 mM, c(NAD$^+$) = 1 mM, c(FMO-E) = 1 U (16.6 μM) (**A**) and 2 U (32.2 μM) (**B**), c(HLADH) = 1 U (7.3 μM) (**A**) and 2 U (14.6 μM) (**B**), buffer: Tris-HCl (100 mM, pH 8.0), 180 rpm, T = 20°C. Reactions (1 mL in total) run in 30 mL glass-vial, single experiment. Lines are only for visual guidance.

Table 3.7. Summary of the convergent cascade reactions applied for the synthesis of γ-butyrolactone.

Reaction number	Ketone [mM]	Diol [mM]	FMO-E [U/mL] (μM)	HLADH [U/mL] (μM)	5h c(GBL) [mM]	24h c(GBL) [mM]	48h c(GBL) [mM]	72h c(GBL) [mM]	Yield [%]	TON[a] [-]
1	20	10	1.0 (16.6)	1.0 (7.3)	10.1	24.6	23.0	21.6	72	904
2	100	50	1.0 (16.6)	1.0 (7.3)	14.5	62.7	97.0	123.4	82	5163
3	100	50	2.0 (33.1)	2.0 (14.6)	28.7	123.3	133.2	134.1	89	2811

[a] The TON values represent μmol lactone product formed per total μmol of FMO-E and HLADH.

The formation of γ-butyrolactone rate decreased during the reactions, which could be the results of reduced concentration of substrates and the deactivation of enzymes. To verify the deactivation of enzymes while using different enzyme amounts, a deactivation test developed by M. J. Selwyn[160] was conducted. The theory of this test is that the product formation is only the function of time and enzyme concentration if all other parameters are kept constant and there is no enzyme deactivation. In this case, when performing enzymatic reactions with different amounts of enzymes, and plotting product concentration versus time multiplied by enzyme concentration, these points should coincide in the same curve. Otherwise, there should be enzyme denaturation, and the amount of enzyme is also the function of time, thus leading to different curves. The γ-butyrolactone concentration (mM) was plotted versus time × total

enzyme concentration (h × U/mL) (**Figure 3.14**). Both graphs showed a similar progress at least up to 5 h, which eliminates a significant enzyme deactivation with low concentration of enzymes. However, the curve with 4 U/mL total enzymes proceeded to higher productivity from 5 h to 24 h than 2 U/mL total enzymes, which showed severer enzyme deactivation in the system with lower enzymes amount.
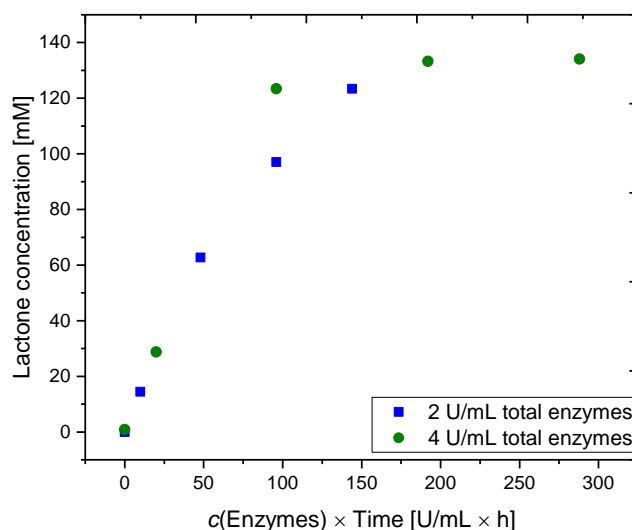
Figure 3.14. Analysis of the performances of the enzymes with 100 mM cyclobutanone and 50 mM 1,4-butanediol using two different enzyme concentrations, FMO-E/HLADH = 1 U/1 U or 2 U/2 U in 1 mL total reaction volume.

3.1.2.3 Effect of reactor on the cascade reaction

As oxygen is the third substrate of FMO-E besides the ketone and the cofactor, it is necessary to investigate the influence of oxygen on the reaction. Herein, the oxygen amount is represented as the headspace ratio of reactor. Therefore, a smaller reactor with the size of 1.5 mL was also used to perform these cascade reactions for comparison. In the case of low substrate concentration (20/10 mM), the smaller reactor led to decreased evaporation of substrate cyclobutanone and resulted in full conversion of both substrates (**Figure 3.15A and B**) while there was still some 1,4-butanediol left in the large reactor resulted from the cyclobutanone evaporation as also mentioned before. The headspace ratio (V_g/V_l) value of large reactor (75 × 28 mm) was 29, which was almost 60-fold higher than that (0.5) of small reactor (32 × 12 mm) and led to obvious reagents evaporation.

On the other hand, it was shown that the larger reactor was preferred when high substrate concentration was applied (**Figure 3.15C and D**) as oxygen now was also one of the limitations. A higher productivity was achieved in the larger reactor due to more available molecular oxygen. The interfacial area ($a_{g/l}$) value in the case of large reactor was calculated as 615 mm^2, which was almost 6-fold higher than that (113 mm^2) of small reactor. It was worth mentioning

that these reactors were closed with cap during the reaction period except taking samples, which meant there would be more oxygen in the reactor with higher value of headspace ratio. In both cases, 1 mL of total reaction volume was applied, thus reactor with higher V_g/V_l value and $a_{g/l}$ value would have more soluble oxygen in the reaction system.
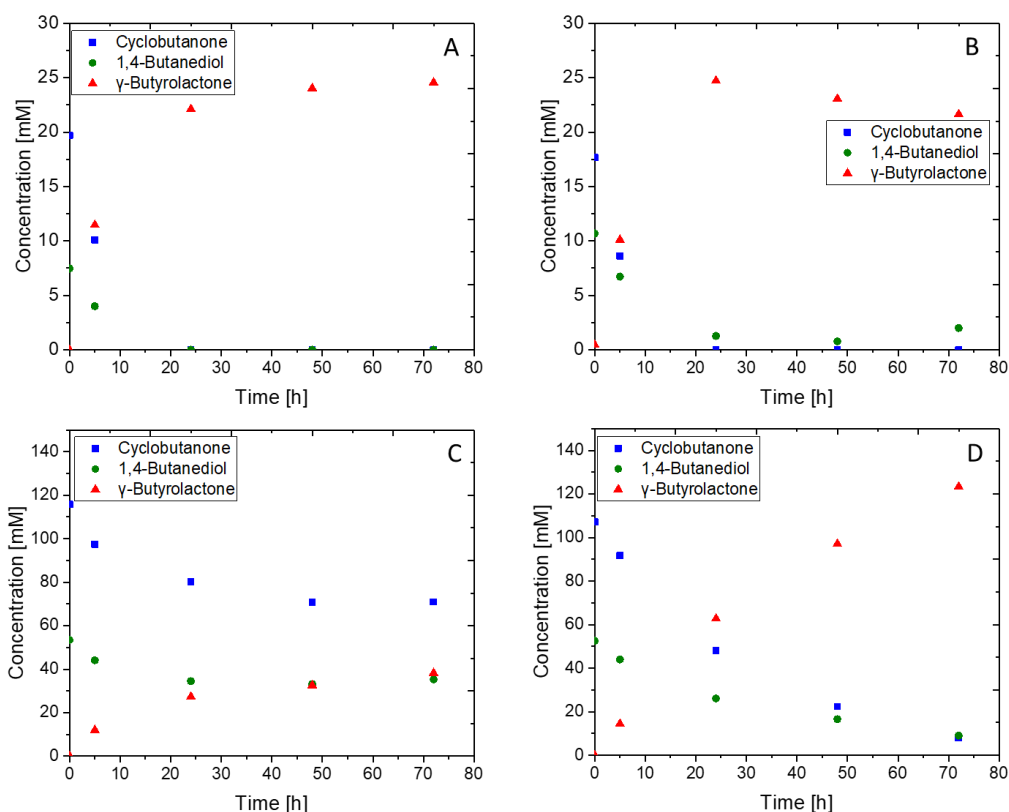
Figure 3.15. The comparison of the performed convergent cascades in 1.5 mL and 30 mL reactors. Reaction conditions: c(cyclobutanone) = 20 mM, c(1,4-butanediol) = 10 mM, c(NAD$^+$) = 1 mM, c(FMO-E) = 1 U (16.6 µM), c(HLADH) = 1 U (7.3 µM), buffer: Tris-HCl (100 mM, pH 8.0), 180 rpm, T = 20°C. Based on the above conditions, c(cyclobutanone) = 20 mM, c(1,4-butanediol) = 10 mM, **A**: reaction (1 mL in total) run in 1.5 mL glass-vial, **B**: reaction (1 mL in total) run in 30 mL glass-vial; c(cyclobutanone) = 100 mM, c(1,4-butanediol) = 50 mM, **C**: reaction (1 mL in total) run in 1.5 mL glass-vial, **D**: reaction (1 mL in total) run in 30 mL glass-vial, single experiment. Lines are only for visual guidance.

3.1.2.4   Interim summary

- The proof-of-concept study of FMO-E-HLADH catalyzed NADH-dependent convergent cascade was successfully demonstrated using cyclobutanone and 1,4-butanediol as the substrates.

- The practical usefulness of this convergent cascade system was demonstrated on a semi-preparative scale (100 mM cyclobutanone and 50 mM 1,4-butanediol) with 134 mM (89%

yield) γ-butyrolactone produced.

- The reactor showed significant effect on the productivity of the cascade reaction by changing the headspace ratio and interfacial area, which could influence the oxygen input and reagent evaporation. The higher headspace ratio and interfacial area would provide more oxygen for the cascade reaction, which is preferred for reaction system with high substrate concentration, but also lead to more reagents evaporation.

3.1.3 NADH-dependent convergent cascade reaction for the synthesis of chiral lactones

In the next set of experiments, racemic bicyclobutanone substrate bicyclo[4.2.0]octan-7-one and the corresponding diol cis-1,2-cyclohexanedimethanol were employed in this convergent cascade (**Scheme 3.5**). As it was reported that FMO-E showed moderate to excellent regioselectivity and enantioselectivity for the Baeyer-Villiger oxidation of racemic fused cycloketones[93]. Thus, the products of FMO-E-catalyzed oxidation of bicyclo[4.2.0]octan-7-one can be normal lactone and abnormal lactone, while the product of HLADH-catalyzed oxidation of cis-1,2-cyclohexanedimethanol is only abnormal lactone.
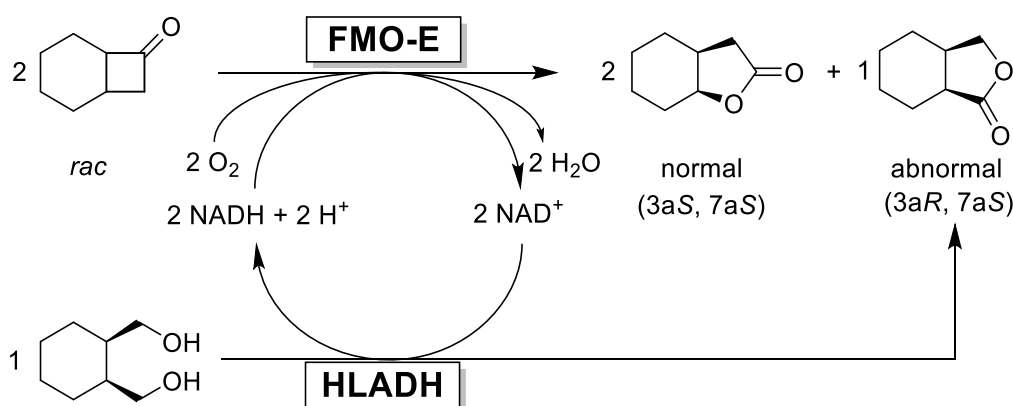
Scheme 3.6. NADH-dependent convergent cascade employing FMO-E and HLADH with racemic bicyclo[4.2.0]octan-7-one and cis-1,2-cyclohexanedimethanol as substrates.

3.1.3.1 Substrates of the cascade reaction

Firstly, the steady-state kinetic parameters of FMO-E towards bicyclo[4.2.0]octan-7-one and HLADH towards cis-1,2-cyclohexanedimethanol were determined using NADH and NAD$^+$ as their cofactors, respectively. The catalytic rate (k_{cat}), Michaelis constant (K_M) and inhibition constant (K_i) were obtained by non-linear regression based on Michaelis-Menten equation without inhibition (**Equation 3.2, FMO-E**) or Michaelis-Menten uncompetitive substrate inhibition equation (**Equation 3.3, HLADH**). The NADH concentration was fixed at 0.1 mM

and NAD$^+$ concentration was fixed at 1.0 mM as previously mentioned.
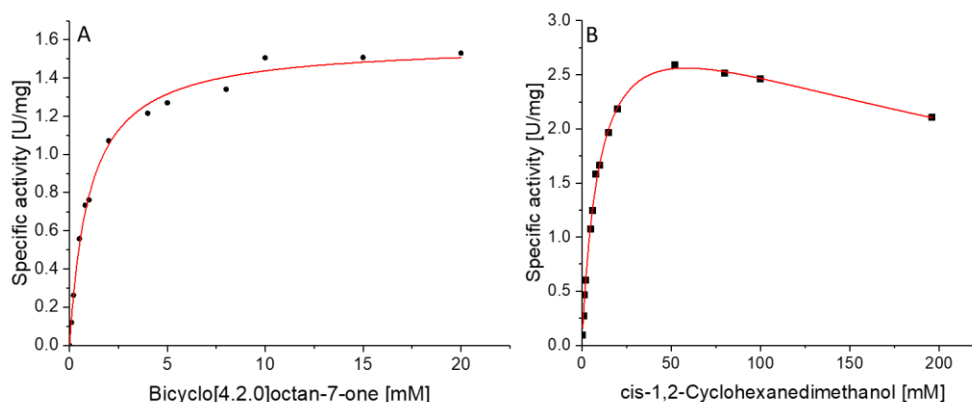
Figure 3.16. The kinetic assay of FMO-E towards bicyclo[4.2.0]octan-7-one (**A**) and HLADH towards cis-1,2-cyclohexanedimethanol (**B**) according to the Michaelis-Menten equation and Michaelis-Menten uncompetitive substrate inhibition equation. Reaction conditions: (A) c(bicyclo[4.2.0]octan-7-one) = 0–20 mM, c(NADH) = 0.1 mM, c(FMO-E) = 0.08 μM, 50 mM pH 7.0 Tris-HCl, 25°C, duplicate measurements; (B) c(cis-1,2-cyclohexanedimethanol) = 0–200 mM, c(NAD$^+$) = 1.0 mM, c(HLADH) = 0.19 μM, 100 mM pH 8.0 Tris-HCl, 25°C, duplicate measurements. The fixed NADH and NAD$^+$ concentration ($\geq$ 5 times of K_M) was chosen based on the preliminary kinetic assay to determine the K_M value of NADH and NAD$^+$.

Both FMO-E and HLADH showed typical Michaelis-Menten behavior towards their substrates (**Figure 3.16**). The K_M and k_{cat} values of FMO-E towards bicyclo[4.2.0]octan-7-one (1.0 mM and 1.7 s^{-1}) were also found to be in the same range with the BVMO standard substrate bicyclo[3.2.0]hept-2-en-6-one (2.4 mM and 2.0 s^{-1}). These data also confirmed the substrate specificity of FMO-E towards (fused) cyclobutanones. HLADH showed similar range of K_M and k_{cat} values (10.4 mM and 2.2 s^{-1}) towards cis-1,2-cyclohexanedimethanol with that of FMO-E towards bicyclo[4.2.0]octan-7-one (**Table 3.8**). But HLADH also showed some extent of substrate inhibition towards cis-1,2-cyclohexanedimethanol with a relatively high K_i value of 326 mM. As it was mentioned before, the kinetic assay of HLADH towards cis-1,2-cyclohexanedimethanol might only represent the step of diol to hydroxy aldehyde with UV assay method.

Table 3.8. Kinetic parameters of FMO-E towards bicyclo[4.2.0]octan-7-one and HLADH towards cis-1,2-cyclohexanedimethanol.

Substrate	v_{max} [U/mg]	K_M [mM]	k_{cat} [s^{-1}]	K_i [mM]
bicyclo[4.2.0]octan-7-one	1.6 ± 0.02	1.0 ± 0.1	1.7	-
cis-1,2-cyclohexanedimethanol	3.3 ± 0.02	10.4 ± 1.3	2.2	326 ± 78

3.1.3.2 Synthesis of chiral bicyclic lactones

In this FMO-E and HLADH coupled convergent cascade reaction, the ratio of normal lactone (N) to abnormal lactone (ABN) decreased from 3.3:1 at 5 h to 1.4:1 at 72 h (N: ABN) starting from 20 mM bicyclo[4.2.0]octan-7-one and 10 mM cis-1,2-cyclohexanedimethanol (**Figure 3.17 A**). The decrease of this ratio mainly resulted from the deactivation of FMO-E which resulted in less normal lactone formation catalyzed by FMO-E. In the case of applying FMO-E alone reported by Riebel et al., the ratio of normal lactone to abnormal lactone was determined as 19:1 (N:ABN)[93].
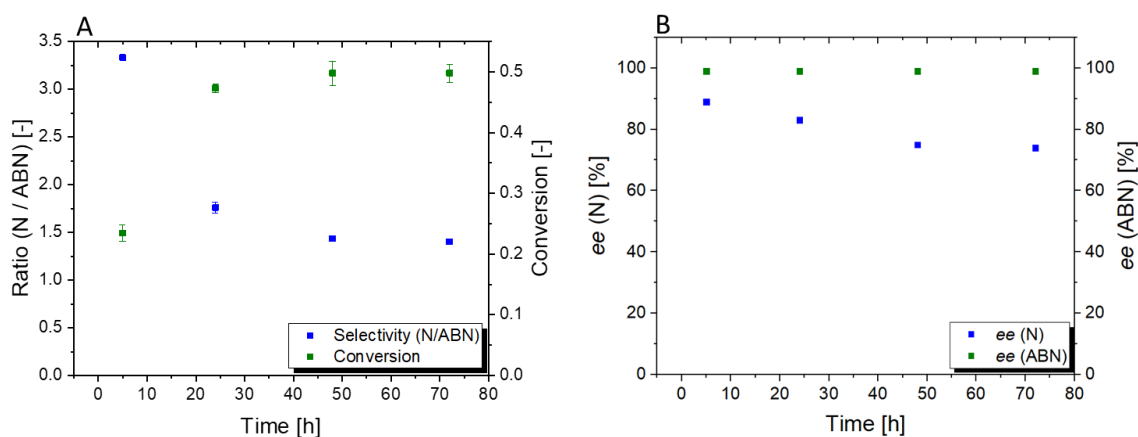
Figure 3.17. The process curve of ratio of normal lactone to abnormal lactone (A) and *ee* values of normal lactone and abnormal lactone (B) in this NADH-dependent convergent cascade employing FMO-E and HLADH with racemic bicyclo[4.2.0]octan-7-one and cis-1,2-cyclohexanedimethanol as substrates.

There was approximate 10 mM bicyclo[4.2.0]octan-7-one left after 72 h, while no cis-1,2-cyclohexanedimethanol could be detected after 48 h (**Figure 3.18**). The *ee* value of the normal lactone was found to be 89% (3a*S*, 7a*S*) at 5 h, which however decreased to 74% (3a*S*, 7a*S*) at 72 h with an analytical yield of 65% (**Figure 3.17 B**). This is because that the Baeyer-Villiger oxidation of bicyclo[4.2.0]octan-7-one catalyzed by FMO-E is a kinetic resolution reaction, which means the enantioselectivity will reduce along with the reaction process. This could be also demonstrated in the work of Riebel et al. that the *ee* value of the normal lactone was 39% (3a*S*, 7a*S*) with a conversion of 81%[93]. On the other hand, the *ee* value of abnormal lactone was kept at >99% (3a*R*, 7a*S*), which was the same with the configuration of the product of HLADH reported in the literature[73]. Hence, it showed that FMO-E and HLADH catalyzed the synthesis of the abnormal lactone with the same enantioselectivity.

In general, there two types of behaviors for BVMO-catalyzed Baeyer-Villiger oxidation of fused cyclobutanones. In the first type, the ratio of normal lactone to abnormal lactone is approximately 50:50 with high enantioselectivities for both lactones while the ratio is

approximately 80:20 (or 90:10) with high enantioselectivity for abnormal lactone and moderate to high *ee* values for normal lactones in the second type[85, 161-163]. Thus, the behavior of FMO-E belongs to the latter case.
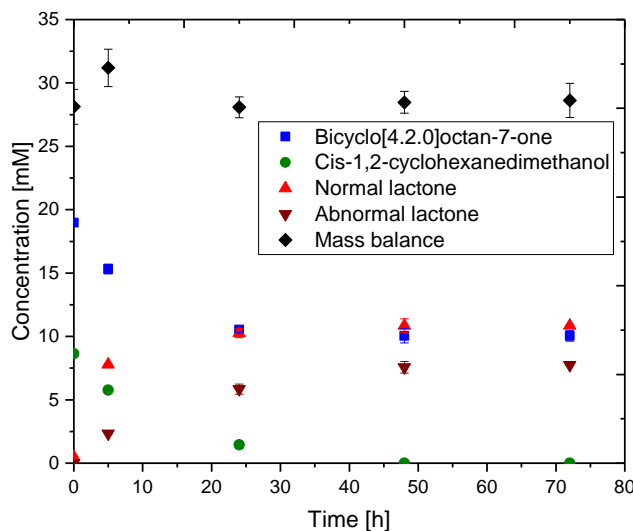
Figure 3.18. Conversion of bicyclo[4.2.0]octan-7-one (■) and cis-1,2-cyclohexanedimethanol (○) to normal lactone (▲) and abnormal lactone (▼). Reaction conditions: c(bicyclo[4.2.0]octan-7-one, 1c) = 20 mM, c(cis-1,2-cyclohexanedimethanol, 2b) = 10 mM, c(NAD$^+$) = 1 mM, c(FMO-E) = 1.0 U (16.6 μM), c(HLADH) = 1.0 U (7.3 μM), buffer: Tris-HCl (100 mM, pH 8.0), 180 rpm, T = 20℃. Reactions (1 mL in total) run in 1.5 mL glass-vials. Standard deviations = 1–7% (experiments performed in duplicates). Lines are only for visual guidance.

3.1.3.3   Interim summary

- The ratio of normal lactone to abnormal lactone in this convergent cascade decreased with the reaction because of the kinetic resolution of the racemic bicyclo[4.2.0]octan-7-one catalyzed by FMO-E and the abnormal lactone generated from the oxidation of cis-1,2-cyclohexanedimethanol catalyzed by HLADH.

- Racemic bicyclo[4.2.0]octan-7-one was converted to normal lactone with an *ee* value of 89–74% (3a*S*, 7a*S*) by FMO-E alone and the abnormal lactone with an *ee* value of >99% (3a*R*, 7a*S*) was synthesized by both FMO-E and HLADH.

3.2　　　Parallel cascade reactions for lactamization

Alcohol dehydrogenases (ADHs) have been widely used for the reduction of carbonyl groups and the oxidation of hydroxy groups[85, 133, 164-165]. Compared with their application in the reduction of prochiral ketones (generating chiral centers), ADH-catalyzed oxidation of alcohols is far less common (destroying chiral centers)[164]. Nevertheless, there are still many reports on the oxidation of diols to the corresponding lactones by ADHs or microorganisms since 1970s[68-69, 75, 155-156, 166-169]. Among these ADHs, horse liver alcohol dehydrogenase (HLADH) has demonstrated to be an effective catalyst in the stereospecific oxidation of only one of the enantiotopic hydroxy groups of acyclic and monocyclic meso-diols or the oxidation of only one selected hydroxy group in a polyhydroxylated molecule[68-69]. Thus, HLADH has been used to convert many diols to the corresponding lactones.

In the ADH-catalyzed lactonization of diols, one hydroxy group is oxidized into aldehyde group and form cyclic hemiacetal (lactol) with another unoxidized hydroxy group via tautermerisation[75, 167]. The lactol intermediates were occasionally observed via GC-MS analysis, but disappeared during the course of the reactions[75]. The lactols are further oxidized to the corresponding lactones by ADH (**Scheme 3.7 A**). ADH-catalyzed lactonization of diols inspires us to have the idea that if amino alcohols, the analogues of diols, can also be directly catalyzed by ADH to the corresponding lactams. To our best knowledge, there is no report on the ADH-catalyzed lactamization of amino alcohols so far. In analogy to ADH-catalyzed lactonization of diols, we propose the reaction mechanism of ADH-catalyzed lactamization of amino alcohols, thus the aldehyde group oxidized from one hydroxy group and the unoxidized hydroxy group form lactal which is further oxidized to the lactam (**Scheme 3.7 B**).
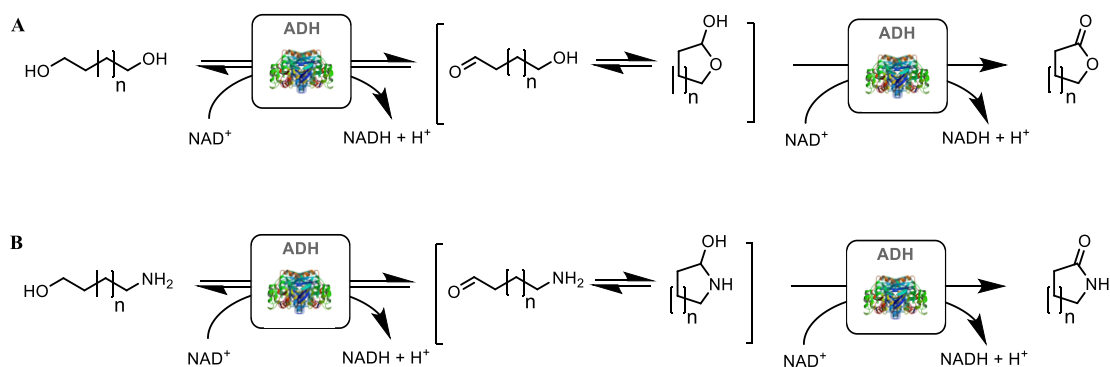
Scheme 3.7. ADH-catalyzed oxidative lactonization of diols (A) and lactamization of amino alcohols (B).

In consequence, three main objectives will be defined in this chapter. Screening of ADHs for the oxidation of amino alcohols is followed by the evaluation of HLADH-catalyzed oxidative lactamization of amino alcohols with stoichiometric amounts of NAD$^+$ using 4-amino-1-

butanol as the model substrate. Finally, HLADH-catalyzed oxidative lactamization of amino alcohols will be improved using only catalytic amounts of NAD^{+} by introducing NAD^{+} regeneration, and the substrate scope of this reaction will be also investigated.

3.2.1 Screening and characterization of ADHs for the oxidation of amino alcohols

3.2.1.1 Screening of ADHs for the oxidation of 4-amino-1-butanol

Though HLADH-catalyzed lactonization of diols is well documented, there are still some reports on other ADH or microorganisms as potential candidates to catalyze oxidation reactions[118, 168-169]. In a set of experiments, we evaluated the ADHs from horse liver (HLADH)[153], *Rhodococcus ruber* DSM 44541 (ADH-A)[170], *Thermus sp.* (TADH)[171] and *Thermoanaerobacter ethanolicus* (*TeS*ADH)[172] using 4-amino-1-butanol as the model substrate by spectrophotometric activity assay. In the spectrophotometric assay, all the evaluated ADHs showed activity in the oxidation of 4-amino-1-butanol (**Figure 3.19**).
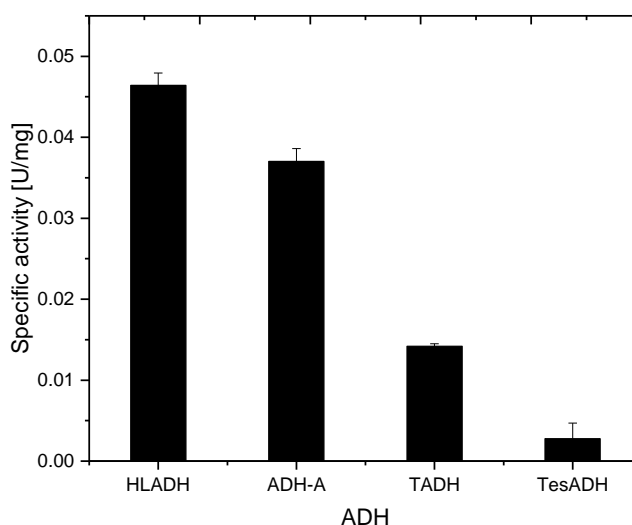
Figure 3.19. Screening of ADHs for the oxidation of 4-amino-1-butanol. Reaction conditions: c(4-amino-1-butanol) = 10 mM, c(NAD(P)[+]) = 1 mM, c(ADH) = 0.27 μM–8.75 μM, 50 mM pH 9.0 CHES buffer, 25°C, duplicate measurements. NADP^{+} was added for the reaction with *TeS*ADH.

Among these evaluated ADHs, HLADH showed the highest activity. However, it should be kept in mind that the activity assay via UV spectroscopy only covers the first step of the lactamization (ADH-catalyzed formation of aldehyde)[75, 118], i.e. not the real lactam formation. Nevertheless, HLADH was selected for the development of ADH-catalyzed lactamization of amino alcohols.

3.2.1.2 Biocatalytic characterization of HLADH

3.2.1.2.1 Effect of pH on the activity and stability of HLADH

Though HLADH is a well-documented enzyme[153], we still investigated the effect of pH on its activity and stability since pH can also influence the lactamization reactions. To display the effect of pH on the activity of HLADH, pH values are plotted against their corresponding relative activities and the result is shown in **Figure 3.20**. The maximum enzyme activity is characterized as 100% relative activity which corresponds to pH 9.0, 50 mM CHES buffer using 10 mM 4-amino-1-butanol as the substrate. The enzyme activity increased with the pH and started to decrease from pH 9.0. That indicates that the HLADH enzyme favors the alkaline environment ranging from pH 8.5 to 10.5. Above pH 10.5, the activity drastically decreases, indicating that a pH higher than 10.5 is not appropriate for the enzyme activity.
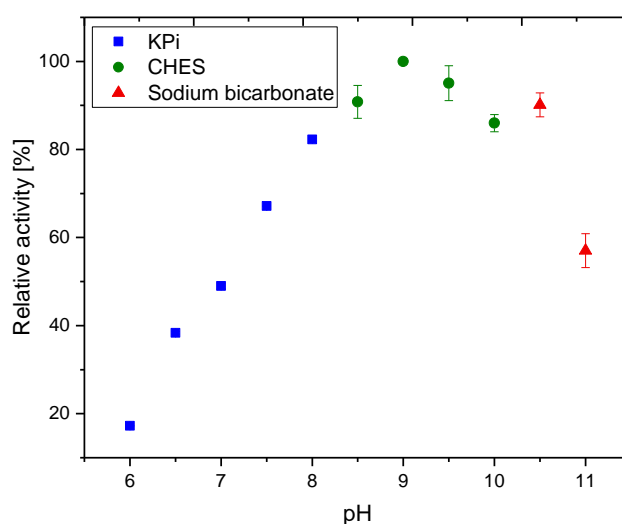
Figure 3.20. Effect of pH on the HLADH activity. Reaction conditions: reaction system (1.0 mL) contained 50 mM buffers with different pH values, 1.0 mM NAD$^+$, 10 mM 4-amino-1-butanol, and 0.43 µM enzyme at 25°C, duplicate measurements. The maximum relative activity of 100% was set to the value obtained at pH 9.0.

To study the effect of pH on the stability of HLADH, the enzyme was incubated for 24 h in different buffers (KP$_i$, CHES and sodium bicarbonate buffer) at 45°C. The results are depicted in the following **Figure 3.21**. After 24 h incubation at 45°C, HLADH in the buffer with pH of 6.5 (50 mM KP$_i$) had the highest residual activity with 84%. HLADH incubated in 50 mM sodium bicarbonate buffer with pH of 10.5 and 11 had the lowest residual activity less than 1%. Based on the results from pH activity analysis of HLADH (**Figure 3.20**), the enzyme activity decreased from pH 9, but there was still some activity (> 50%) to be seen in both pH 10.5 and 11.0. But in this experiment, the residual activity was less than 1% for pH 10.5 and 11.0. Thus,

the pH did affect the enzyme stability and resulted in the low activity of HLADH inside pH 10.5 and 11.0. HLADH is relatively stable from pH 6.0 to 9.0.
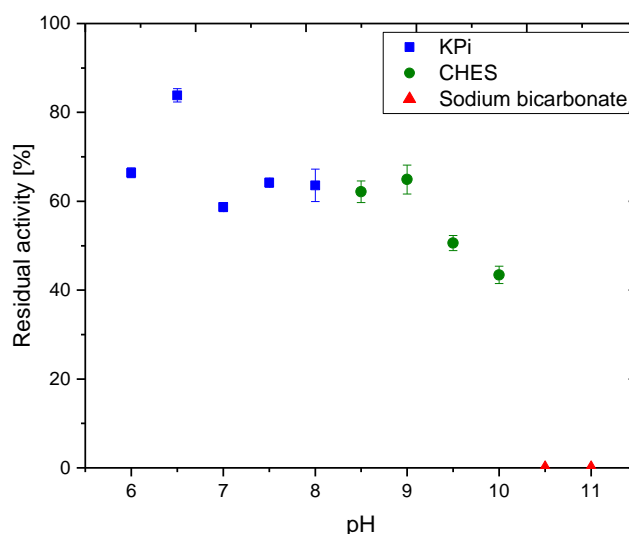
Figure 3.21. Effect of pH on the HLADH stability. 500 μL of 1.0 mg/mL (25 μM) enzyme solution in 50 mM buffer with different pH values was incubated at 45°C and the residual activity was measured with standard ADH activity assay using 10 mM 4-amino-1-butanol as substrate after 24 h, duplicate measurements. The maximum residual activity of 100% was determined for each individual reaction before the incubation.

3.2.1.2.2 Determination of HLADH steady-state kinetic parameters

Next, the substrate scope of HLADH-catalyzed amino alcohols oxidation was explored by UV assay. Two further aliphatic amino alcohols (5-amino-1-pentanol and 6-amino-1-hexanol) and two aromatic amino alcohols ((2-(2-aminoethyl)phenyl)-methanol and (2-(aminomethyl)phenyl) methanol) were evaluated. All aliphatic amino alcohols showed significant UV oxidation activity with HLADH, while no activity was observed for the two evaluated aromatic amino alcohols (data not shown). A further kinetic analysis of the three aliphatic substrates was performed with HLADH by UV assay. The kinetic analysis was done by purified HLADH *via* Ni-NTA affinity chromatography (**Figure 3A**).

The investigation of enzymatic reaction kinetics is essential for the process development and optimization. At a high substrate concentration, there is often an inhibition caused by the substrate itself and can be seen from the form of the graph (Michaelis-Menten graph) that rises with the substrate concentration and then sinks until zero or near a specific value asymptotically. This is caused by substrate that not only binds to the active site of the enzyme but also binds to the non-active site (allosteric) and resulted to the reduction of the production rate[173].

HLADH is one well-known enzyme that catalyzes the reversible oxidation of a wide range of alcohols to aldehydes or ketones. This kind of reaction obeys the Theorell-Chance reaction

mechanism, i.e. the enzyme firstly binds the coenzyme NAD^+ before binding the substrate and the product is released prior to the reduced coenzyme NADH upon oxidation of the alcohols[174-175]. However, many alcohols at the concentrations above K_M are HLADH inhibitors[176-178]. At high concentrations, alcohols act as inhibitors that bind the HLADH-NAD^+ complex, thus leading to an inactive enzyme form.
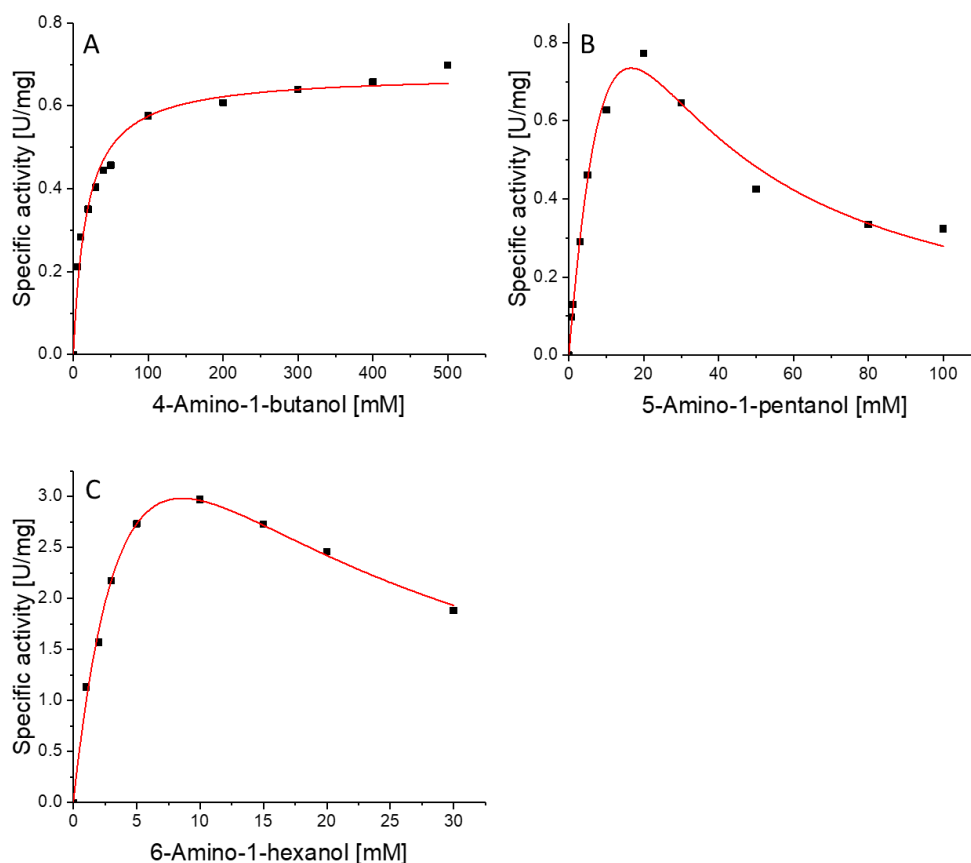
Figure 3.22. The steady-state kinetic assay of HLADH towards 4-amino-1-butanol (A), 5-amino-1-pentanol (B) and 6-amino-1-hexanol (C) according to the Michaelis-Menten equation. Reaction conditions: (A) c(4-amino-1-butanol) = 0–500 mM, c(NAD^+) = 1.0 mM, c(HLADH) = 0.44 μM, 50 mM CHES (pH 9.0), 25°C, duplicate measurements; (B) c(5-amino-1-pentanol) = 0–100 mM, c(NAD^+) = 10.0 mM, c(HLADH) = 0.85 μM, 50 mM CHES (pH 9.0), 25°C, duplicate measurements; (C) c(6-amino-1-hexanol) = 0–30 mM, c(NAD^+) = 10.0 mM, c(HLADH) = 0.85 μM, 50 mM CHES (pH 9.0), 25°C, duplicate measurements. The fixed NAD^+ concentration ($\geq$ 5 times of K_M) was chosen based on the preliminary kinetic assay to determine the K_M value of NAD^+.

Surprisingly, no substrate inhibition was observed up to 500 mM 4-amino-1-butanol while there was significant substrate inhibition in the case of 1,4-butanediol[75] and many alcohols are the inhibitors of HLADH at high concentrations[119, 179]. The non-linear fitting and parameters estimations were conducted using Originlab Pro 2017 based on Michaelis-Menten equation without inhibition (**Equation 3.4**). The v_{max} and K_M values of HLADH with 4-amino-1-butanol

as the substrate were 0.68 ± 0.02 U/mg and 17.8 ± 2.2 mM, respectively (**Table 3.9**). In contrast to 4-amino-1-butanol, kinetics of HLADH towards 5-amino-1-pentanol and 6-amino-1-hexanol showed an uncompetitive inhibition by the substrate. The inhibition started to appear at around 20 mM with 5-amino-1-pentanol and around 10 mM with 6-amino-1-hexanol (**Figure 3.22**). The non-linear fitting and parameters estimations were calculated using Originlab Pro 2017 based on Michaelis-Menten equation with uncompetitive substrate inhibition (**Equation 3.5**). v_{max}, K_M and K_i values for 5-amino-1-pentanol were 3.35 ± 1.57 U/mg, 29.6 ± 16.9 mM and 9.33 ± 5.30 mM and for 6-amino-1-hexanol were 7.64 ± 1.18 U/mg, 6.71 ± 1.48 mM and 11.0 ± 2.63 mM, respectively (**Table 3.9**). These results show that HLADH has higher affinity towards 5-amino-1-pentaol and 6-amino-1-henxanol. But on the other hand, the two substrates would cause also inhibition easily.

$$v = \frac{v_{max} \cdot c_{sub}}{K_M + c_{sub}} \qquad\qquad \textbf{Equation 3.4}$$

$$v = \frac{v_{max} \cdot c_{sub}}{K_M + c_{sub} \cdot (1 + \frac{c_{sub}}{K_{i,sub}})} \qquad\qquad \textbf{Equation 3.5}$$

Table 3.9. Kinetic parameters of HLADH towards amino alcohols.

Substrate	v_{max} [U/mg]	K_M [mM]	K_i [mM]	K_i / K_M [-]
4-amino-1-butanol[a]	0.82 ± 0.07	34.9 ± 10.4	-	-
4-amino-1-butanol[b]	0.68 ± 0.02	17.8 ± 2.2	-	-
4-amino-1-butanol[c]	0.73 ± 0.01	3.77 ± 0.30	-	-
5-amino-1-pentanol	3.35 ± 1.57	29.6 ± 16.9	9.33 ± 5.30	0.32
6-amino-1-hexanol	7.64 ± 1.18	6.71 ± 1.48	11.0 ± 2.63	1.64

[a] pH 7.0 [b] pH 9.0 [c] pH 11.0

Not like the common sense that pH has significant effect on the activity of enzyme is well studied, the effect of pH on the affinity is far less far explored. This assumption, is supported by the rather low affinity of HLADH towards 4-amino-1-butanol at lower pH values (**Figure 3.23**). The kinetic assay done at pH 7.0 revealed a K_M value for the amino alcohol as 34.9 mM, whereas that of at pH 11.0 was 3.77 mM (**Table 3.9**). These results indicate that the affinity of HLADH towards substrate increases with the pH. The effect of pH on enzyme affinity was also documented in the literature[175, 180].
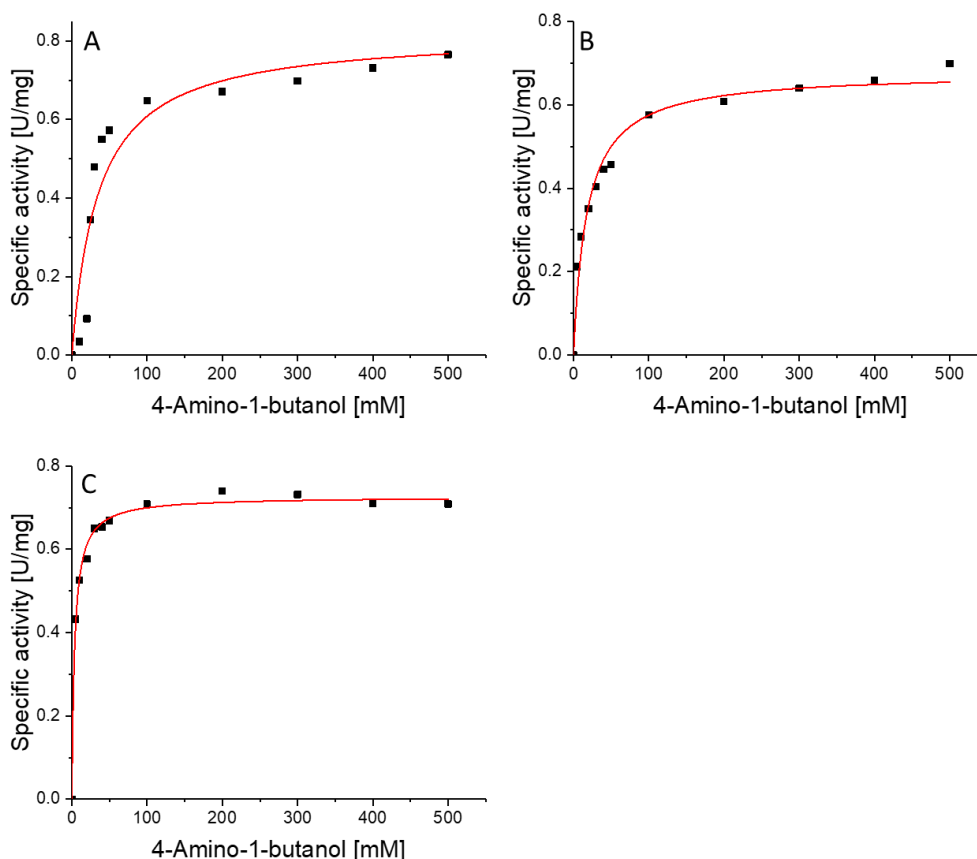
Figure 3.23. The steady-state kinetic assay of HLADH towards 4-amino-1-butanol at pH 7.0 (A), pH 9.0 (B) and pH 11.0 (C) according to the Michaelis-Menten equation. Reaction conditions: c(4-amino-1-butanol) = 0–500 mM, c(NAD$^+$) = 1.0 mM, c(HLADH) = 0.44 μM, 50 mM pH 7.0 KP$_i$ (A), 50 mM pH 9.0 CHES (B), 50 mM pH 11.0 sodium bicarbonate (C), 25°C, duplicate measurements; The fixed NAD$^+$ concentration ($\geq$ 5 times of K_M) was chosen based on the preliminary kinetic assay to determine the K_M value of NAD$^+$.

3.2.1.3   Interim summary

- HLADH was selected as the biocatalyst for further research among the four evaluated ADHs.

- The optimal pH of HLADH is pH 9.0 and it is relatively stable from pH 6.0 to 9.0.

- Steady-state kinetic investigation revealed that there was no substrate inhibition with 4-amino-1-butanol up to 500 mM while the substrate inhibition was observed from approximate 20 mM with 5-amino-1-pentanol and from approximate 10 mM with 6-amino-1-hexanol for HLADH.

3.2.2 Evaluation of HLADH-catalyzed oxidative lactamization of 4-amino-1-butanol

In the sub-chapter 3.2.1, spectrophotometric activity assay was applied for the screening of AHDs. As it was aforementioned that this method might only cover the first step of lactamization (ADH-catalyzed formation of aldehyde). Thus, it is important to perform reactions to confirm the real lactam formation after HLADH was selected as the target biocatalyst (**Scheme 3.7B**). Generally speaking, there are many factors, such as pH, buffer type, temperature, substrate concentration, cofactor concentration, enzyme loading that have influence on the enzymatic reactions. For the proof of concept study, we fixed the temperature (25°C), substrate concentration (10 mM) and enzyme loading (0.1 mg/mL) as a rule of thumb and evaluated other two important parameters: pH and ionic strength of buffer.

3.2.2.1 Effect of pH on the lactamization

We suspected the pH of the reaction mixture having a significant effect on the performance of the enzymatic oxidative lactamization reaction. First, like any other enzymatic reactions, the HLADH-catalyzed oxidation is pH-dependent. Second, the intramolecular ring-closure necessitates deprotonated amines to function as nucleophile. Therefore, we performed a range of HLADH-catalyzed oxidations of model substrate 4-amino-1-butanol and analyzed the reaction mixtures for their content in the desired γ-lactam.

The oxidized nicotinamide cofactors (NAD^+) is essential for the HLADH-catalyzed oxidation of alcohols. To circumvent the limitation of NAD^+, stoichiometric amounts of NAD^+ (20 mM, one step reaction consumes one equivalent of NAD^+) was added in the system. The HLADH kinetic analysis towards NAD^+ showed that there was no inhibition up to 20 mM (**Figure 3.24**). Therefore, the influence of NAD^+ can be excluded when evaluating the effect of pH on the lactam formation with stoichiometric amounts of NAD^+.
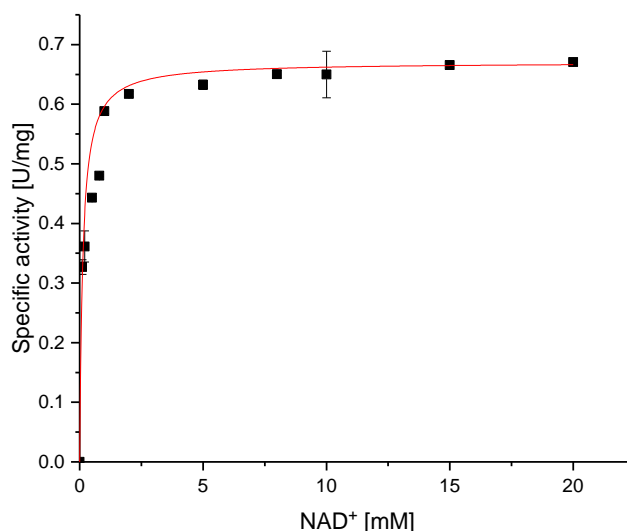
Figure 3.24. The kinetic assay of HLADH towards NAD^+ using 4-amino-1-butanol as the substrate according to the Michaelis-Menten equation. Reaction conditions: c(4-amino-1-butanol) = 100 mM, $c(NAD^+)$ = 0–20 mM, c(HLADH) = 0.5 μM, 50 mM pH 9.0 CHES buffer, 25°C, duplicate measurements. The fixed 4-amino-1-butanol concentration ($\geq$ 5 times of K_M) was chosen based on the previous kinetic assay to determine the K_M value of 4-amino-1-butanol (17.8 ± 2.2).

Indeed, the yield of γ-lactam steadily increased with increasing pH at least up to pH 11. Based on our previous experiments, HLADH exhibited the highest activity in oxidative direction whereas it steadily increased with increasing pH up to pH 9.0 (**Figure 3.20**). Hence, the still increasing productivity at elevated pH values may most likely be attributed to the increasing non-protonation state of the amine (R-NH_2) (**Figure 3.25**), which is reasonable considering that the intramolecular ring-formation necessitates the nucleophilic, non-protonated amine functionality. The plot of ratio of NH_2 to NH_3^+ against pH was determined by Henderson–Hasselbalch equation (**Equation 3.6**).

$$\text{pH} = \text{p}K_a + \log(\frac{c(NH_2)}{c(NH_3^+)})$$
Equation 3.6
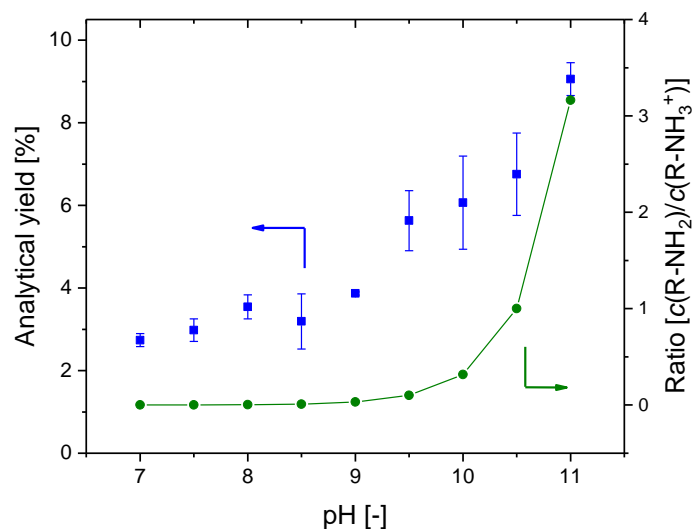
Figure 3.25. The effect of pH on the lactam formation (blue squares) with stoichiometric amounts of NAD$^+$ and the ratio of NH$_2$ to NH$_3^+$ (oliver circles) based on the pH. Reaction conditions: c(4-amino-1-butanol) = 10 mM, c(NAD$^+$) = 20 mM, c(HLADH) = 0.1 mg/mL (0.01 U/mL, 2.5 μM), buffer: KP$_i$ (50 mM, pH 7.0–8.0), CHES (50 mM, pH 8.5–10.0), sodium bicarbonate (50 mM, pH 10.5–11.0), 900 rpm, 25°C and 24 h. Duplicate reactions (1 mL in total) run in 1.5 mL glass-vials. The pK_a value of R-NH$_2$ and R-NH$_4^+$ was chosen as 10.5 as an average value for primary amine/ammonium ion.

Additionally, the protonation state may also affect the kinetic characteristics of the enzyme with the amino alcohol. This assumption, is supported by the rather low affinity of HLADH towards 4-amino-1-butanol at lower pH values (**Figure 3.23**). The kinetic assay done at pH 7.0 revealed a K_M value for 4-amino-1-butanol as 34.9 mM, whereas that of at pH 11.0 was 3.8 mM (**Table 3.8**).

However, the analytical yield of the lactam formation was less than 10% for all pH values even with stoichiometric amounts of NAD$^+$ (**Figure 3.25**). The low yield should be the issue of thermodynamics, since HLADH-catalyzed oxidation of alcohols is thermodynamically unfavorable and the reaction is reversible[179]. Therefore, the lactam yield could be increased by addressing the thermodynamics problem in principle.

3.2.2.2   Effect of ionic strength on the lactamization

Besides the pH of buffer, ionic strength can also significantly affect the thermodynamic feasibility of a particular reaction direction. Moreover, amino acid residues, which undergo protonation-deprotonation reactions, are involved in binding of substrates and conversion to products. CHES (pH 9.5) buffer was selected as the model buffer to evaluate the effect of buffer concentration on the lactam formation as there was a lactam yield jump from pH 9.0 to 9.5 (**Figure 3.25**). The evaluation was based on 10 mM 4-amino-1-butanol using stoichiometric amounts of cofactor in CHES buffer (pH 9.5) with different ionic strengths from 10 mM to

1000 mM. The highest lactam yield was found in CHES buffer with ionic strength of 250 mM in which the yield is 1.8 times of that in CHES buffer with ionic strength of 50 mM (**Figure 3.26**). There was no lactam detected in CHES buffer with ionic strength of 10 mM indicating the importance of buffer for enzymatic reaction.
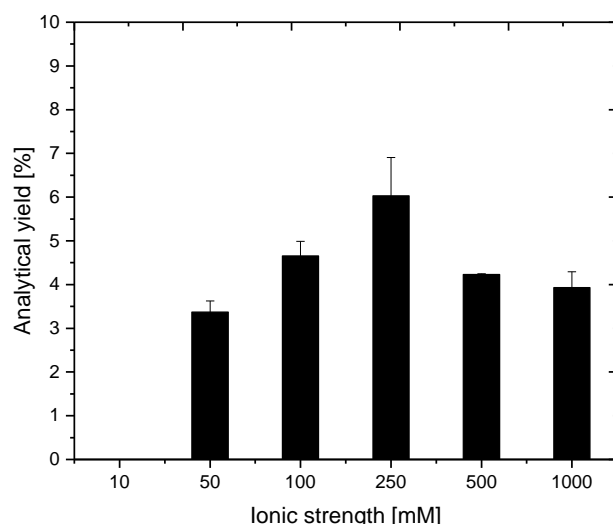
Figure 3.26. The effect of ionic strength on the lactam formation using stoichiometric amounts of NAD^+. Reaction conditions: c(4-amino-1-butanol) = 10 mM, $c(NAD^+)$ = 20 mM, c(HLADH) = 0.1 mg/mL (0.01 U/mL, 2.5 µM), pH 9.5 CHES (10–1000 mM), 900 rpm, 25°C, and 24 h. Duplicate reactions (1 mL in total) run in 1.5 mL glass-vials.

3.2.2.3   Interim summary

- The lactam yield increased with increasing pH mainly because the high pH increased non-protonation state of the amine ($R-NH_2$), which facilitated intramolecular ring-formation of the intermediate.

- The HLADH-catalyzed lactamization of 4-amino-1-butanol with stoichiometric NAD^+ showed the highest yield in the CHES buffer with ionic strength of 250 mM.

- The HLADH-catalyzed lactamization product yield of 4-amino-1-butanol with stoichiometric NAD^+ was quite low (< 10%) because of the thermodynamic limitation.

3.2.3   Improvement of HLADH-catalyzed oxidative lactamization of amino alcohols

So far, stoichiometric amounts of NAD^+ were used to evaluate the effect of pH and ionic strength on the HLADH-catalyzed lactamization of 4-amino-1-butanol. However, this obviously is not desirable from an economic point of view since NAD^+ is quite expensive[181]. Moreover, the lactam yield was less than 10% under the optimized pH and ionic strength conditions. In this point of view, it was still quite interesting to employ one NAD^+ regeneration system in the reaction not only for the economical NAD^+ regeneration but also for driving the

equilibrium to the lactam formation direction.

3.2.3.1 Regeneration of NAD⁺

In cofactor dependent enzymatic reduction reactions, the reduced nicotinamide cofactor (NAD(P)H) can be regenerate using enzymes like formate dehydrogenase (FDH) or glucose dehydrogenase (GDH). Particularly FDH has been widely used in the industry for the reduced cofactor regeneration[182]. In contrast, so far enzymes for the oxidized nicotinamide cofactor (NAD(P)⁺) are less explored. The enzymatic can be either substrate coupled or enzyme coupled. The substrate coupled cofactor regeneration methods normally suffer from some in principle drawbacks. Due to the low thermodynamic driving force, large molar surpluses of the co-substrate have to be applied in the system to shift the equilibrium to the product direction[183]. However, most enzymes are not stable in such conditions. Moreover, the surpluses of co-substrate would lead to significant waste which impairs the atom efficiency of the reactions. The common enzymatic NAD(P)⁺ regeneration methods are summarized in **Table 3.10**[183].

Table 3.10. Common enzymatic NAD(P)⁺ regeneration methods.

Enzyme	Co-substrate/Co-product	Waste[e]
GluDH[a]	α-ketoglutarate/glutamate	146
LDH[b]	pyruvate/lactate	90
ADH[c]	acetone/2-propanol	58
NOX1 or NOX2[d]	oxygen/H_2O (or H_2O_2)	18 (or 34)

[a] Glutamate dehydrogenase [b] Lactate dehydrogenase [c] Alcohol dehydrogenase [d] NADH oxidase [d] Product mass per mole NAD(P)⁺ regenerated

NAD(P)H oxidase (NOX) is one interesting enzyme class for the oxidized nicotinamide cofactor regeneration due to its some intrinsic advantages, namely enabling the use of molecular oxygen as the co-substrate and generating H_2O or H_2O_2 as the by-product, thus generating few organic waste chemicals in the reaction system which simplifies the downstream process[184]. Moreover, the high redox potential of oxygen is also a high thermodynamic driving force for the coupled reactions. Normally, H_2O forming NOX is prior to H_2O_2 forming NOX as the H_2O_2 will cause enzyme deactivation. In this study, a H_2O forming NADH oxidase variant V193R/V194H from *Streptococcus mutans* (*Sm*NOX) was selected as it had been proved to be a highly active and relatively stable enzyme, which could be expressed in *Escherichia coli* and is not dependent on FADH or DTT addition[185-187].

3.2.3.2 Biocatalytic characterization of *Sm*NOX

H_2O forming NADH oxidase from *Streptococcus mutans* (*Sm*NOX) was identified by Higuchi and his co-workers in 1993[185]. It is a monomer oxidase containing one molar FAD per monomer with a molecular weight of 50 kDa and its activity is independent of additional FAD. Later it was cloned and expressed in *Escherichia coli* to study its molecular properties by Higuchi and his co-workers in 1996[186]. *Sm*NOX is a strictly NADH-dependent oxidase, which means it can only oxidize NAD^+. The cofactor specificity of *Sm*NOX was engineered by Glieder and his co-workers in 2014 with two mutations (V193R/V194H) to show high activity for both NAD^+ and $NADP^+$[187]. This variant will be characterized and applied for the NAD^+ regeneration.

3.2.3.2.1 Purification of *Sm*NOX

Expression of *Sm*NOX was carried out in *E. coli* BL21 (DE3) and purified by Ni-NTA affinity chromatography method. The purification table for *Sm*NOX is shown in **Table 3.11**, with a corresponding SDS-PAGE in **Figure 3.27** which shows the purified *Sm*NOX band with an approximate 50 kDa molecular weight. The purification process had a high enzyme yield of 31.4 mg/g wet cell.
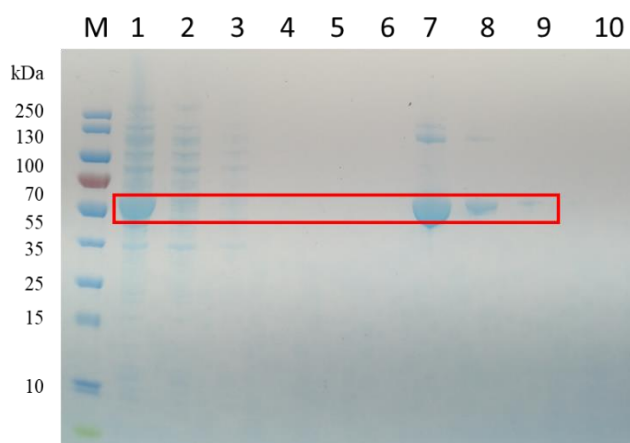
Figure 3.27. SDS-PAGE analysis of different fractions taken during the purification of *Sm*NOX (50 kDa). Lane 1: cell free extract; lane 2: flow through; Lane M: PageRuler Prestained Protein Ladder (Thermo Fisher); lane 3-6: washing fractions; lane 7-11: elution fractions.

Table 3.11. Summary of *Sm*NOX purification steps.

Purification steps[a]	V [mL]	Protein [mg]	Specificity activity[b] [U/mg]	Total activity [U]	Purification factor [-]	Yield [%]
CFE	10	165	3.2	524	-	100
UF	3.8	62.7	3.6	226	1.13	43.1

[a] CFE: Cell free extract, UF: Ultrafiltration

[b] General NOX activity assay with 0.1 mM NADH as substrate

3.2.3.2.2 Effect of pH on the activity and stability of *Sm*NOX

*Sm*NOX activity profile with respect to pH was measured with purified enzyme. The optimum pH of activity was found at pH 7.0 (50 mM KP$_i$), which is consistent with the data of literature[185]. Below pH 7.0, activity decreased slowly and still had 73% activity left. At pH values above 7.0, *Sm*NOX activity fell off constantly before almost reached zero at pH 11.0 (**Figure 3.28**).
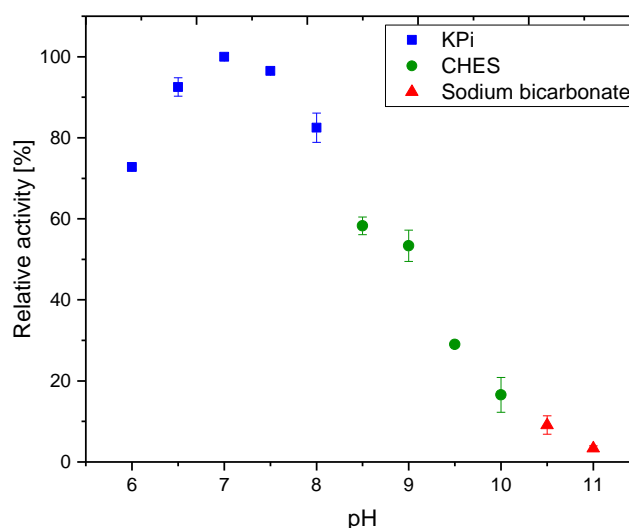
Figure 3.28. Effect of pH on *Sm*NOX activity. Reaction conditions: reaction system (1.0 mL) contained 50 mM buffers with different pH, 0.1 mM NADH, and 0.17 µM enzyme solution at 25℃, duplicate measurements. The maximum relative activity of 100% was set to the value obtained at pH 7.0.

To study the effect of pH on the stability of *Sm*NOX, it was incubated in different buffers with pH from 6.0 to 11.0 at 25℃ for 24 h. The results are depicted on the bellow **Figure 3.29**. After 24 h incubation at 25℃, *Sm*NOX inside pH 10.0 (50 mM CHES) had the highest residual activity with 75% activity left. *Sm*NOX was relatively stable from pH 6.0 to 10.0, but it was unstable in alkaline condition (pH > 10.0).
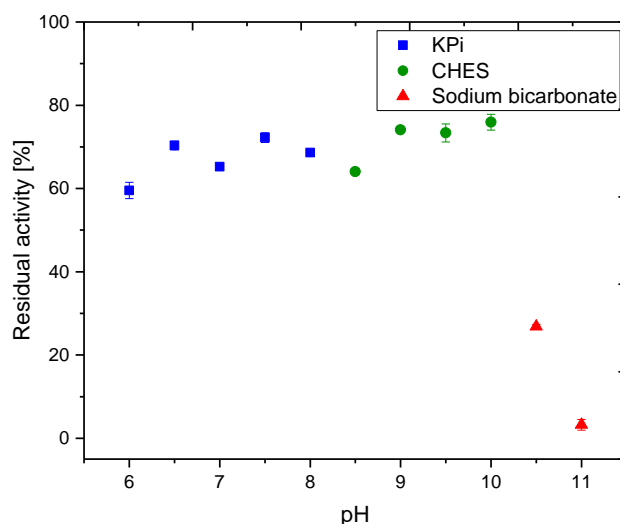
Figure 3.29. Effect of pH on *Sm*NOX stability. 500 μL of 1.0 mg/mL (25 μM) enzyme solutions in 50 mM buffers with different pH were incubated at 25°C and the residual activities were measured after 24 h, duplicate measurements. The maximum residual activity of 100% was determined for each individual reaction before the incubation.

3.2.3.2.3 Effect of temperature on *Sm*NOX long-term stability

The stability of *Sm*NOX was analyzed by incubating purified enzyme in 50 mM KP_i buffer (pH 7.0) at 25°C, 40°C and 50°C for varied period of time and the residual activity was measured (**Figure 3.30**). *Sm*NOX was relatively stable at 25°C and 40°C, but labile at 50°C, giving half-life times of 33 h, 5.6 h and 0.2 h, respectively (**Table 3.12**). Based on the results, the further HLADH-*Sm*NOX coupled cascade reactions would be performed at 25°C.
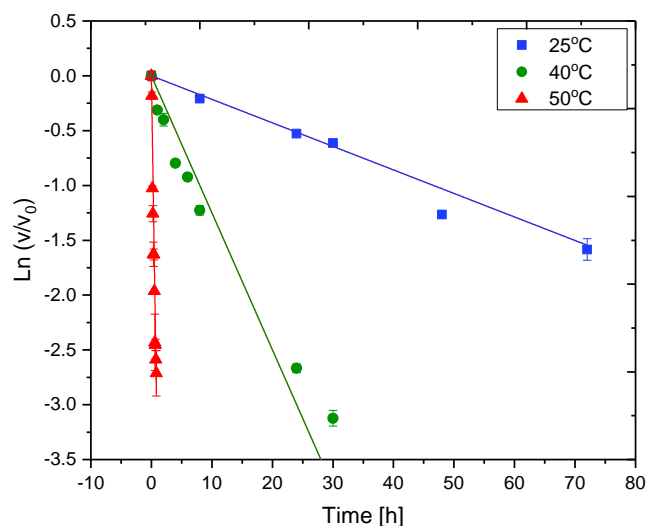
Figure 3.30. Long-term stability analysis for the determination of the half-life times of *Sm*NOX at 25°C, 40°C, and 50°C. 500 μL of 1.0 mg/mL (25 μM) enzyme solutions in 50 mM KP_i buffer (pH 7.0) were incubated at 25°C, 40°C, and 50°C and the residual activities were measured after 24 h, duplicate measurements.

Table 3.12. Summary of half-life times of *Sm*NOX at 25°C, 45°C and 50°C.

T [°C]	k_{des} [h^{-1}]	$\tau_{1/2}$ [h]
25	0.021	33
40	0.125	5.6
50	3.479	0.2

3.2.3.3 HLADH-catalyzed oxidative lactamization of amino alcohols with NAD$^+$ regeneration

As mentioned before, the application of NAD$^+$ regeneration system may shift the equilibrium of the reaction to the lactam formation side. To validate this hypothesis, HLADH-catalyzed oxidative reactions of 4-amino-1-butanol with and without *Sm*NOX-catalyzed NAD$^+$ regeneration were compared. Under identical conditions, HLADH-catalyzed oxidation of 4-amino-1-butanol with catalytic amounts of NAD$^+$ (5 mol-%) and *in situ* NAD$^+$ regeneration promoted by *Sm*NOX excelled over the reaction using stoichiometric NAD$^+$ by more than doubled yield of γ-lactam (**Figure 3.31**). Hence, we concluded that the usage of cofactor regeneration system (by employing *Sm*NOX enzyme) had a great potential to improve the lactam formation. However, the lactam yield was still far away from the satisfied level, which necessitates further optimization.
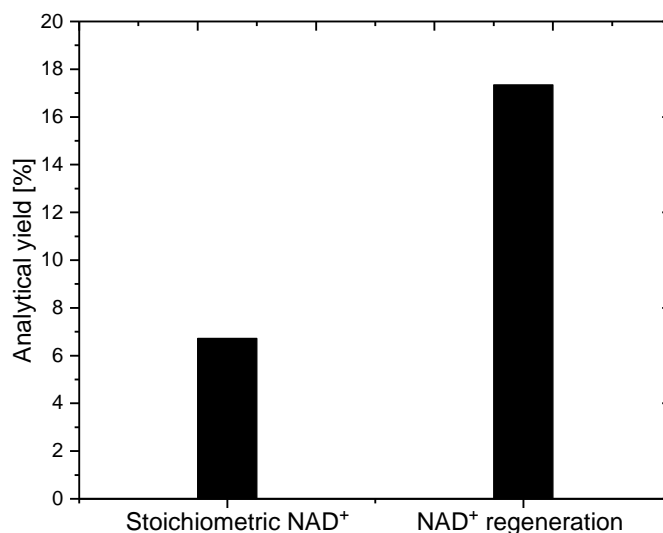
Figure 3.31. Comparison of lactam formation with stoichiometric amount of NAD$^+$ and with NAD$^+$ regeneration. Stoichiometric NAD$^+$: c(4-amino-1-butanol) = 10 mM, c(NAD$^+$) = 20 mM, c(HLADH) = 0.1 mg/mL (0.006 U/mL, 2.5 μM), 250 mM CHES (pH 9.5), and 900 rpm, 25°C, 24 h; *In situ* NAD$^+$ regeneration: c(4-amino-1-butanol) = 10 mM, c(NAD$^+$) = 1.0 mM, c(HLADH) = 0.1 mg/mL (0.006 U/mL, 2.5 μM), c(*Sm*NOX) = 0.5 mg/mL (10 μM), 250 mM CHES (pH 9.5), 900 rpm, 25°C, and 24 h. One reaction (1 mL in total) run in 1.5 mL glass-vials.

The bi-enzymatic parallel cascade system described here is influenced by several parameters, such as temperature (T), O$_2$ amount (the headspace ratio = (Headspace volume (mL)/(Volume

of the reaction mixture (mL)), pH, substrate concentration (c(4-amino-1-butanol)), HLADH concentration (c(HLADH)), SmNOX concentration (c(SmNOX)), NAD^+ concentration (c(NAD^+)) and reaction time (t). Each of these parameters can directly and interactively influence the final product yield. To identify the key parameters, a Design of Experiment (DoE) approach was applied to investigate detailed analysis of interactions between the various reaction parameters. For screening purposes, the above mentioned eight reaction parameters were evaluated for their impacts on the target response (i.e. product yield) and three parameters (pH, c(HLADH), and c(NAD^+)) were identified as the vital ones. Temperature was set up at 20°C since SmNOX was unstable at elevated temperature and substrate concentration was fixed at 10 mM. 1.5 mM GC vial was chosen as the reactor. From the economic point of view, NAD^+ concentration was used in catalytic amount level (1 mM). To ensure sufficient NAD^+ regeneration and compensate the relatively poor stability of SmNOX compared with HLADH, approximate 100-fold activity excess of SmNOX was applied in the system. The reaction was carried out for 24 hours as longer reaction time could result in the product hydrolysis.

As discussed in chapter 3.2.2, pH had significant effect on the lactam formation by influencing the oxidation of alcohols and the intramolecular ring-closure. Thus, pH should be revaluated as SmNOX was introduced into the system. Based on the previous results, a series of buffers with ionic strength of 250 mM from pH 7.0 to 11.0 were selected as the reaction media. The bi-enzymatic reaction exhibited a broad range between pH 8.0 and 10.0 (**Figure 3.32**), which can be attributed to the compromise of HLADH and SmNOX pH profiles. Among these pHs, pH 8.0 KP_i buffer was chosen as the buffer for further ionic strength revaluation as the analytical yield of lactam was the highest (81%) in this buffer.
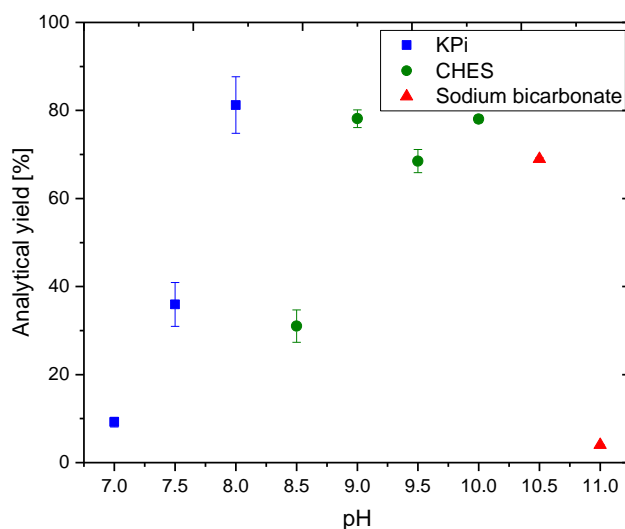
Figure 3.32. The effect of pH on the lactam formation of reaction with *in situ* NAD$^+$ regeneration. Reaction conditions: c(4-amino-1-butanol) = 10 mM, c(NAD$^+$) = 1 mM, c(HLADH) = 1.0 mg/mL (25 μM, 0.06 U/mL), c(*Sm*NOX) = 1.0 mg/mL (20 μM, 5.39 U/mL), buffer: KP$_i$ (250 mM, pH 7.0–8.0), CHES (250 mM, pH 8.5–10.0), sodium bicarbonate (250 mM, pH 10.5–11.0), 900 rpm, 25°C, 24 h. Duplicate reactions (1 mL in total) run in 1.5 mL glass-vials.

The ionic strength of KP$_i$ at pH 8.0 was varied to find the optimal ionic strength for the lactamization reaction with cofactor regeneration (**Figure 3.33**). Interestingly, the analytical yield of lactam reached 95% at pH 8.0 KP$_i$ buffer with the ionic strength of 50 mM, which indicates that the pH and ionic strength of buffer have the interactive influence on the lactam formation. Therefore, the optimal buffer for the HLADH/*Sm*NOX-catalyzed oxidative lactamization of amino alcohols was 50 mM pH 8.0 KP$_i$ buffer.
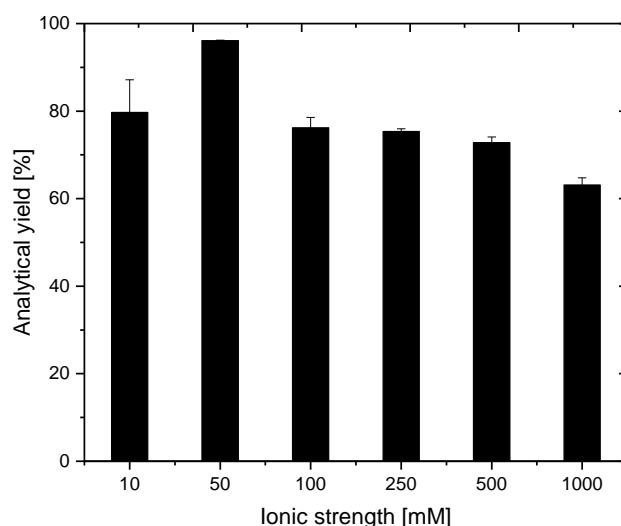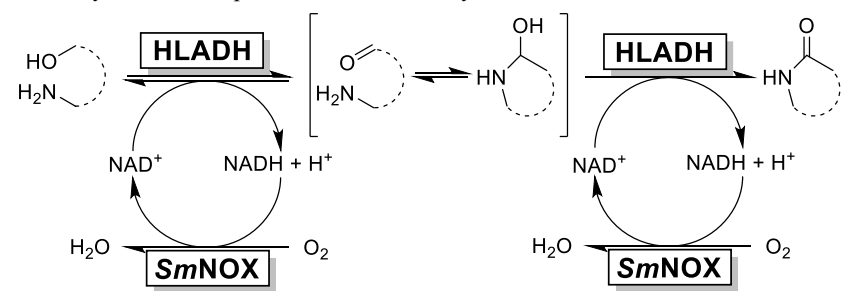
Figure 3.33. The effect of ionic strength on the lactam formation NAD$^+$ regeneration. Reaction conditions: c(4-amino-1-butanol) = 10 mM, c(NAD$^+$) = 1 mM, c(HLADH) = 1.0 mg/mL (25 µM, 0.06 U/mL), c(SmNOX) = 1.0 mg/mL (20 µM, 5.39 U/mL), pH 8.0 KP$_i$ (10–1000 mM), 900 rpm, 25°C, and 24 h. Duplicate reactions (1 mL in total) run in 1.5 mL glass-vials.

Next, the substrate scope of the oxidative lactamization system was explored within the identified conditions. Two further aliphatic amino alcohols (5-amino-1-pentanol and 6-amino-1-hexanol) and two aromatic amino alcohols ((2-(2-aminoethyl)phenyl)-methanol and (2-(aminomethyl)phenyl) methanol) were evaluated. While the two homologues of 4-amino-1-butanol were readily converted (albeit at lower rates, **Table 3.13**), the two aromatic amino alcohols were converted very slowly (**Figure 3.34**). The product yield decreased with the decreasing length of the aliphatic amino alcohol chain. As shown in **Table 3.13**, 5-amino-1-pentanol and 6-amino-1-hexanol were converted to the corresponding lactams with much less yield than 4-amino-1-butanol (95%), only resulting in 45% and 20% yield, respectively. The results are reasonable as formation of the five-membered ring of lactam is sterically more favored compared to six- and especially seven-membered rings[80]. The previous kinetic analysis of the three aliphatic substrates (**Figure 3.22**) revealed that the 'best substrate' i.e. 4-amino-1-butanol, which gave the highest yield was not most readily converted by HLADH. As shown in **Table 3.9**, both v_{max} and K_M for this substrate were less favourable as compared to the other two substrates. On the other hand, this substrate, in contrast to the others, did not exhibit any excess substrate inhibition. But as mentioned above, the UV activity assay might only cover the first reaction step, i.e., ADH-catalyzed oxidation of hydroxy group. The oxidation of the lactal intermediate or the competitive loss of water pathway could also be the limitation for the final lactam formation. Only trace amount (< 1% yield) of 1-isoindolinone could be found and no 3,4-dihydro-2H-isoquinolin-1-one was detected in the system.

Table 3.13. Preliminary substrate scope of the HLADH-catalyzed oxidative lactamization of amino alcohols[a].

Substrate		Product		Yield[b] [%]
4-Amino-1-butanol	(structure)	γ-butyrolactam	(structure)	95
5-Amino-1-pentanol	(structure)	δ-valerolactam	(structure)	34
6-Amino-1-hexanol	(structure)	ε-caprolactam	(structure)	15
(2-(2-aminoethyl)phenyl)-methanol	(structure)	1-isoindolinone	(structure)	< 1
(2-(aminomethyl)phenyl) methanol	(structure)	3,4-dihydro-2H-isoquinolin-1-one	(structure)	n.d.

[a] Conditions: 10 mM substrate, 1.0 mM NAD+, 1.0 mg/mL HLADH (25 μM), 1.0 mg/mL SmNOX (20 μM), 50 mM pH 8.0 KPi, 25°C, 900 rpm, 24 h.

[b] Analytical yield.

A typical time-course for the conversion of three aliphatic amino alcohols is given in **Figure 3.34**. The three reactions proceeded smoothly at the first 5 h and then slowed considerably. This figure shows that the equilibrium was almost reached within 5 hours for the three substrates. The slight decrease of δ-valerolactam and ε-caprolactam from 5 h to 24 h can to a large extent be the result of the undesired hydrolysis of products. Furthermore, evaluation of products hydrolysis in the reaction conditions (25°C, 900 rpm) revealed that these lactams really underwent hydrolysis, especially for δ–valerolactam (**Figure 3.36**). The turnover number (TON) value of HLADH (mol_{lactam}/mol_{HLADH}) for the synthesis of γ-butyrolactam was 380, whereas the TON values for the synthesis of δ-valerolactam and ε-caprolactam were found as 152 and 56, respectively.
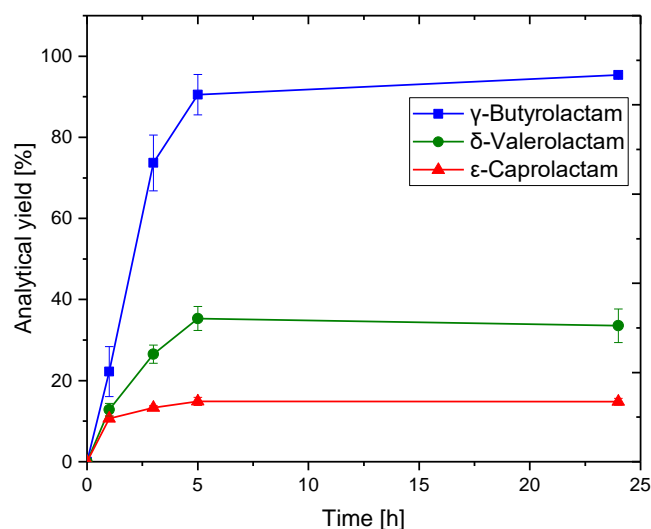
Figure 3.34. The HLADH-catalyzed oxidative lactamization of amino alcohols. Reaction conditions: c(amino alcohol) = 10 mM, c(NAD$^+$) = 1 mM, c(HLADH) = 1.0 mg/mL (0.1 U/mL, 25 µM), c(SmNOX) = 1.0 mg/mL (5 U/mL, 20 µM), buffer: pH 8.0 KP$_i$ (50 mM), 25°C, 900 rpm. Square = γ-butyrolactam, circle = δ-valerolactam, and triangle = ε-caprolactam. Duplicate reactions (1 mL in total) run in 1.5 mL glass-vials.

The residual percentage of each product for the time span of 2 days was approximately around 90%. This means that there was a hydrolysis process of the product in each reaction system. However, the products were relatively stable inside aqueous media with different pH (from pH 7.0 to 11.0) within the period of time, but the residual percentage of γ-butyrolactam decreased dramatically after 2 days and then stabilized again after day 5 with 60% (**Figure 3.35**). For both δ-valerolactam and ε-caprolactam (**Figure 3.36** and **3.37**), they hydrolyzed fast in the first day but then the residual percentage saw a little increase and kept in around 80–90% for the rest time. Among the analyzed products, ε-caprolactam showed the highest residual percentage of 88%–90% after 7 days, compared to γ-butyrolactam with 62%–65% and δ-valerolactam with 75%–82%. The pH of buffers showed no significant influence on the lactam hydrolysis.
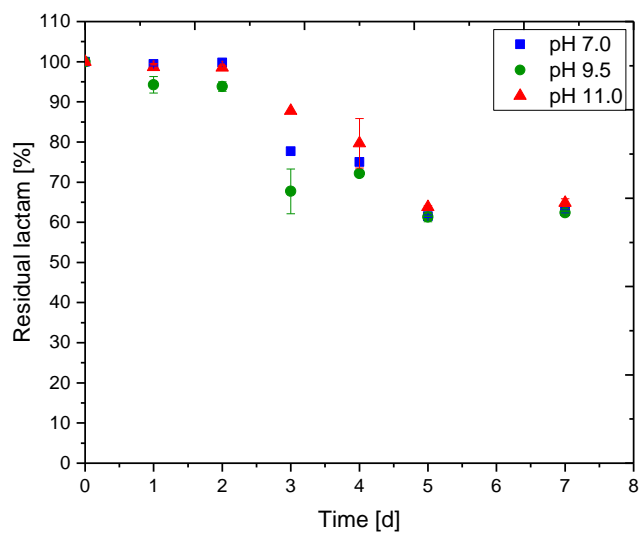
Figure 3.35. Hydrolysis of 10 mM γ-butyrolactam in aqueous solution. Buffers: potassium phosphate buffer 50 mM pH 7.0, CHES buffer pH 9.5, sodium bicarbonate buffer pH 11.0.
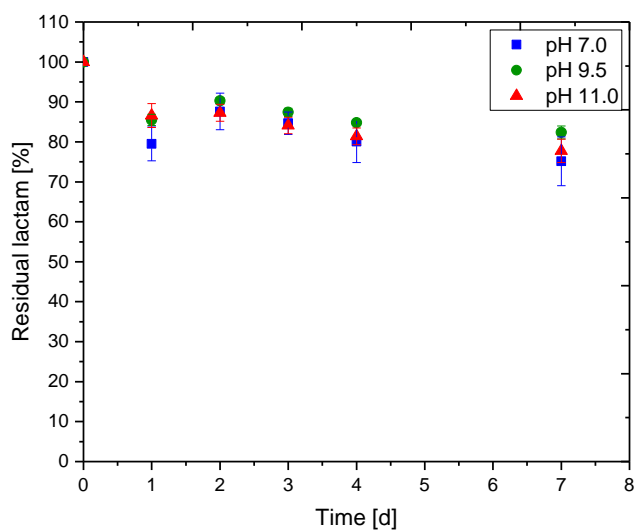
Figure 3.36. Hydrolysis of 10 mM δ-valerolactam in aqueous solution. Buffers: potassium phosphate buffer 50 mM pH 7.0, CHES buffer pH 9.5, sodium bicarbonate buffer pH 11.0.
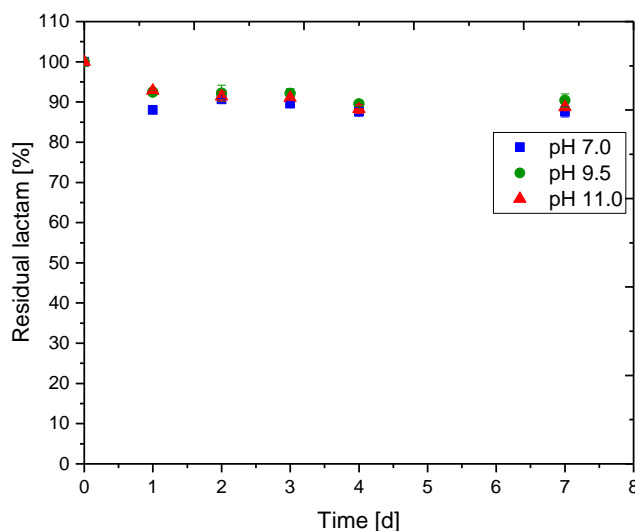
Figure 3.37. Hydrolysis of 10 mM ε-caprolactam in aqueous solution. Buffers: potassium phosphate buffer 50 mM pH 7.0, CHES buffer pH 9.5, sodium bicarbonate buffer pH 11.0.

Next, the synthesis of γ-butyrolactam with 10 mM 4-amino alcohol in 0.1 L scale using cell free extracts of HLADH and *Sm*NOX was performed resulting in 81% analytical yield. The isolated crude product (40 mg) with 47% isolation yield after extraction and evaporation was proved by NMR analysis (^{1}H and ^{13}C; **Figure B14** and **B15**). The purity of the isolated product was only approximately 20%, which meant the product isolation step was the main limitation for the production of γ-butyrolactam. Nevertheless, this parallel cascade reaction proved a simple efficient synthesis of lactam directly starting from the amino alcohol using two enzymes.

3.2.3.4 Interim summary

- NADH oxidase from *Streptococcus mutans* (*Sm*NOX) promoted NAD$^+$ *in situ* regeneration could significantly improve the HLADH-catalyzed lactamization of amino alcohols.

- The pH and ionic strength of the buffer had an interactive influence on the lactam formation. 50 mM pH 8.0 KP$_i$ buffer was selected as the final reaction medium as the comprise of activities of FMO-E and HLADH.

- This parallel cascade reaction system up to now was limited to only convert aliphatic amino alcohols. The γ-butyrolactam (5-membered) was synthesized with up to 95% analytical yield, whereby the yield decreased with increasing ring-size (38% for 6-membered δ-valerolactam and 14% for 7-membered ε-caprolactam).

- The products hydrolysis was another issue to consider when performing these reactions since the three lactams hydrolyzed up to 20% in aqueous buffer after one day.

4   DISCUSSION AND OUTLOOK

The detailed results concerning the two newly designed cascades have been presented and discussed in chapter 3. The aim of this chapter is to present overall discussion regarding to the relaxed cofactor specificity and stability of FMO-E, substrate scope, oxygen supply, evaluation of the cascade reactions as well as future perspectives and remarks.

4.1   Overall discussion

4.1.1   Relaxed cofactor specificity and narrow substrate scope of FMO-E

In order to obtain a better understanding on how FMO-E can catalyze Baeyer-Villiger oxidation with relaxed nicotinamide cofactors, homology modelling of FMO-E was conducted and compared with the crystal structures of a type I BVMO (PDB: 1W4X[188]) and a type I FMO (PDB: 2VQ7[189]) by Riebel et al.[93]. The comparison showed that these three enzymes use different mechanisms to catalyze Baeyer-Villiger oxidation (**Figure 4.1**).
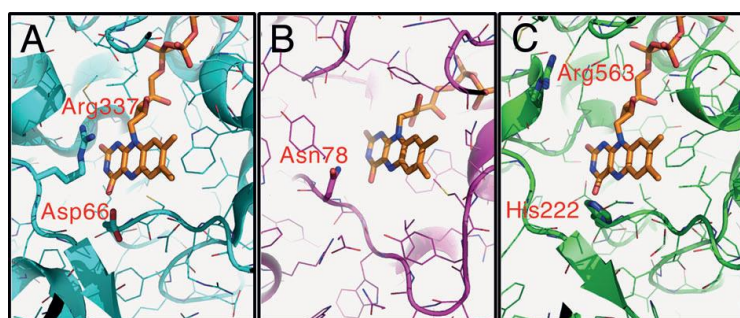
Figure 4.1. Comparison of the active site architectures of A) PDB:1W4X as a type I BVMO, B) 2VQ7 as a type I FMO, and C) FMO-E as the type II FMO. The picture is taken from Riebel et al. (2014)[93].

The NADPH specific type I BVMOs contain one strictly conserved arginine residue for the oxidation catalysis[188], while the counterpart of arginine in type I FMO is an asparagine[189]. However, no such residues could be identified in the homologous structure positions of FMO-E. Two conserved residues His222 and Arg563 were found to locate closely to the isoalloxazine part of FAD cofactor among those type II FMOs including FMO-E. Through site-directed mutagenesis, these two residues were verified to be crucial for the FAD binding. However, there was no conclusive evidence to show that whether these two residues were essential for the catalysis.

Another type II FMO, flavin-containing monooxygenase from *Stenotrophomonas maltophilia* (*SM*FMO), has been crystallized to investigate its cofactor promiscuity on molecular level[95].

The conserved arginine residue in NADPH-dependent BVMO, which is involved in binding the ribose phosphate, is replaced by a glutamine in 193 position (Gln193) in *SM*FMO. The absence of the interaction between positively charged arginine and negatively charged phosphate oxygen leads to the relaxed cofactor specificity. However, the molecular weight of *SM*FMO is only 39 kDa, which is significantly smaller than that of FMO-E (64 kDa). Therefore, the sequence identity between FMO-E and *SM*FMO was so low (19%) that the conserved Gln193 residue of *SM*FMO could not be located in the modelled structure of FMO-E[190]. Thus, the promiscuity of cofactor specificity of FMO-E is more difficult to explain. Interestingly, FMO-E contains one extra extension of approximately 160 residues in the N-terminal compared with *SM*FMO[93]. This may be the molecular basis for the much higher efficiency of FMO-E catalyzed Baeyer-Villiger oxidations than *SM*FMO.

FMO-E showed efficient activity towards the desymmetrization of many prochiral cyclobutanones resulting in lactones with moderate to good enantioselectivity[93, 119]. It could also catalyze the regiodivergent conversion of many racemic fused cyclobutanones with the preferential formation of normal lactones[93]. Nevertheless, similar to the substrate selectivity of *SM*FMO, the Baeyer-Villiger oxidation activity of FMO-E was also restricted to (fused) cyclobutanones. FMO-E did not exhibit any Baeyer-Villiger oxidation activity towards all other analyzed bulkier cycloketones with either NADH or NADPH as cofactor. This feature of narrow substrate scope of FMO-E is a significant disadvantage over the broad and versatile substrate scopes of many other well-known type I BVMOs, such as *Acinetobacter* CHMO and CHMO from *Comamonas sp.* strain NCIMB 9782 (CPMO).

4.1.2   Stability of FMO-E

A number of drawbacks have been identified for the industrial application of oxidoreductases, such as low enzyme stability in organic solvent and at high substrate concentrations, inhibition by substrate and product, insufficient oxygen transfer as well as need for cofactor regeneration. Among these disadvantages, the instability of enzymes is always an important issue as oxidoreductases are relatively unstable compared to hydrolases, which dominate the enzymes already applied in industry. CHMO$_{Acineto}$ has been engineered by Codexis Inc. (USA) for the enantioselective production of (*S*)-omeprazole, the active pharmaceutical ingredient (API) of the proton-pump inhibitor Nexium, on a multi dozen-gram scale[191]. Though multiple rounds of mutagenesis resulting in 41 mutations were conducted to improve stability and other parameters of CHMO$_{Acineto}$ to be on industrial application level, it demonstrated the high potential of BVMO. It is so far the only known industrial process from BVMOs, but there are plenty of conceptual application studies reported, such as production of polyesters monomers[192-194],

synthesis of API intermediates[195] and metabolites[196].

In the case of BVMOs, not only thermostability but also oxidative stability should be addressed. The need of oxidative stability is determined by the mechanism of this kind of enzymes[145]. Oxygen reacts with FAD tightly bound to the enzyme to form the alkylhydroperoxide intermediate, which reacts with the carbonyl group of substrates through nucleophilic addition to form the short-lived Criegee intermediate. The corresponding product in addition to water and oxidized FAD are released after the rearrangement and cleavage of the intermediate. The oxidized FAD is then reduced by the nicotinamide NAD(P)H mediated reduction[197-199]. Formation of hydrogen peroxide is observed due to the slow decay of the formed peroxiflavin if no substrate is present. Consequently, the amino acids will be oxidized by the highly reactive hydrogen peroxide leading to the activity of enzymes. Among all the protein amino acids, cysteine and methionine are the two residues containing sulfur atoms, which are the major sites for the oxidation of the protein[200-204]. This oxidation can not only occur in the residues of active site of enzymes, but also can occur at the distal parts of enzymes through remote effects[205-207].

In a recently reported work, the mutagenesis-independent stabilization of class B flavin monooxygenases was achieved by adding an engineered formulation of additives including natural cofactors NADPH and FAD as well as superoxide dismutase and catalase as antioxidants[148]. This way could easily improve the half-life time of $CHMO_{Acineto}$ by 10^3–10^4-fold without any laborious protein engineering work by random mutagenesis or rational design. FMOs can produce H_2O_2 and $NADP^+$ from molecular oxygen and NADPH in an uncoupling reaction[137, 208]. Any approaches mitigating the effects of reactive oxygen species (ROS) could contribute to the stabilization of $CHMO_{Acineto}$. This protocol was also practical for other two enzymes of this class, monooxygenase from *Pseudomonas putida* (OTEMO) and FMO-E. From the economical point of view, only low concentration of NADPH and FAD were added with FMO-E. As expected, the half-life time of FMO-E with 10 μM FAD and 0.1 mM NADPH at 30°C was 2.6 times longer than without these cofactors (**Table 3.4**)[119]. The concentration of NADPH also had significant influence on the stabilization of FMOs. Its positive effect had a steep jump at approximate 1 mM NADPH. Therefore, the stabilization of FMO-E would be much increased if higher concentration of NADPH used. The addition of superoxide dismutase and catalase also further strengthen this stabilization of FMO-E. Surprisingly, NADH did not show any beneficial effect on the stabilization of FMO-E even at up to 2.5 mM concentration (**Table 3.4**).

4.1.3 Oxygen supply

Oxygen limitation is indeed a major drawback when performing intensive oxygen dependent biocatalytic reactions due to the low solubility of oxygen in aqueous solution at the standard operation conditions (atmospheric pressure and room temperature)[184, 209]. Since oxygen is a substrate of FMO and NOX, the limited oxygen transfer rate would have negative effect on the FMO and NOX-mediated oxidation reactions. This was proved by the work of Baldwin et al. where the product formation rate increased with the increased oxygen transfer rate using a high concentration of recombinant *E. coli* cells overexpressing CHMO[210]. In our case, the productivity of FMO-E coupled convergent cascade reaction conducted in a reactor with a larger interfacial area between gas phase and liquid phase was 6-fold higher than that in a reactor with lower value (**Figure 3.16C and D**). Another recently reported work also showed that the baffled flasks could strongly improve the oxygen transfer rate of a BV oxidation catalyzed by immobilized whole cells expressing CHMO, thus leading to higher reaction rate[211].

A stirred tank reactor aerated through bubbling with air or oxygen can provide sufficient oxygen transfer rate for the reaction. In a process development for ADH/NOX coupled system, the authors found that a gassed stirred tank reactor was a promising reactor as it could provide external oxygen supply for the system[212]. The bubble aerated reaction in the stirred tank reactor gave full conversion after 2.5 h whereas the reaction without additional oxygen supply needed 28 h for the full conversion. However, the interfacial deactivation of enzymes should not be ignored when the enzymes were sensitive to the gas-liquid interface, which is in the case of most FMOs. Then, the aeration can be achieved with a membrane, which made gas dissolved into liquid. However, the additional mass transfer resistance through the membrane may make it less sufficient in terms of the flux of oxygen supplied into the reaction medium compared to bubbled system. Thus, a large specific membrane area is needed. In a CHMO-coupled fed-batch cascade synthesis of poly-ε-caprolactone, the sufficient oxygen membrane aeration was achieved by placing one silicone tube into an oxygen-aerated bottle[193]. With the cooperation with fed-batch operation adding the substrate cyclohexanol and *in situ* product removal of ε-caprolactone, up to 283 mM product 6-hydroxyhexanoic acid could be achieved without productivity loss within 20 h.

4.1.4 Evaluation of cascade reactions

Biocatalysis has been established as the complement to conventional methods for the production of optically pure chiral compounds and recognized as an emerging technology for decades. Biocatalytic processes could be considered as green methods in terms of safety and

environmental issues. However, the most discussed disadvantages for biocatalytic processes are the high costs of catalyst and the low productivity[213]. Therefore, it necessitates fast and simple assessment for biocatalytic processes.

In the case of convergent cascade reaction for the synthesis of γ-butyrolactone, the TON value for the enzymes ($mol_{lactone}/mol_{FMO-E\ and\ HLADH}$) could reach 5163, whereas the TON value for NAD^+ was 123. On the other hand, the TON values for the enzyme ($mol_{lactame}/mol_{HLADH}$) and NAD^+ were 380 and 9.5 for the synthesis of γ-butyrolactam by the parallel cascade reaction. The TON values for NAD^+ of these two reactions were far away from the laboratory requirement (1000-10,000)[214]. The productivity of γ-butyrolactone and γ-butyrolactam considering enzymes was 7.9 kg product/kg free enzyme and 0.8 kg product/kg free enzyme. Admittedly, the productivity obtained from the two cascades was a long way off the requirement for the fine chemicals (>670 kg product/kg free enzyme)[213]. This could result from the low substrate concentration and low stability of the FMO-E and *Sm*NOX in the two cascades.

4.2 Outlook

4.2.1 Crystal structure and protein engineering of FMO-E

The comparison of structure of *SM*FMO with the structure of a NADPH-dependent FMO from *Methylophaga aminisulfidivorans* (mFMO) revealed that the cofactor promiscuity of *SM*FMO may be due to the substitution of Arg234/Thr235 couple in the NADPH phosphate recognition site in mFMO, for Gln193/His194 couple in SMFMO[95]. Similarly, FMO from *Cellvibrio sp.* BR (CFMO) and FMO from *Pseudomonas stutzeri* NF13 (*PS*FMO) were found to possess Ser202/Thr203 couple and Gln194/Glu195 couple in the putative phosphate recognition site, respectively[215]. Through the study among *SM*FMO, CFMO and *PS*FMO, it was known that FMO with Gln/His couple in the phosphate recognition site favors NADH binding slightly and FMO with Ser/Thr couple showed no preferential activity with both cofactors[215]. Up to now, the molecular determinants of the cofactor promiscuity of FMO-E is still unclear due to the absence of the crystal structure. Therefore, the elucidation of the structure of FMO-E would shed light on the structural and catalytic properties, especially for the mechanism of its relaxed cofactor specificity. The k_{cat} value (2.0 s^{-1}) of FMO-E was approximately two orders of magnitude higher than that of *SM*FMO (0.029 s^{-1}) when using NADH as the cofactor. The comparison of the structures of FMO-E and *SM*FMO would provide some evidence for the high Baeyer-Villiger reaction efficiency of FMO-E. Though the direct engineering of NADH specificity in NADPH-dependent flavoprotein monooxygenases is not a trivial, the molecular understanding of nicotinamide cofactor promiscuity of FMO-E would provide new insights on

the cofactor specificity engineering of other NADPH-dependent FMOs. Thus, the above-described features of FMO-E make it an ideal candidate to conduct the crystallization studies, which would allow to understand the mechanisms behind these properties.

Cyclohexanone monooxygenase from *Rhodococcus sp.* HI-31 (CHMO_Rhodo) has been extensively investigated for the enzymatic mechanism using several structures showing the movement of enzyme domains during the catalytic circles[216-218]. However, the first published crystal structure of BVMO is phenylacetone monooxygenase (PAMO) from *Thermobifida fusca* as it is a relatively thermostable and solvent tolerant BVMO. The structure of prototype CHMO_Acineto could not solved due to its low stability. Thus, the main challenge for the crystal structure determination of FMO-E would be its unstable nature.

The number of newly identified and characterized BVMO is rapidly growing due to the genome mining efforts. However, one can also use protein engineering technologies to tailor enzymes to improve some properties for specific application as well as searching for new enzymes with new properties. There are different methods when conducting protein engineering depending on the available knowledge about enzyme's structure and catalytic mechanism[219]. If little of structure and mechanism knowledge is known for the enzyme of interest, then the random mutagenesis by methods such as error-prone PCR (epPCR) is the only choice. But the subsequent massive high-throughput screening efforts need to be employed to identify the target mutants. If the crystal structure of the enzyme is known, then the rational design by methods such as site-directed mutagenesis can be used to engineer the enzyme with much smaller number of mutants to screen.

One target of the protein engineering of FMO-E is to broaden its substrate scope. In the case of broadening the substrate spectrum of PAMO[220-223], most of these studies were performed by the comparison of the crystal structure of PAMO with the homology models of CHMO_Acineto or CHMO_Rhodo, since they have broader substrate spectrum. In the case of FMO-E, the comparison of the crystal structure of FMO-E with homology models of CHMO_Acineto or CHMO_Rhodo would help us identify key residues in the active pocket of FMO-E. As aforementioned, FMO-E exhibits low stability, which is a major hinder for its application. Oppermann and Reetz increased the oxidative stress stability and thermostability of CHMO_Acineto by mutating all the methionine and cysteine residues[145]. As the sulfur atom containing residues, methionine and cysteine are the typical target sites to improve the oxidative sensitivity of enzymes. Another important approach to improve the thermostability of CHMO_Acineto is the means of introduction of disulfide bonds. In the study conducted by van Beek and coworkers, a computational protocol was used to predict disulfide bonds by introducing cysteine pairs. A small library was

created and several stabilizing disulfide bonds were identified. The similar strategy was also used by Schmidt and coworkers to improve the thermostability of CHMO$_{Acineto}$ using another program to predict the potential disulfide bonds[224]. In the case of FMO-E, these strategies can be employed to promote its oxidative stability and thermostability.

4.2.2   Fusion enzymes for cascade reactions

In this thesis, two different redox-neutral cascades were developed for the synthesis of lactones and lactams. The combination of redox enzymes in one-pot reactions without isolation of intermediates offer considerable advantages: time and materials needed for the recovery of product is reduced, reversible reactions can be driven to completion and the harmful or unstable compounds can be kept at the minimum level. Redox enzymes that usually require expensive nicotinamide cofactors are mostly coupled in a cascade (FMO-E and HLADH, HLADH and *Sm*NOX) to achieve self-sufficient cofactor regeneration rendering the reaction systems more efficient and economical. However, these cascade reactions are still far away from practical industrial application due to some drawbacks, such as the above-mentioned low stability and low catalytic efficiency i.e. the low TONs of enzymes.

An approach that could address these problems is to produce these coupled enzymes in fused version, in which the coupled enzymes are expressed into one multifunctional enzyme. Many studies have shown that enzymes or functional proteins optimized by fusion constructs could have various advantages, such as improved catalytic efficiency, stability, expression, and solubility[225-226]. In theory, in the cascade reactions catalyzed by fusion enzyme, the product from one enzyme could directly transfer into the active site of another enzyme as the fused enzymes are in close proximity. This has been proven in the case of a bifunctional aldolase/kinase enzyme for more efficient C-C bond formation[227]. The proximity of active sites in the fused enzyme promoted the aldol reaction rate by 20-fold. A recent study described the synthesis of ε-caprolactone from cyclohexanol by a fusion enzyme of ADH and CHMO[228]. This fusion enzyme could convert 200 mM cyclohexanol to final product with a >99% conversion whereas the reaction catalyzed by the two separate enzymes only gave a conversion of 42%[228].

Compared to the isolated enzymes, the whole cell biotransformations have some intrinsic features. The enzymes utilized in the cell are more stable due to the natural environment inside the cell. Moreover, many whole cell systems offer the internal cofactor regeneration by only adding the co-substrates. In a recently published work by the group of Bornscheuer, a CHMO and an ADH were cloned into one vector and co-expressed in *E. coli*. A multi-enzyme cascade reaction catalyzed by the whole cell containing the co-expressed enzymes showed higher

conversion than the cascade reaction catalyzed by individual whole cells[229]. This study also proves the potential application of fusion enzyme in whole cell form.

Though there is no conclusion how to design a stable and efficient fusion protein, it is worth trying to combine FMO-E and HLADH as well as HLADH and *Sm*NOX into fusion enzymes for the cascade reactions. The possible proximity of active sites of enzymes could make the "substrates transport distance" shorter thus leading to higher catalytic efficiency. In addition, the fusion enzyme could also make the enzyme-coupled cofactor regeneration possible in low-water media, which has the benefits of using hydrophobic substrates at high concentrations and preventing the undesired autohydrolysis of products.

4.2.3   Effect of reactor on oxygen supply

Oxygen supply of the reactions was significantly influenced by the geometry of the reactors as shown in the overall discussion part. Energy input or in other words stirring speed is another important point for the oxygen supply in the reactor. In general, the geometry of the stirrer and the reactor, the speed of the stirrer (rpm) as well as the type of aeration are the parameters that could influence the oxygen input into the reaction system. Theoretically, the oxygen supply for the reaction is directly determined by the interfacial area between the gas and liquid which is influenced by the energy input.

In this PhD thesis, the effect of reactor on oxygen supply in the two cascade reactions was only investigated qualitatively by the definition of oxygen amount as headspace ratio, which equals head space volume per volume of reaction mixture. It is of high interest to study the effect of reactor on oxygen supply quantificationally by defining the oxygen amount as the result of interfacial area in the future. For this point, the experiments can be performed in reactors with the same headspace ratio at different height-diameter ratios (H/D).

5   SUMMARY

In this PhD study, one convergent cascade and a parallel cascade, both being NADH-dependent, were developed for the synthesis of lactones and lactams, respectively. The main results are summarized below:

1. NADH-dependent convergent cascade reactions for lactonization

- FMO-E showed relaxed cofactor specificity since it could accept both NADPH and NADH as cofactor. The k_{cat} value of FMO-E towards NADH was in the same range (1-20 s^{-1}) with many other typical class B flavoprotein MOs, indicating it was a potent biocatalyst with NADH as the cofactor.

- FMO-E is identified as a relatively unstable enzyme since its half-life time at 30°C was only 2.21 h. The phosphorylated nicotinamide cofactor NADPH was found to significantly improve its thermostability. 0.1 mM NADPH combined with 10 μM FAD could increase the half-life time of FMO-E at 30°C by 2.6-fold. However, the unphosphorylated nicotinamide cofactor NADH did not show any beneficial effect on the stability of FMO-E.

- FMO-E only showed Baeyer-Villiger oxidation activity towards cyclobutanones and fused cyclobutanones, indicating its narrow substrate scope.

- The proof-of-concept study of this NADH-dependent convergent cascade consisting of FMO-E and HLADH was successfully demonstrated using cyclobutanone and 1,4-butanediol as the substrates. More than 130 mM γ-butyrolactone with an analytical yield of 89% were obtained when applying 100 mM cyclobutanone and 50 mM 1,4-butanediol in this cascade.

- The reactor showed significant effect on the productivity of the cascade reaction by changing the headspace ratio and interfacial area, which could influence the oxygen input and reagent evaporation. The higher headspace ratio and interfacial area would provide more oxygen for the cascade reaction, which is preferred for reaction system with high substrate concentration, but also lead to more substrate evaporation.

- The ratio of normal lactone to abnormal lactone in the synthesis of chiral lactones decreased during the course of the process because of deactivation of FMO-E and the increased abnormal lactone generated from the oxidation of cis-1,2-cyclohexanedimethanol catalyzed by HLADH.

- Racemic bicyclo[4.2.0]octan-7-one was converted to normal lactone with an *ee* value of 89–74% (3a*S*, 7a*S*) by FMO-E alone and the abnormal lactone with an *ee* value

of >99% (3a*R*, 7a*S*) was synthesized by both FMO-E and HLADH.

2. Parallel cascade reactions for lactamization

- HLADH showed the highest activity toward 4-amino-1-butanol *via* UV-Vis spectroscopy activity assay and was selected as the candidate biocatalyst for the research among the four evaluated ADHs (HLADH, ADH-A, TADH and *TeS*ADH).

- Steady-state kinetic investigation revealed that there was no substrate inhibition with 4-amino-1-butanol up to 500 mM while the substrate inhibition was observed from approximate 20 mM with 5-amino-1-pentanol and from approximate 10 mM with 6-amino-1-hexanol for HLADH.

- Both the pH and ionic strength of buffer showed significant effects on HLADH-catalyzed lactamization of amino alcohols. The lactam yield increased with increasing pH mainly because the high pH increased non-protonation state of the amine (R-NH_2), which facilitated intramolecular ring-formation of the amine aldehyde intermediate.

- The HLADH-catalyzed lactamization product yield of 4-amino-1-butanol with stoichiometric NAD^+ was quite low (< 10%) even at alkaline conditions because of the unfavorable thermodynamics.

- NADH oxidase from *Streptococcus mutans* (*Sm*NOX) promoted NAD^+ *in situ* regeneration could significantly improve the HLADH-catalyzed lactamization of amino alcohols up to 95% analytical yield when using 4-amino-1-butanol as the substrate under optimized conditions.

- Up to now, this parallel cascade reaction system is limited to aliphatic amino alcohols as substrates. The formation of the five-membered ring of γ-lactam is sterically more favored as compared to six- and seven-membered lactam rings. The γ-butyrolactam (5-membered) was synthesized with up to 95% analytical yield, whereby the yield decreased with increasing ring-size (38% for 6-membered δ-valerolactam and 14% for 7-membered ε-caprolactam).

- The preparation of γ-butyrolactam was performed in 0.1 L scale using cell free extracts of HLADH and *Sm*NOX. The isolated crude product after extraction and evaporation was proved by NMR analysis.

Overall, this presented PhD study represents the first application of FMO-E in a NADH-dependent convergent cascade for the synthesis of achiral and chiral lactones as well as the directed approach for the lactamization of aliphatic amino alcohols catalyzed by HLADH.

A   MATERIALS AND METHODS

A 1   Materials

A 1.1   Chemicals

Racemic bicyclo[4.2.0]octan-7-one (CAS: 54211-18-6), octahydrobenzofuran-2-one (CAS: 553-86-6), (2-(aminomethyl)phenyl)methanol (CAS: 4152-92-5), (2-(2-aminoethyl)phenyl)methanol (CAS: 76518-29-1), 1-isoindolinone (CAS: 480-91-1) and 3,4-dihydro-2H-isoquinolin-1-one (CAS: 1196-38-9) were kindly provided by Dr. Florian Rudroff and Dr. Anna K. Ressmann (TU Wien, Austria). All other chemicals were of analytical grade and purchased from Sigma–Aldrich (Steinheim, Germany), Carl Roth (Karlsruhe, Germany), Merck (Darmstadt, Germany), Fluka (Buchs, Switzerland) or Acros Organics (Geel, Belgium) and used without further purification. Ni-NTA affinity resin was purchased from Expedeon (Cambridgeshire, UK) while Strep–Tactin®XT resin was purchased from IBA GmbH (Göttingen, Germany). BCA protein quantification kit (Pierce™) was purchased from Thermo Scientific (Rockford, USA).

A 1.2   Plasmids and strains

The recombinant pBAD vector (with a N-terminal strep tag: WSHPQFEK) containing FMO-E gene was from Prof. Marco W. Fraaije (University of Groningen, the Netherlands). The recombinant pET-28b plasmids containing HLADH gene and *Sm*NOX gene were from Dr. Diederik Johannes Opperman (University of Free State, South Africa). The recombinant pET-22b(+) plasmid containing ADH-A gene and recombinant pET-21a plasmid containing *Te*SADH gene were from Prof. Dr. Wolfgang Kroutil (University of Graz, Austria). The recombinant pASZ2 plasmid containing TADH gene was from our institute. Chemically competent E. *coli* DH5α, BL21 (DE3), Top10 cells were purchased from Invitrogen (Carlsbad, USA).

A 1.3   Equipments

HP 6890 Series GC	Agilent Technologies, Waldbronn, Germany
Agilent GC ChemStation Rev. B.01.01.[164]	Agilent Technologies, Waldbronn, Germany
Hydrodex ß-PM (25 m × 0.25 mm) GC column	Macherey-Nagel, Düren, Germany
Agilent 1100 Series HPLC	Agilent Technologies, Waldbronn, Germany
Agilent OpenLAB CDS ChemStation Edition	Agilent Technologies, Waldbronn, Germany
EC 100/3 NUCLEODUR C18 Gravity, 3 µm, 100 × 3	Macherey-Nagel, Düren, Germany
Unikon XL UV/Vis spectrophotometer	Goebel Instrumentelle Analytik GmbH, Hallertau, Germany
Libra S12 UV/Vis spectrophotometer	Biochrom GmbH, Berlin, Germany
Brinkmann Rm6 MGW Lauda Water Bath	Lauda Dr. R. Wobser GmbH, Lauda-Königshofen, Germany
Sartorius CP224S balance	Sartorius, Göttingen, Germany
Sartorius LC2200P balance	Sartorius, Göttingen, Germany
Beckman Coulter Avanti J-25i centrifuge	Beckman Coulter GmbH, Krefeld, Germany
Hettich® Universal 320R centrifuge	Andreas Hettich GmbH, Tuttlingen, Germany
Hettich® MIKRO 200R centrifuge	Andreas Hettich GmbH, Tuttlingen, Germany
Eppendorf 5415D centrifuge	Eppendorf AG., Hamburg, Germany
Labor-pH-Meter 766	Knick Elektronische Messgeräte GmbH, Berlin, Germany
Infinite® 200 PRO multimode microplate reader	Tecan Group Ltd, Männedorf, Switzerland
GC vial	Klaus Trott Chromatographie-Zubehör, Kriftel, Germany
Snap-cap vials, 75 × 28 mm, 30 mL	neoLab Migge GmbH, Heidelberg, Germany
Christ Alpha 2-4 lyophilizer	Christ, Osterode am Harz, Germany
Microbiological incubator	Salus Labs, Flint, US
CERTOMAT® R benchtop shaker	Sartorius, Göttingen, Germany
Infors HT shaker	Infors AG, Bottmingen, Switzerland
HLC Heating-ThermoMixer MHR 11	DITABIS Digital Biomedical Imaging Systems AG, Pforzheim, Germany
Multifunction cooling ThermoMixer MKR 13	DITABIS Digital Biomedical Imaging Systems AG, Pforzheim, Germany
Heathrow Scientific Vortexer™	Daigger Scientific, Vernon Hills, USA
Bandelin SONOPULS-Ultrasonic Homogenizer HD 2070	Bandelin electronic GmbH, Berlin, Germany
MS 73 ultrasonic homogenizer probe	Bandelin electronic GmbH, Berlin, Germany
VARIOKLAV® classic laboratory autoclaves	HP Medizintechnik GmbH, Oberschleißheim, Germany
Mini-PROTEAN® Tetra Vertical Electrophoresis Cell	Bio-Rad Laboratories, Hercules, USA
Millipore centrifuge ultrafilter (30 kDa)	Merck Chemicals GmbH, Darmstadt, Germany
Msc Advantage clean bench	Thermo fisher scientific, Illinois, USA

A 2 Methods

A 2.1 Heterologous expression and purification of enzymes

A 2.1.1 Heterologous expression and purification of ADH-A

ADH from *Rhodococcus ruber* DSM 44541 (ADH-A) was expressed with plasmid pET-22b(+) in E. *coli* BL21 (DE3)[170]. First, the recombinant plasmids were transformed into the chemically competent E. *coli* BL21 (DE3). The transformation was performed by the following procedure: (1) Pipette 1–2 µL of plasmid into the vial of competent cells and mix by tapping gently; (2) incubate on ice for 30 min; (3) incubate at 42°C in a water bath for 30 s for heat shock followed by on ice for 5 min; (4) add 800 µL SOC medium to the vial and incubate at 37°C and 120 rpm for 1 h; (5) spread 200 µL of cells on LB (lysogeny broth) agar plate containing 100 µg/mL ampicillin and then incubate at 37°C overnight (~ 16 h).

For preculture, 20 mL LB medium containing 100 µg/mL ampicillin and 0.75 mM $ZnCl_2$ in 100 mL baffled flask was inoculated with one colony from the LB agar plate and then incubated at 37°C and 120 rpm overnight (~ 16 h). 10 mL of the preculture was used to inoculate 400 mL TB medium containing 100 µg/mL ampicillin and 0.75 mM $ZnCl_2$ in 2 L baffled flask, which was then incubated at 37°C and 120 rpm. After OD_{600} reached 0.6–0.8, IPTG was added to a final concentration of 0.5 mM and the incubation was continued at room temperature (~22°C) for 24 h. The cells were harvested by centrifugation at 5238 × g at 4°C for 10 min.

Cell pellets obtained after centrifugation were resuspended in Tris-HCl buffer (20 mM, pH 7.5, ~10 mL per gram of wet cell) and disrupted by sonication (Sartorius Labsonic M) on ice at 60% amplitude and 0.4 cycle for 4 times – 4 min each – with 4 min resting on ice between the cycles. The soluble protein was separated from the cell debris by centrifugation at 32735 × g for 20 min. The supernatant was heat-treated in water bath at 80°C for 20 min to precipitate the thermally unstable proteins. The precipitate was separated by centrifugation at 32735 × g for 30 min at 4°C. The supernatant was deep-frozen at -80°C. The SDS-PAGE of purified ADH-A was shown in **Figure A1**.
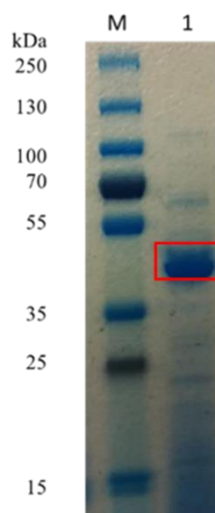
Figure A1. SDS-PAGE analysis of the purified ADH-A (35 kDa). Lane M: PageRuler Prestained Protein Ladder (Thermo Fisher); lane 1: purified ADH-A after heat treatment.

A 2.1.2 Heterologous expression and purification of TADH

ADH from *Thermus sp.* ATN1 (TADH) was expressed with plasmid pASZ2 in *E. coli* BL21 (DE3)[171]. The transformation of recombinant TADH plasmid was the same with the procedures of ADH-A.

For preculture, 20 mL LB medium containing 100 μg/mL ampicillin in 100 mL baffled flask was inoculated with one colony from the LB agar plate and then incubated at 37°C and 120 rpm overnight (~ 16 h). 10 mL of the preculture was used to inoculate 400 mL TB medium containing 100 μg/mL ampicillin in 2 L baffled flask, which was then incubated at 37°C and 120 rpm. After OD^{600} reached 0.6–0.8, IPTG was added to a final concentration of 0.5 mM and the incubation was continued at room temperature (~22°C) for 24 h. The cells were harvested by centrifugation at 5238 × g at 4°C for 10 min.

The purification of recombinant TADH plasmid was the same with the procedures of ADH-A. The SDS-PAGE of purified TADH was shown in **Figure A2**.
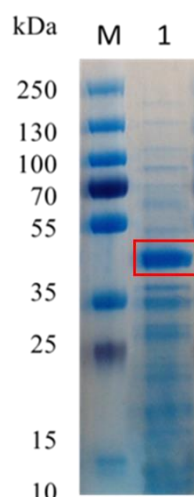
Figure A2. SDS-PAGE analysis of the purified TADH (37 kDa). Lane M: PageRuler Prestained Protein Ladder (Thermo Fisher); lane 1: purified TADH after heat treatment.

A 2.1.3   Heterologous expression and purification of HLADH

HLADH was expressed with plasmid pET-28b in E. *coli* BL21 (DE3)[153]. First, the recombinant plasmids were transformed into the chemically competent E. *coli* BL21 (DE3). The transformation was performed by the following procedure: (1) Pipette 1–2 μL of plasmid into the vial of competent cells and mix by tapping gently; (2) incubate on ice for 30 min; (3) incubate at 42°C in a water bath for 30 s for heat shock followed by on ice for 5 min; (4) add 800 μL SOC medium to the vial and incubation at 37°C and 120 rpm for 1 h; (5) spread 200 μL of cells on LB agar plate containing 50 μg/mL kanamycin and then incubate at 37°C overnight (~ 16 h).

For preculture, 20 mL LB medium containing 50 μg/mL kanamycin in 100 mL baffled flask was inoculated with one colony from the LB agar plate and then incubated at 37°C and 120 rpm overnight (~ 12 h). 10 mL of the preculture was used to inoculate 400 mL LB medium containing 50 μg/mL kanamycin in 2 L baffled flask, which was then incubated at 37°C and 120 rpm. After OD_{600} reached 0.6–0.8, IPTG was added to a final concentration of 0.5 mM and the incubation was continued at room temperature (~22°C) for 24 h. The cells were harvested by centrifugation at 5238 × g at 4°C for 10 min.

Cell pellets obtained after centrifugation were resuspended in lysis buffer (10 mM Tris-HCl, pH 7.5, 0.1 mM Pefabloc, 1 mg/mL lysozyme; ~10 mL per gram of wet cell) and disrupted by sonication (Sartorius Labsonic M with MS 73 probe) on ice at 60% amplitude and 0.4 cycle for 4 times – 4 min each – with 4 min resting on ice between the cycles. The soluble protein was separated from the cell debris by centrifugation at 32735 × g for 30 min at 4 °C.

The cell free extract (CFE) was twice applied to the Ni-NTA column slowly which was equilibrated with 10 bed volumes of binding buffer (50 mM NaH_2PO_4, 300 mM NaCl, 10 mM imidazole, pH 8.0) in advance. The column was washed with 10 bed volumes of washing buffer (50 mM NaH_2PO_4, 300 mM NaCl, 20 mM imidazole, pH 8.0) to remove the unbound proteins. At the end, 5x of 1 bed volume of elution buffer (50 mM NaH_2PO_4, 300 mM NaCl, 250 mM imidazole, pH 8.0) was added to the column to elute the bound enzyme. 5 µL of samples were collected from each wash- and elution fraction for subsequent SDS-PAGE analysis. Then the column was washed with 10 bed volumes of the following buffers: (1) MES buffer at pH 5.0 to regenerate the column, (2) deionized water, (3) 20% (v/v) ethanol. Finally, the column was stored in 20% ethanol (v/v) at 4°C.

All the fractions containing the purified enzymes according to the SDS-PAGE (**Figure A3**) were collected for further ultrafiltration using centrifugal ultrafiltration unit (Millipore, 10 kDa, 1389 × g). Afterwards, the concentrated enzyme solution was diluted with desalting buffer (10 mM, Tris-HCl, 1.0 mM DTT, 25% (glycerol, v/v), pH 7.5) twice to 100 times dilution and finally concentrated to less than 1.0 mL. The obtained purified enzyme was stored at −80°C by aliquoting in micro-reaction tubes (each 100 µL). The concentration of protein and activity of enzyme were measured for each step and a typical purification was summarized in **Table A1**. The productivity of HLADH was 7.5 mg/g wet cell.
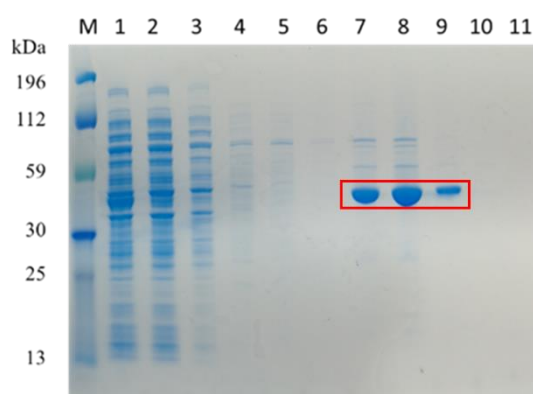
Figure A3. SDS-PAGE analysis of different fractions taken during the purification of HLADH (40 kDa). Lane M: PageRuler Prestained Protein Ladder (Thermo Fisher); lane 1: cell free extract; lane 2: flow through; lane 3-6: washing fractions; lane 7-11: elution fractions.

Table A1. Summary of HLADH purification steps.

Purification steps[a]	V [mL]	Protein [mg]	Specificity activity [U/mg][b]	Total activity [U]	Purification factor [-]	Yield [%]
CFE	20	56	0.237	13.3	-	100
UF	1.5	4.2	0.471	2.0	2	14.9

[a] CFE: Cell free extract, UF: Ultrafiltration

[b] ADH activity assay using 10 mM 1,4-butanediol as the substrate

A 2.1.4 Heterologous expression and purification of *Te*SADH

ADH from *Thermoanaerobacter ethanolicus* (*Te*SADH) was expressed with plasmid pET-21a in E. *coli* BL21 (DE3)[172]. The transformation, expression and purification of recombinant *Te*SADH was similar with the procedures of HLADH, the only difference was that the antibiotic was ampicillin. The SDS-PAGE of *Te*SADH purification was shown in **Figure A4**.
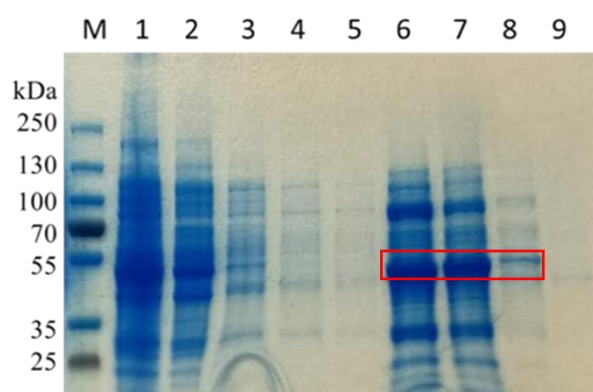
Figure A4. SDS-PAGE analysis of different fractions taken during the purification of *Te*SADH (38 kDa). Lane M: PageRuler Prestained Protein Ladder (Thermo Fisher); lane 1-5: washing fractions; lane 6-9: elution fractions.

A 2.1.5 Heterologous expression and purification of *Sm*NOX

*Sm*NOX were expressed with plasmid pET-28b in E. *coli* BL21 (DE3). The transformation, expression and purification of *Sm*NOX was the same with HLADH. The SDS-PAGE of *Sm*NOX purification was shown in **Figure 4.9**. The concentration of protein and activity of enzyme were measured for each step and a typical purification was summarized in **Table 4.3**.

A 2.1.6 Heterologous expression and purification of FMO-E

For preculture, 20 mL LB medium containing 50 µg/mL ampicillin in 100 mL baffled flask was inoculated with one colony on the plate and then incubated at 37°C and 180 rpm overnight (~ 12 h). 10 mL of the preculture was used to inoculate 400 mL×3 LB medium containing 100 µg/mL ampicillin and 0.002% (w/v) L-arabinose in 2 L baffled flask, which was then incubated at room temperature (~ 22°C) and 120 rpm for 32 h. The cells (final OD_{600} = 4.4)

were harvested by centrifugation at 8,000 rpm (5238 × g) at 4°C for 10 min. 4.4 g wet cells were obtained from 1.2 L of culture medium (wet cell yield = 3.7 g cell/L medium).

Cell pellets obtained after centrifugation were resuspended in lysis buffer (10 mM Tris-HCl, pH 7.5, 10 μM FAD, 0.1 mM Pefabloc, 1 mg/mL lysozyme; ~ 10 mL per gram of wet cell) and disrupted by sonication (Sartorius Labsonic M with MS 73 probe) on ice at 60% amplitude and 0.4 cycle for 4 times – 4 min each – with 4 min resting on ice between the cycles. The soluble protein was separated from the cell debris by centrifugation at 20,000 rpm (32735 × g) for 30 min at 4°C.

Purification of FMO-E from the CFE was done by using Strep-Tactin® Sepharose (IBA GmbH, Germany). Difference from the manufacturer manual: FAD (10 μM), DTT (1.0 mM) and glycerol (10%, v/v) were added in the buffers. The CFE was slowly loaded on to the column two times and the column was washed with 5 times of 1 CV (5 mL) Buffer W (100 mM Tris-HCl, pH 8.0, 150 mM NaCl, 1 mM EDTA, 10 μM FAD, 1.0 mM DTT, 10% glycerol (v/v)). The wash fractions (1 CV each) were collected and 5 μL of each fraction was taken for subsequent SDS-PAGE analysis. Then the combined protein was eluted by Buffer BXT (100 mM Tris-HCl, pH 8.0, 150 mM NaCl. 1 mM EDTA, 50 mM biotin, 10 μM FAD, 1.0 mM DTT, 10% glycerol (v/v)). Firstly 0.6 CV Buffer BXT as elution fraction 1 (E1) was added, then 1.6 CV (E2) and finally 1.0 CV (E3) were added. 5 μL of each fraction was taken for subsequent SDS-PAGE analysis. 2 CV of 10 mM NaOH was added to the column to regenerate resin and then the NaOH was immediately removed by adding 8 CV of Buffer W. Then the column was stored in Buffer W at 4°C.

All fractions containing the purified enzymes according to the result of SDS-PAGE analysis were collected for further ultrafiltration using centrifugal ultrafiltration unit (Millipore, 10 kDa, 1389 × g). Afterwards, the concentrated enzyme solution was diluted with desalting buffer (10 mM phosphate buffer, pH 6.5, 1.0 mM DTT, 10 μM FAD, 25% glycerol (v/v)) for twice to 100 times dilution and finally concentrated to less than 1.0 mL. The reason of the used phosphate buffer at pH 6.5 is because FMO-E has the highest stability in this buffer and pH.

A 2.2   Analysis of FMO-E, ADHs, SmNOX activities

A 2.2.1   Analysis of FMO-E activity

The activity of purified FMO-E was determined spectrophotometrically by monitoring the decrease of absorbance of NADPH or NADH over time at 340 nm. The reaction mixture (1.0 mL) typically contained 50 mM pH 7.5 Tris-HCl (1.0 mM DTT, 1.0 mM EDTA, 10 μM

FAD, 10% glycerol (v/v)), 0.1 mM NADPH or NADH, 10 mM ketone substrate, 1.0% (v/v) DMSO (from the substrate stock solution), and 10 μL enzyme at 25°C. The absorption at 340 nm was followed over a period of 1 min and the activity was subsequently determined from the recorded linear slope following **Equation A1**. The assay for the negative control was performed without the substrate. One unit (U) is defined as the amount of enzyme that consumes 1 μmol NADH or NADPH per minute under the defined conditions.

$$A_{spec}[\mu mol \cdot min^{-1} \cdot mg^{-1}] = \frac{(\Delta Abs_{sample} - \Delta Abs_{blank}) \cdot V_R \cdot D}{\varepsilon \cdot d \cdot V_S \cdot C_L}$$ **Equation A1**

$\varepsilon = 6220 \ M^{-1}cm^{-1}$

ΔAbs = measure slope at 340 nm per minute

V_R = total volume of the reaction mixture (here 1.0 mL)

V_S = volume of the enzyme solution (here 10 μL)

d = path length of the cuvette (here 1 cm)

D = dilution factor of the enzyme

C_L = protein concentration of enzyme solution (mg mL^{-1})

A 2.2.2   Analysis of ADHs activity

The activity assay of ADHs was performed spectrophotometrically by monitoring the increase of the absorbance of NADH or NADPH over time at 340 nm. The reaction mixture (1.0 mL) typically contained 50 mM pH 9.0 CHES, 1.0 mM NAD$^+$, 10 mM substrates and 10 μL enzyme solution at 25°C. The absorption at 340 nm was followed over a period of 1 min and the activity was subsequently determined from the recorded linear slope following **Equation A1**. The assay for the negative control was performed without the substrate. One unit (U) is defined as the amount of enzyme that generate 1 μmol NADH or NADPH per minute under the defined conditions.

A 2.2.3   Analysis of *Sm*NOX activity

The activity assay of *Sm*NOX was performed spectrophotometrically by monitoring the decrease of the absorbance of NADH over time at 340 nm. The reaction mixture (1.0 mL) typically contained 50 mM pH 7.0 KP$_i$ buffer, 0.1 mM NADH and 10 μL enzyme solution at 25°C. The absorption at 340 nm was followed over a period of 1 min and the activity was subsequently determined from the recorded linear slope, also following **Equation A1**. One unit (U) is defined as the amount of enzyme that consumes 1 μmol NADH per minute under the defined conditions.

A 2.3 Characterization of FMO-E

A 2.3.1 Effect of pH on FMO-E activity and stability

The effect of pH on the enzyme activity was determined by performing the enzyme activity assay at a pH range from 5.0 to 9.0. Sodium acetate buffer (5.0, 5.5), sodium phosphate buffer (6.0, 6.5, 7.0, 7.5) and Tris-HCl buffer (7.5, 8.0, 8.5, 9.0) were selected based on their *pK*a values. The stability of FMO-E was determined by incubating 50 µL of 1.0 mg/mL (16 µM) purified enzyme at 4°C in different pH (5.0, 5.5, 6.0, 6.5, 7.0, 7.5, 8.0, 8.5 and 9.0) buffers and the residual activity was detected after 24 h.

A 2.3.2 Effect of temperature on FMO-E activity and stability

The effect of the temperature on enzyme activity was determined by performing the activity assay at temperature range from 20–45°C (20, 25, 30, 35, 40, and 45°C) in 50 mM Tris-HCl buffer (pH 7.5). The buffer was equilibrated at each temperature in advance and the activity assay was performed as described before. The stability of the FMO-E was determined by measuring the residual activity at 25 °C after incubating 50 µL of 1.0 mg/mL (16 µM) purified enzyme in 50 mM Tris-HCl buffer (pH 7.5) at various temperatures from 20–45°C (20, 25, 30, 35, 40, and 45°C) for 10 min.

A 2.3.3 Effect of cosolvent on activity of FMO-E

The effect of the cosolvent on enzyme activity was determined by performing the standard FMO-E activity assay in 50 mM pH 7.5 Tris-HCl buffer with different contents of organic solvents from 0% to 30% (v/v). C_{50} (the concentration of solvent in buffer at which half inactivation of the enzyme is observed) was used to describe the tolerance of FMO-E towards organic solvents.

A 2.3.4 Effect of cofactor on FMO-E long-term stability

The effect of the cofactors (FAD, NADH and NADPH) on the long-term stability of FMO-E was investigated. According to the published research of Dr. Florian Rudroff (TU Wien), four kinds of cofactor components (10 µM FAD, 10 µM FAD + 0.1 mM NADH, 10 µM FAD + 0.1 mM NADPH, 10 µM FAD + 2.5 mM NADH) were selected. The half-life times of FMO-E (1.0 mg/mL, 16 µM) at 30°C with different cofactors were determined by detecting the residual activity at different time points (0, 1, 3, 5, and 8 h). The half-life times ($\tau_{1/2}$) were calculated based on **Equation A2**.

$$\tau_{1/2} = \frac{\ln 2}{k_{des}} \qquad\qquad \textbf{Equation A2}$$

$\tau_{1/2}$: Half life time [h]

k_{des}: Deactivation constant [h^{-1}]

A 2.3.5   Effect of co-solvent on FMO-E activity

The effect of co-solvent on FMO-E activity was determined by performing the activity assay with various concentration of co-solvent from 0% to 30% (v/v) in 50 mM pH 7.5 Tris–HCl buffer. Six kinds of water miscible organic solvents, methanol (MeOH), dimethyl sulfoxide (DMSO), ethanol (EtOH), 1,4-dioxane, acetone and acetonitrile (ACN) were investigated. The concept of C$_{50}$ is introduced to describe the effect of co-solvent on enzyme activity, which means the concentration (v/v) of co-solvent at which half activity left. The activity assay was performed as described before.

A 2.3.6   Determination of FMO-E kinetic parameters

The kinetic constants (at fixed NAD(P)H concentration) were determined by measuring the initial velocities with various concentrations of the substrate. The activity assay was performed spectrophotometrically by monitoring the decrease of the absorbance of NAD(P)H over time at 340 nm and the extinction coefficient of 6220 M^{-1}cm^{-1}. The reaction mixture (1.0 mL) typically contained 50 mM Tris-HCl (pH 7.5, 1.0 mM DTT, 1.0 mM EDTA, 10 μM FAD, 10% glycerol (v/v)), 0.1 mM NAD(P)H, 0–20 mM ketone substrates, 1.0–5.0% (v/v) DMSO, and 10 μL FMO-E solution (8 μM) at 25°C. The assay for the negative control was performed without the substrate.

The kinetic constants (at fixed substrate concentration) were determined by measuring the initial velocities with various concentrations of NAD(P)H. The activity assay was performed spectrophotometrically by monitoring the decrease of the absorbance of NAD(P)H over time at 340 nm and the extinction coefficient of 6220 M^{-1}cm^{-1}. The reaction mixture (1.0 mL) typically contained 50 mM Tris-HCl (pH 7.5, 1.0 mM DTT, 1.0 mM EDTA, 10 μM FAD, 10% glycerol (v/v)), 10 mM substrate, 0–0.1 mM NAD(P)H, 1.0–5.0% (v/v) DMSO, and 10 μL FMO-E solution (8 μM) at 25°C. The assay for the negative control was performed without the substrate.

Bicyclo[3.2.0]hept-2-en-6-one was used as the model substrate to study FMO-E's kinetic parameters. Both NADH and NADPH were used as the cofactor with this substrate. Then, the kinetic parameters were calculated with MATLAB (R2015a, The MathWorks, USA) based on

the Michaelis-Menten double-substrate equation (**Equation A3**).

$$v = \frac{v_{max} \cdot c_{sub} \cdot c_{NAD(P)H}}{\left(K_{M_{Sub}} + c_{sub}\right) \cdot (K_{M\_NAD(P)H} + c_{NAD(P)H})}$$
(**Equation A3**)

Like the model substrate bicyclo[3.2.0]hept-2-en-6-one, FMO-E's kinetic study towards other two cyclobutanone substrates with NADH as the cofactor were also performed at the same conditions. Then, the kinetic parameters were calculated with Origin 8.5.1 (2011, OriginLab Corporation, USA) based on the Michaelis-Menten single-substrate equation (**Equation A4**), while the NADH concentration is fixed to 0.1 mM, 10-fold higher than the K_M value for NADH.

$$v = \frac{v_{max} \cdot c_{sub}}{K_{M\_Sub} + c_{Sub}}$$
(**Equation A4**)

A 2.4   Characterization of HLADH

A 2.4.1   Effect of pH on HLADH activity and stability

The effect of pH on HLADH activity was determined by performing the activity assay at a pH range from 7.5 to 12.0. Tris–HCl buffer (7.5, 8.0, 8.5, 9.0), CHES buffer (9.0, 9.5, 10.0), sodium bicarbonate buffer (10.0, 10.5, 11.0) and disodium hydrogen phosphate buffer (11.0, 11.5, 12.0) with concentration of 50 mM were selected based on their pK_a values. The stability of HLADH was determined by incubating 500 μL of 0.1 mg/mL (2.5 μM) of the purified enzyme at 25°C in different pH (6.0, 6.5, 7.0, 7.5, 8.0, 8.5, 9.0, 9.5, 10.0, 10.5 and 11.0) buffers with concentration of 50 mM and the residual activity was detected after 24 h.

A 2.4.2   Determination of HLADH kinetic parameters

The kinetic constants were determined by measuring the initial rates with various concentrations of amino alcohol substrates. The activity assay was performed spectrophotometrically by monitoring the increase absorbance of NADH in time at 340 nm and the extinction coefficient of 6220 $M^{-1}cm^{-1}$. The reaction mixture (1.0 mL) typically contained 50 mM CHES (pH 9.0), 1.0 mM NAD^+, 0–500 mM amino alcohol substrate and 10 μL HLADH (0.85 μM) solution at 25°C. The assay for the negative control was performed without the substrate. Three aliphatic amino alcohols, 4-amino-1-butanol, 5-amino-1-pentanol and 6-amino-1-hexanol, were analyzed for the enzyme kinetics. The non-linear fitting and parameters estimations were conducted using Originlab Pro 2017 based on Michaelis-Menten equation without inhibition (**Equation A4**) or Michaelis-Menten uncompetitive substrate inhibition

equation (**Equation A5**), as the cofactor concentration is fixed. The NAD$^+$ concentrations used in the initial rates assays were predetermined to have the saturation conditions.

$$v = \frac{v_{max} \cdot c_{sub}}{K_M + c_{sub} \cdot (1 + \frac{c_{sub}}{K_{i,sub}})} \qquad \textbf{Equation A5}$$

A 2.5   Characterization of *Sm*NOX

A 2.5.1   Effect of pH on *Sm*NOX activity

The effect of pH on the *Sm*NOX activity was determined by performing the activity assay at 50 mM buffer with pH range from 6.0 to 11. KP$_i$ buffer (6.0, 6.5, 7.0, 7.5, and 8.0), CHES buffer (8.5, 9.0, 9.5, and 10.0) and sodium bicarbonate buffer (10.5 and 11.0) were selected based on their pKa values. The highest activity was normalized as 100%. The effect of pH on the stability of *Sm*NOX was determined by incubating 500 µL of 1.0 mg/mL (20 µM) of the purified enzyme in 50 mM buffer with pH from 6.0 to 11.0 at 25°C. KP$_i$ buffer (6.0, 6.5, 7.0, 7.5, and 8.0), CHES buffer (8.5, 9.0, 9.5, and 10.0) and sodium bicarbonate buffer (10.5, 11.0) were selected based on their *pK*a values. The residual activity was measured after 24 h.

A 2.5.2   Effect of temperature on *Sm*NOX long-term stability

The effect of temperature on the long-term stability of the *Sm*NOX was studied by measuring the half-life times of *Sm*NOX at different temperatures. The half-life times of *Sm*NOX at 30°C, 40°C, 50°C were determined by incubating 500 µL of 1.0 mg/mL (20 µM) of the purified enzyme in 50 mM KP$_i$ buffer (pH 7) at the above temperatures. The samples of enzyme at 30ºC were taken at 0h, 1h, 4h, 8h, 24h, 30h, 48h, 72h, samples of enzyme at 40ºC were taken at 0h, 1h, 2h, 4h, 6h, 8h, 24h, 30h and samples of enzyme at 50ºC were taken every 5 min for 1h. The residual activities were detected using the above *Sm*NOX activity assay method at 25 ºC. The half-life times ($\tau_{1/2}$) were calculated based on **Equation 2**.

A 2.5.3   Determination of *Sm*NOX kinetic parameters

The kinetic constants were determined by measuring the initial rates with various concentration of NADH. The activity assay was performed spectrophotometrically by monitoring the decrease absorbance of NADH in time at 340 nm and the extinction coefficient of 6220 M^{-1}cm^{-1}. The reaction mixture (1.0 mL) typically contained air saturated 50 mM KP$_i$ (pH 7.0), 0–0.2 mM NADH and 10 µL *Sm*NOX (0.085 µM) enzyme solution at 25°C. The non-linear fitting and parameters estimations were conducted using Originlab Pro 2017 based on Michaelis-Menten

equation without inhibition (**Equation A5**).

A 2.6   Convergent cascade reactions with FMO-E and HLADH

The reaction system (1.0 mL) in 1.5/30 mL glass vial consists of 20/100 mM ketone substrates (cyclobutanone or bicyclo[4.2.0]octan-7-one), 10/50 mM diol substrates (1,4-butanediol or cis-1,2-cyclohexanedimethanol), 1.0 mM NAD^+, 1.0/2.0 U of FMO-E, 1.0/2.0 U of HLADH, 100 mM Tris-HCl (pH 8.0). The reactions were performed at 20°C with 900 rpm (1.5 mL glass vial) or180 rpm (35 mL glass vial) shaking speed. Four negative controls (without NAD^+, without FMO-E, without HLADH and without both enzymes) were carried out at the same conditions. Samples (50 μL) were taken at the indicated time intervals (0, 1, 3, 5, 24, 48 and 72 h) through extraction (250 μL EtOAc with 2 mM methyl benzoate as the internal standard). After centrifuging (13,000 rpm; 1 min) and separating the two phases, the EtOAc layer was dried with $MgSO_4$, and then transferred to GC vials and analyzed by GC.

A 2.7   HLADH-catalyzed lactamization of amino alcohol with stoichiometric NAD^+

A 2.7.1   Effect of buffer pH on the lactamization

4-Amino-1-butanol was selected as the model substrate to investigate the influence of pH on the lactam formation. The evaluation was based on 10 mM 4-amino-1-butanol using stoichiometric amounts of cofactor (20 mM NAD^+) in 50 mM buffer with different pH values from 6.0 to 11.0. KP_i buffer (7.0, 7.5, and 8.0), CHES buffer (8.5, 9.0, 9.5, and 10.0) and sodium bicarbonate buffer (10.5 and 11.0) were selected based on their pKa values. The reaction (1 mL) took place in a GC Vial (1.5 mL) consisting of 10 mM 4-amino-1-butanol, 20 mM NAD^+, 0.1 mg/mL HLADH (0.006 U/mL, 2.5 μM) and different pH buffers. The reactions were carried out on a thermo-shaker kept at 25°C with 900 rpm shaking speed for 24 hours.

A 2.7.2   Effect of ionic strength of buffer on the lactamization

4-Amino-1-butanol was selected as the model substrate and CHES buffer (pH 9.5) as the reaction medium to investigate the influence of ionic strength on the lactam formation. The evaluation was based on 10 mM 4-amino-1-butanol using stoichiometric amounts of cofactor (20 mM NAD^+) in CHES buffer (pH 9.5) with different ionic strengths from 10 mM to 1000 mM. The reaction (1 mL) took place in a GC Vial (1.5 mL) consisting of 10 mM 4-amino-1-butanol, 20 mM NAD^+, 0.1 mg/mL HLADH (0.01 U/mL, 2.5 μM) and CHES buffer (pH 9.5) with different ionic strengths. The reactions were carried out on a thermo-shaker fixed at 25°C

with 900 rpm shaking speed for 24 hours.

A 2.8 HLADH-catalyzed lactamization of amino alcohol with *in situ* NAD⁺ regeneration

A 2.8.1 Effect of buffer pH on the lactamization

4-Amino-1-butanol was selected as the model substrate to investigate the influence of pH on the lactam formation. The evaluation was based on 10 mM 4-amino-1-butanol using SmNOX for *in situ* NAD^+ regeneration in 50 mM buffer with different pH values from 6.0 to 11.0. KP_i buffer (7.0, 7.5, and 8.0), CHES buffer (8.5, 9.0, 9.5, and 10.0) and sodium bicarbonate buffer (10.5 and 11.0) were selected based on their pKa values. The reaction (1 mL) took place in a GC Vial (1.5 mL) consisting of 10 mM 4-amino-1-butanol, 1.0 mM NAD^+, 1.0 mg/mL HLADH (0.06 U/mL, 2.5 μM), 1.0 mg/mL SmNOX (5.39 U/mL, 20 μM), and different pH buffers. The reactions were carried out on a thermo-shaker kept at 25°C with 900 rpm shaking speed for 24 hours.

A 2.8.2 Effect of ionic strength of buffer on the lactamization

4-Amino-1-butanol was selected as the model substrate and KP_i buffer (pH 8.0) as the reaction medium to investigate the influence of ionic strength on the lactam formation. The evaluation was based on 10 mM 4-amino-1-butanol using SmNOX for *in situ* NAD^+ regeneration in KP_i buffer (pH 8.0) with different ionic strengths from 10 mM to 1000 mM. The reaction (1 mL) took place in a GC Vial (1.5 mL) consisting of 10 mM 4-amino-1-butanol, 1.0 mM NAD^+, 1.0 mg/mL HLADH (0.06 U/mL, 2.5 μM), 1.0 mg/mL SmNOX (5.39 U/mL, 20 μM) and KP_i buffer (pH 8.0) with different ionic strengths. The reactions were carried out on a thermo-shaker fixed at 25°C with 900 rpm shaking speed for 24 hours.

A 2.8.3 Substrate scope of HLADH-catalyzed lactamization of amino alcohol

The substrate scope of HLAH-catalyzed oxidative lactamization was investigated under the optimized reaction conditions. Two further aliphatic amino alcohols (5-amino-1-pentanol and 6-amino-1-hexanol) and two aromatic amino alcohols ((2-(2-aminoethyl)phenyl)-methanol and (2-(aminomethyl)phenyl) methanol) were evaluated. The lactamization reactions (1.0 mL) took place in a GC vial (1.5 mL) consisting of 10 mM amino alcohol substrate, 1.0 mM NAD^+, 1.0 mg/mL HLADH (2.5 μM), 1.0 mg/mL SmNOX (20 μM), pH 8.0, 50 mM KP_i buffer. The reactions were performed on a shaker at 25°C with 900 rpm shaking speed for 24 hours.

A 2.9   Design of Experiments (DoE) for evaluation of key parameters of the reaction

A 2.9.1   Screening of reaction parameters

Design of Experiments (DoE) approach was used to screen the lactamization reaction with NAD+ regeneration with several key factors involved. For screening purposes, eight reaction parameters (i.e., T, O_2, pH, c(4-amino-1-butanol), c(HLADH), c(SmNOX), c(NAD^+), t) were evaluated for their impacts on the target response (i.e. product yield). A 'fractional factorial design' as a balanced subset of the full factorial at two levels was developed using the software program Design-Expert® Software Version 10 (Stat-Ease, USA).

Table A2. Summary of the DoE for screening of the reaction parameters

Objective	Screening
Process Model	Linear
Design	Fractional Factorial
Levels	2
Runs in Design	16
Center Points	3
N = Number of experiments	19

The design developed for the screening of eight reaction parameters is shown in **Table A3**.

Table A3. List of experiments designed based on a 'fraction factorial design' for the screening of reaction parameters

Reaction No	T [°C]	O₂[a] [-]	pH [-]	c(4-amino-1-butanol) [mM]	c(HLADH) [mg/mL]	c(SmNOX) [mg/mL]	c(NAD⁺) [mM]	t [h]	Product yield [%]
1	25	19	9.5	55	0.55	0.55	5.05	36	1.47
2	25	19	9.5	55	0.55	0.55	5.05	36	1.81
3	20	34	7	10	1	1	0.1	48	3.70
4	30	34	12	10	1	0.1	0.1	24	0.20
5	20	4	12	100	1	0.1	0.1	48	0.14
6	30	4	12	100	0.1	0.1	10	24	0.28
7	30	34	12	100	1	1	10	48	0.18
8	30	34	7	100	0.1	0.1	0.1	48	0.60
9	20	4	7	100	0.1	1	10	48	0.42
10	20	4	12	10	1	1	10	24	32.58
11	30	4	7	10	1	0.1	10	48	21.37
12	30	34	7	10	0.1	1	10	24	1.72
13	20	34	7	100	1	0.1	10	24	11.32
14	20	4	7	10	0.1	0.1	0.1	24	3.22
15	25	19	9.5	55	0.55	0.55	5.05	36	2.20
16	30	4	12	10	0.1	1	0.1	48	0.70
17	20	34	12	100	0.1	1	0.1	24	0.43
18	20	34	12	10	0.1	0.1	10	48	2.82
19	30	4	7	100	1	1	0.1	24	5.02

[a] Oxygen amount represented as the headspace ratio $= \dfrac{Headspace\ volume\ (mL)}{Volume\ of\ the\ reaction\ mixture\ (mL)}$

A 2.9.2 Experimental procedure for performing the experiments designed for screening

Stock solutions of 4-amino-1-butanol (1 M), NAD⁺ (10 mM, 500 mM and 1000 mM) were prepared in distilled water. Target protein concentrations in the experiments were for HLADH, 0.1 mg/mL (0.006 U/mL), 0.55 mg/mL (0.033 U/mL) and 1 mg/mL (0.06 U/mL), and for SmNOX, 0.1 mg/mL (0.539 U/mL), 0.55 mg/mL (2.965 U/mL) and 1 mg/mL (5.39 U/mL). The stock solutions of 4-amino-1-butanol (10 µL, 55 µL and 100 µL), and buffer (729.4–963.94 µL), were added into the capped glass vials (5 mL, 20 mL or 35 mL of total volume) containing HLADH (0.1–1 mg) and SmNOX (0.1–1 mg). Reactions were started by the addition of NAD⁺ (10 µL, 10.05 µL). The initial reaction conditions were: 10–100 mM 4-amino-1-butanol, 0.1–10 mM NAD⁺, 0.1–1 mg/mL (0.006–0.06 U/mL) HLADH and 0.1–1 mg/mL (0.539–5.39 U/mL) SmNOX (**Table A3**). Reaction mixtures (19 reactions, 1 mL of total volume each) were kept in capped glass vials (5 mL, 20 mL and 35 mL) at 20–30°C and orbitally shaken at 180 rpm.

A 2.10   Hydrolysis of lactone and lactam products

A 2.10.1 Hydrolysis of γ-butyrolactone

γ-Butyrolactone was investigated for its stability in the aqueous medium. It was prepared as 20 mM solution in 100 mM Tris-HCl (pH 8.0 and pH 9.0). 1 mL of these solutions in 1.5 mL GC vials were put on a thermo-shaker kept at 20°C and 900 rpm shaking speed simulating the reaction condition. Samples were taken every day and the residual product concentration was assayed by GC.

A 2.10.2 Hydrolysis of lactams

Three lactam products, γ-butyrolactam, δ-valerolactam and ε-caprolactam were investigated for their stability in the aqueous medium. They were prepared as 10 mM solution in three kinds of pH (7.0, 9.5 and 11.0) in potassium phosphate buffer, CHES buffer and sodium bicarbonate buffer with concentration of 50 mM. 1 mL of these solutions in 1.5 mL GC vials were put on a thermo-shaker kept at 25°C and 900 rpm shaking speed simulating the reaction condition. Samples were taken every day and the residual product concentration was assayed by GC.

A 2.11   Sample preparation for gas chromatography (GC) analysis

Samples (25/50 μL) were taken at the indicated time intervals through extraction (250 μL EtOAc with 2 mM methyl benzoate as the internal standard). After centrifuging (13,000 rpm; 1 min) and separating the two phases, the EtOAc layer was dried with anhydrous $MgSO_4$. To analyse cyclobutanone, the use of EtOAc at high purity (99.8%) was especially important. All reaction components were then analyzed by gas chromatography (GC) and the methods were developed with Hydrodex ß-PM (25 m x 0.25 mm x 0.25 μm) column. Peaks were identified by standards.

A 2.12   Synthesis of reference compounds

[1]H and ^{13}C spectra were recorded from $CDCl_3$ solutions on a Bruker Advance UltraShield 400 (400 MHz) spectrometer and chemical shifts (δ) are reported in ppm using tetramethylsilane as internal standard coupling constants (J) are in Hertz (Hz). The following abbreviations were used to explain the multiplicities: s = singlet, d = doublet, q = quartet, m = multiplet.

A 2.12.1 Synthesis of bicyclo[4.2.0]octan-7-one

Synthesis of bicyclo[4.2.0]octan-7-one was performed as previously described in literature[230]. Analytical data was in accordance with literature.

^{1}H-NMR (400 MHz, CDCl$_3$): δ_H = 1.00 – 1.25 (m, 3H), 1.34 – 1.47 (m, 1H), 1.48 – 1.62 (m, 2H), 1.88 – 1.99 (m, 1H), 2.08 – 2.19 (m, 1H), 2.37 – 2.52 (m, 2H), 3.06 – 3.17 (m, 1H), 3.20 – 3.31 (m, 1H) ppm.

^{13}C-NMR (100 MHz, CDCl$_3$): δ_C = 21.4, 22.5, 22.6, 22.7, 29.6, 52.3, 56.8, 210.2 ppm.

A 2.12.2 Synthesis of hexahydro-2(3H)-benzofuranone

Bicyclo[4.2.0]octan-7-one (113 mg, 0.91 mmol) was dissolved in dichloromethane (0.5 ml) and added to a suspension of mCPBA (77%, 306 mg, 1.5 equiv.) in dichloromethane (0.5 ml), which formed a clear and colorless solution after a few minutes of stirring at room temperature. Over the course of the reaction a thick white suspension forms due to precipitation of the corresponding benzoic acid. Stirring was continued for 18 h until complete conversion of starting material could be detected by TLC. Then triethylamine (1.0 mL) was added dropwise, followed by addition of H$_2$O (1.0 mL) and the biphasic mixture was stirred for 30 min. The organic layer was diluted with DCM (10 mL), washed with H$_2$O (2 x 10 mL), 2N HCl (10 mL) and brine, then dried and concentrated. Crude material was purified by column chromatography (7 g SiO$_2$, LP/EtOAc = 20:1-3:1) to obtain the product as colorless oil in 66% yield.

^{1}H-NMR (400 MHz, CDCl$_3$): δ_H = 1.22 – 1.29 (m, 2H), 1.43 – 1.54 (m, 2H), 1.60 – 1.76 (m, 3H), 2.01 – 2.13 (m, 1H), 2.25 (dd, J = 16.8, 2.7 Hz, 1H), 2.32 – 2.44 (m, 1H), 2.61 (dd, J = 16.7, 6.8 Hz, 1H), 4.51 (q, J = 4.2 Hz, 1H) ppm.

^{13}C-NMR (100 MHz, CDCl$_3$): δ_C = 20.0, 22.9, 27.3, 27.9, 35.0, 37.6, 79.3, 177.7 ppm.

Analytical data in accordance with literature[231].

A 2.13 Preparative synthesis of γ-butyrolactam for NMR analysis

Synthesis of γ-butyrolactam was performed in 100 mL scale using 10 mM 4-amino-1-butanol, 1.0 mM NAD$^+$, HLADH cell free extract (14 U) and *Sm*NOX cell free extract (450 U) in 50 mM pH 8.0 KP$_i$ buffer stirring with overhead impeller at room temperature. After 24 hours the reaction mixture was stopped and extracted with the same volume of EtOAc for 3 times. The pooled organic layer was then dried over anhydrous Na$_2$SO$_4$ and filtered with a microfiltration membrane (PVDF). The clear organic phase was removed firstly by a rotary evaporator under reduced pressure and further by a vacuum over at room temperature.

The sample was analysed by ^{1}H-NMR and ^{13}C-NMR by preparation of 10 mg of the sample in 1 mL chloroform-d1. The NMR spectrum was recorded at 400 MHz (^{1}H and ^{13}C).

B   APPENDIX

B 1   Sequence of enzymes used in this work

FMO-E from *Rhodococcus jostii* RHA1

```
MTTTFSDTDLRTDAQAWLDGFSRFLAAELAPTAVFAPQAYWRDVLAFTGDLRTFSDEIPAELLRRQELTK
ATNIRIAEDRTPPRLVERAGIPCLEVIFEFDTLAGSAVGVARLVDVPERGLLVRSLFTTLDQLADHPERT
GEHRPVGQADSSKFGGPNWLDRRIAAQAYENRDPDVLIVGGGQSGLTLAARLGQLDVDALVVDTHARPGD
NWRTRYHALTLHNAVWLNDLPYMPFPATWPQFVPKDKLAGWFEAYVEAMEINFWGTTAFIGGDYDEQSQS
WVARVRRGDGTVRTLRPKHVVIATGVSGIPYVPELPGLSQFAGRTLHSSEYDDANDFAGQRVVIIGTGNS
AHDVAQDLHAHGIDVTMVQRSSTTIVSVDPSAAAADASYLTAPTLEDCDLLSMATVYPDLYTGSQMITAT
MKELDKDLVAALNRIGFRTDYGEEDTGQQMKFMRRGGGYYLNVGCSDLLISGQVGLVQYADTAGFVAEGL
SLTNGDVVEADAVILATGYQTQQEGVRALLGDEIADAVGPIWGYDDEGEVRNTWRRTAQPGLWFSSGNFQ
LCRIYSKVLAMQIRTELDNG
```

Horse liver alcohol dehydrogenase (HLADH)

```
MSTAGKVIKCKAAVLWEEKKPFSIEEVEVAPPKAHEVRIKMVATGICRSDDHVVSGTLVTPLPVIAGHEA
AGIVESIGEGVTTVRPGDKVIPLFTPQCGKCRVCKHPEGNFCLKNDLSMPRGTMQDGTSRFTCRGKPIHH
FLGTSTFSQYTVVDEISVAKIDAASPLEKVCLIGCGFSTGYGSAVKVAKVTQGSTCAVFGLGGVGLSVIM
GCKAAGAARIIGVDINKDKFAKAKEVGATECVNPQDYKKPIQEVLTEMSNGGVDFSFEVIGRLDTMVTAL
SCCQEAYGVSVIVGVPPDSQNLSMNPMLLLSGRTWKGAIFGGFKSKDSVPKLVADFMAKKFALDPLITHV
LPFEKINEGFDLLRSGESIRTILTF
```

NADH oxidase from *Streptococcus mutans* variant V193R/V194H (*Sm*NOX)

```
MSKIVIVGANHAGTAAINTILDNYGSENEVVVFDQNSNISFLGCGMALWIGKQISGPQGLFYADKESLEA
KGAKIYMESPVTAIDYDAKRVTALVNGQEHVESYEKLILATGSTPILPPIKGAAIKEGSRDFEATLKNLQ
FVKLYQNAEDVINKLQDKSQNLNRIAVVGAGYIGVELAEAFKRLGKEVILIDRHDTCLAGYYDQDLSEMM
RQNLEDHGIELAFGETVKAIEGDGKVERIVTDKASHDVDMVILAVGFRPNTALGNAKLKTFRNGAFLVDK
KQETSIPDVYAIGDCATVYDNAINDTNYIALASNALRSGIVAGHNAAGHKLESLGVQGSNGISIFGLNMV
STGLTQEKAKRFGYNPEVTAFTDFQKASFIEHDNYPVTLKIVYDKDSRLVLGAQMASKEDMSMGIHMFSL
AIQEKVTIERLALLDYFFLPHFNQPYNYMTKAALKAK
```

ADH from *Rhodococcus ruber* DSM 44541 (ADH-A)

```
MKAVQYTEIGSEPVVVDIPTPTPGPGEILLKVTAAGLCHSDIFVMDMPAAQYAYGLPLTLGHEGVGTVAELGEGVT
GFGVGDAVAVYGPWGCGACHACARGRENYCTRAADLGITPPGLGSPGSMAEYMIVDSARHLVPIGDLDPVAAAPLT
DAGLTPYHAISRVLPLLGPGSTAVVIGVGGLGHVGIQILRAVSAARVIAVDLDDDRLALAREVGADAAVKSGAGAA
DAIRELTGGQGATAVFDFVGAQSTIDTAQQVVAVDGHISVVGIHAGAHAKVGFFMIPFGASVVTPYWGTRSELMEV
VALARAGRLDIHTETFTLDEGPAAYRRLREGSIRGRGVVVP
```
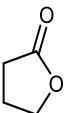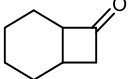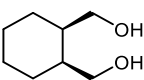
ADH from *Thermus sp.* ATN1 (TADH)
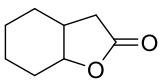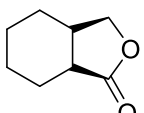
MRAVVFENKERVAVKEVNAPRLQHPLDALVRVHLAGICGSDLHLYHGKIPVLPGSVLGHEFVGQVEAVGEGIQDLQ
PGDWVVGPFHIACGTCPYCRRHQYNLCERGGVYGYGPMFGNLQGAQAEILRVPFSNVNLRKLPPNLSPERAIFAGD
ILSTAYGGLIQGQLRPGDSVAVIGAGPVGLMAIEVAQVLGASKILAIDRIPERLERAASLGAIPINAEQENPVRRV
RSETNDEGPDLVLEAVGGAATLSLALEMVRPGGRVSAVGVDNAPSFPFPLASGLVKDLTFRIGLANVHLYIDAVLA
LLASGRLQPERIVSHYLPLEEAPRGYELFDRKEALKVLLVVRG
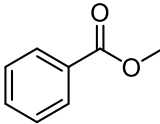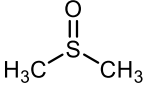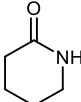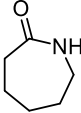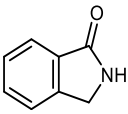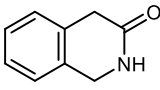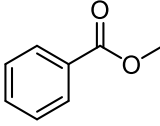
ADH from *Thermoanaerobacter ethanolicus* (*Te*SADH)

MKGFAMLSIGKVGWIEKEKPAPGPFDAIVRPLAVAPCTSDIHTVFEGAIGERHNMILGHEAVGEVVEVGSEVKDFK
PGDRVVVPAITPDWWTSEVQRGYHQHSGGMLAGWKFSNVKDGVFGEFFHVNDADMNLAHLPKEIPLEAAVMIPDMM
TTGFHGAELADIELGATVAVLGIGPVGLMAVAGAKLRGAGRIIAVGSRPVCVDAAKYYGATDIVNYKDGPIESQIM
NLTEGKGVDAAIIAGGNADIMATAVKIVKPGGTIANVNYFGEGEVLPVPRLEWGCGMAHKTIKGGLCPGGRLRMER
LIDLVFYKPVDPSKLVTHVFQGFDNIEKAFMLMKDKPKDLIKPVVILA

B 2   GC methods and spectra

Table B1. GC methods used in this work.

Entry	Chemical		Temperature profile			t_R [min]
			R [°C/min]	T [°C]	H [min]	
1	Cyclobutanone		-	70	5	2.9
			20	230	0	
			R [°C/min]	T [°C]	H [min]	
2	1,4-Butanediol		-	70	5	10.7
			20	230	0	
			R [°C/min]	T [°C]	H [min]	
3	γ-Butyrolactone (GBL)		-	70	5	9.2
			20	230	0	
			R [°C/min]	T [°C]	H [min]	
4	Bicyclo[4.2.0]octan-7-one		-	100	5	11.4
			2.3	150	0	
			50	230	2	
			R [°C/min]	T [°C]	H [min]	
5	Cis-1,2-Cyclohexanedimethanol		-	100	5	29.5
			2.3	150	0	
			50	230	2	
			R [°C/min]	T [°C]	H [min]	
6	Octahydrobenzofuran-2-one (normal lactone)		-	100	5	27.0 (n.d.)
			2.3	150	0	27.1 (3a*S*,7a*S*)
			50	230	2	
7	(3a*R*,7a*S*)-Hexahydroisobenzofuran-1(3H)-one		R [°C/min]	T [°C]	H [min]	
			-	100	5	
			2.3	150	0	25.9

			R [°C/min]	T [°C]	H [min]	
	(abnormal lactone)		50	230	2	
			R [°C/min]	T [°C]	H [min]	
			-	70	5	9.9
8	Methyl benzoate (internal standard)		20	230	0	
			R [°C/min]	T [°C]	H [min]	
			-	100	5	8.7
			2.3	150	0	
			50	230	2	
			R [°C/min]	T [°C]	H [min]	
			-	70	5	8.2
9	Dimethy sulfoxide (DMSO)		20	230	0	
			R [°C/min]	T [°C]	H [min]	
			-	100	5	4.7
			2.3	150	0	
			50	230	2	
10	γ-Butyrolactam		R [°C/min]	T [°C]	H [min]	
			-	70	5	11.4
			20	230	7	
11	-Valerolactam		R [°C/min]	T [°C]	H [min]	
			-	70	5	12.3
			20	230	7	
12	-Caprolactam		R [°C/min]	T [°C]	H [min]	
			-	70	5	12.9
			20	230	7	
13	1-Isoindolinone		R [°C/min]	T [°C]	H [min]	
			-	100	5	15.6
			20	200	0	
			2	230	5	
14	3,4-Dihydro-2H-isoquinolin-1-one		R [°C/min]	T [°C]	H [min]	
			-	100	5	16.3
			20	200	0	
			2	230	5	
15	Methyl benzoate (internal standard)		R [°C/min]	T [°C]	H [min]	
			-	70	5	9.8
			20	230	7	
			R [°C/min]	T [°C]	H [min]	
			-	100	5	7.2
			20	200	0	
			2	230	5	

Detector: FID; Carrier gas: N2; T (Injector): 250°C; T (Detector): 250°C; Total flow rate: 10.9 mL/min; Column flow rate: 0.4 mL/min; Split ratio: 20; Pressure: 0.413 bar. GC column: HYDRODEX β-PM (25 m × 0.25 mm).
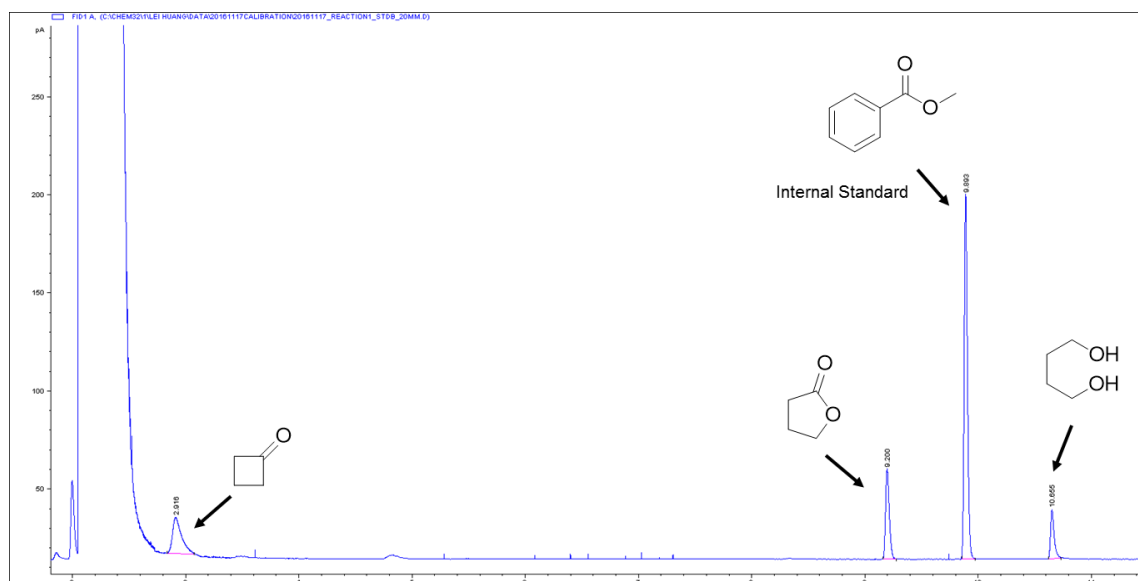
Figure B1. A GC chromatogram example of a calibration sample of cyclobutanone, 1,4-butanediol and γ-butyrolactone with an internal standard (methyl benzoate).
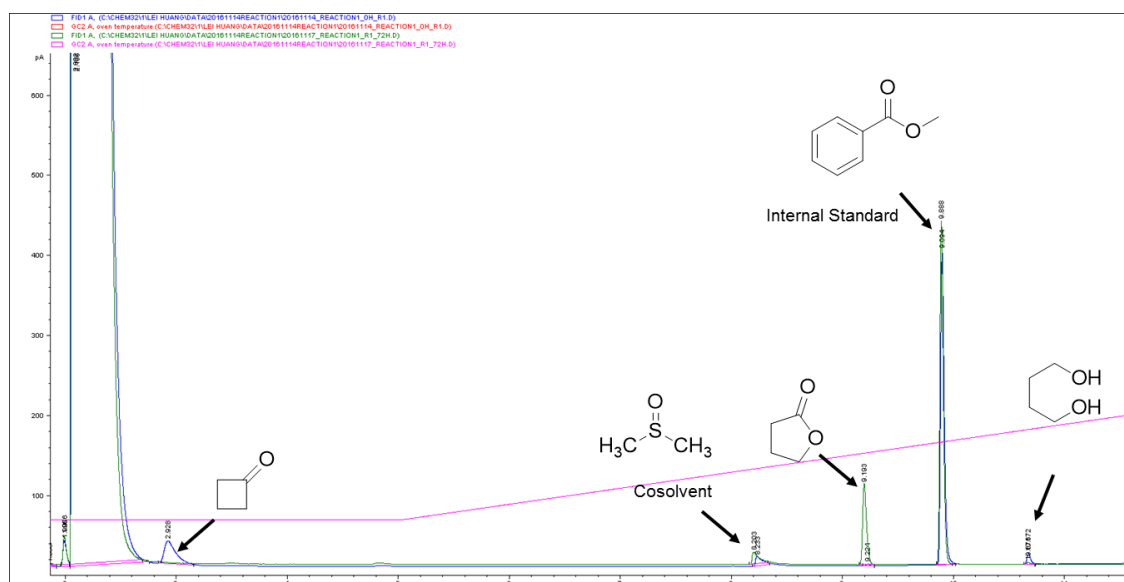
Figure B2. The chromatograms of reaction samples (blue/green= time 0/72 h). Reaction conditions: c(cyclobutanone) = 20 mM, c(1,4-butanediol) = 10 mM, c(NAD$^+$) = 1 mM, c(FMO-E) = 1.0 U (16.6 μM), c(HLADH) = 1.0 U (7.3 μM), buffer: Tris-HCl (100 mM, pH 8.0), 180 rpm, T = 20°C. Reactions (1 mL in total) run in 30 mL glass-vials.
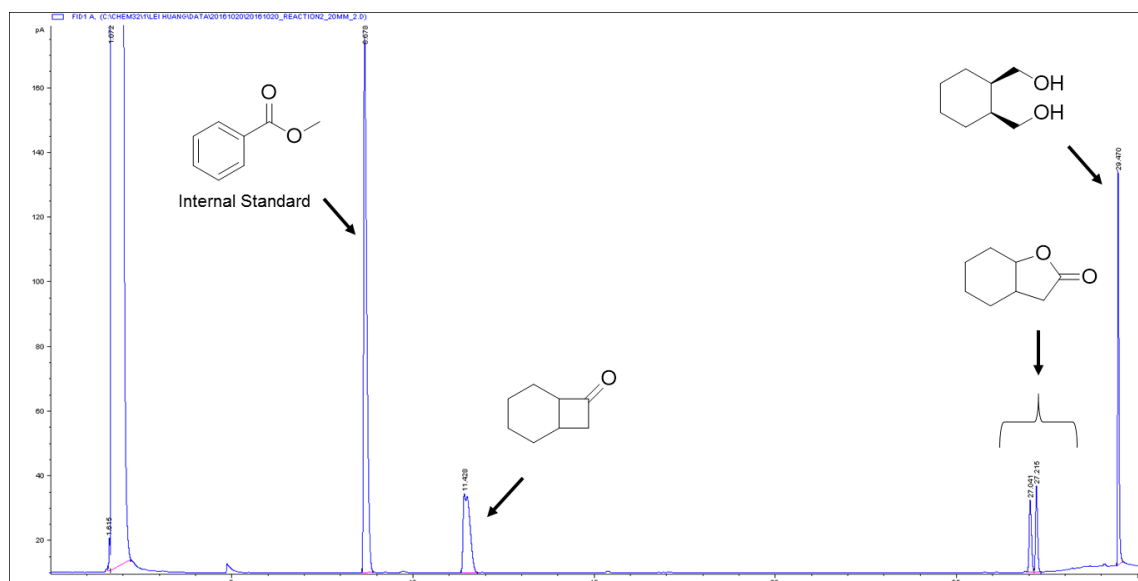
Figure B3. A GC chromatogram example of a calibration sample of bicyclo[4.2.0]octan-7-one, *cis*-1,2-cyclohexanedimethanol and octahydrobenzofuran-2-one with an internal standard (methyl benzoate). Baseline separation of bicyclo[4.2.0]octan-7-one was not possible.
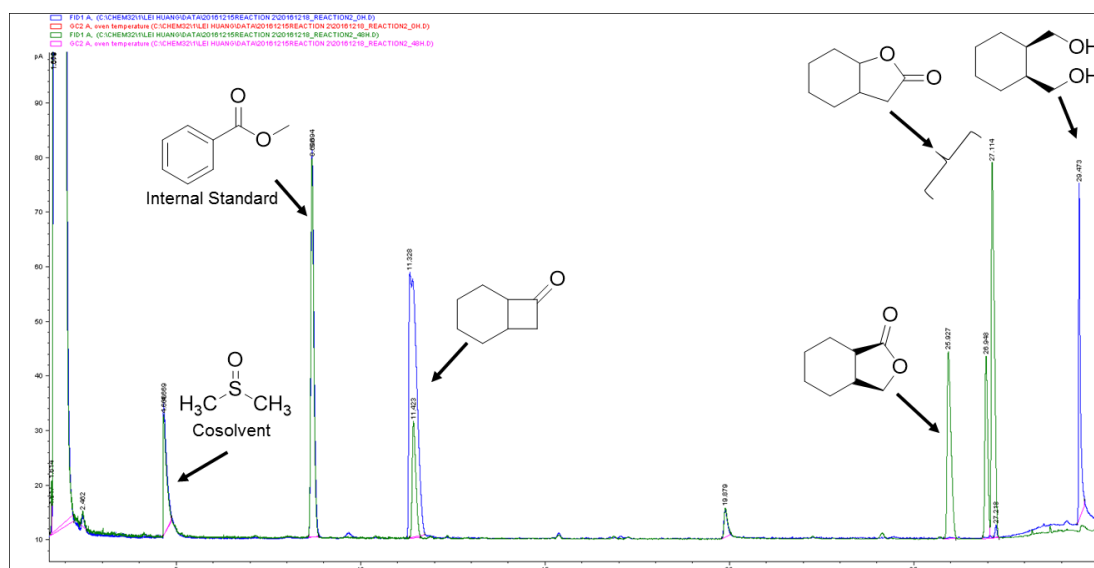
Figure B4. The chromatograms of reaction samples (blue/green= time 0/48 h). Reaction conditions: c(Bicyclo[4.2.0]octan-7-one) = 20 mM, c(cis-1,2-cyclohexanedimethanol) = 10 mM, c(NAD$^+$) = 1 mM, c(FMO-E) = 1 U (16.6 µM), c(HLADH) = 1 U (7.3 µM), buffer: Tris-HCl (100 mM, pH 8.0), 180 rpm, T = 20°C. Reactions (1 mL in total) run in 30 mL glass-vials.
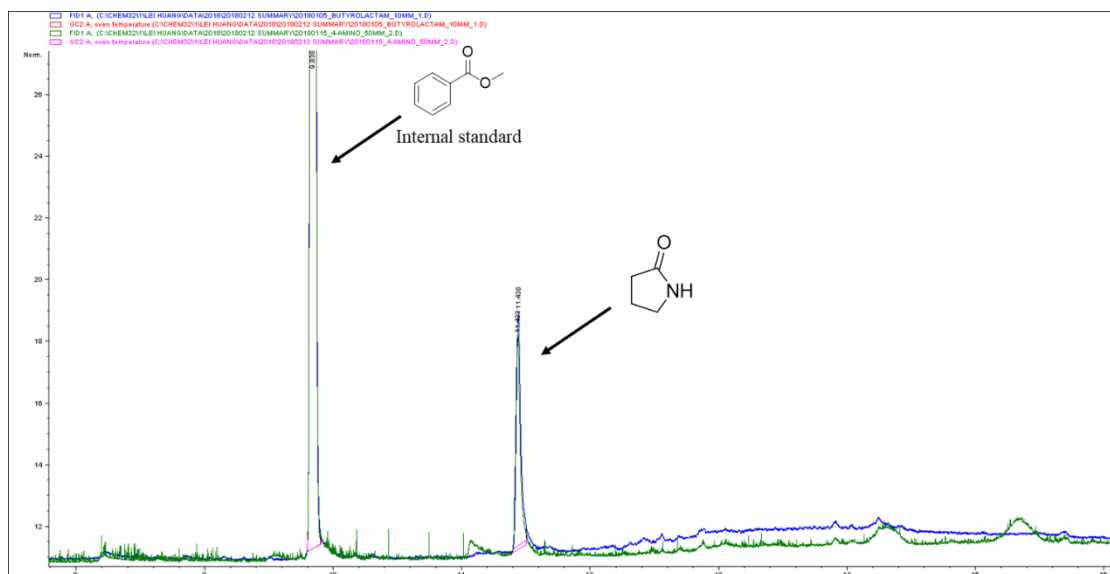
Figure B5. The chromatograms of reference γ-butyrolactam and reaction sample (blue/green= 10 mM γ-butyrolactam/sample of 24 h). Reaction conditions: c(4-amino-1-butanol) = 10 mM, c(NAD$^+$) = 1 mM, c(HLADH) = 1.0 mg/mL, c(SmNOX) = 1.0 mg/mL, buffer: 50 mM pH 8.0 KP$_i$, 900 rpm, T = 25°C, t = 24 h.
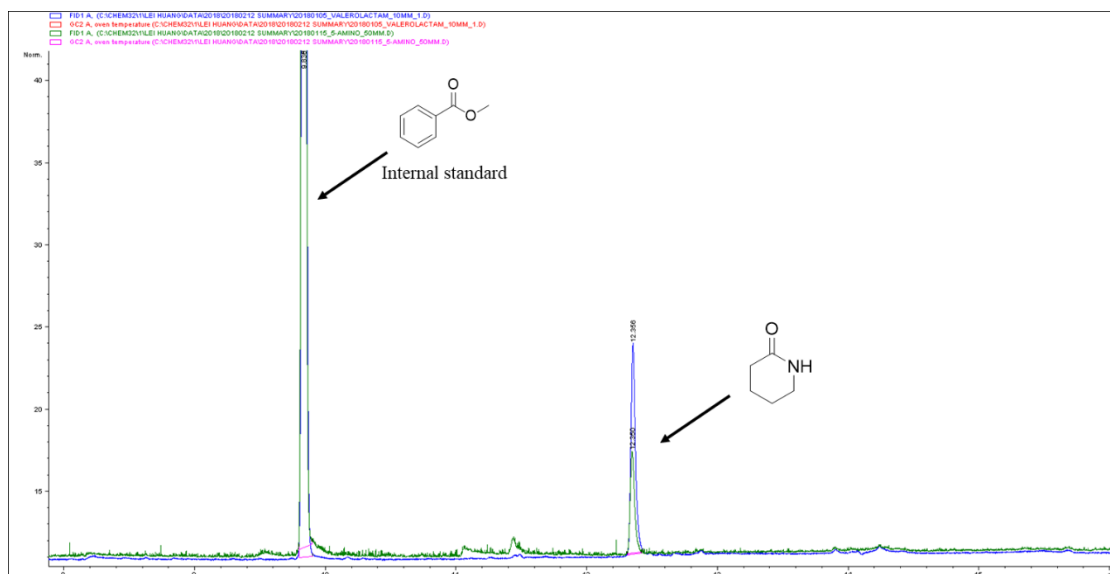
Figure B6. The chromatograms of reference δ-valerolactam and reaction sample (blue/green= 10 mM δ-valerolactam/sample of 24 h). Reaction conditions: c(5-amino-1-pentanol) = 10 mM, c(NAD$^+$) = 1 mM, c(HLADH) = 1.0 mg/mL, c(SmNOX) = 1.0 mg/mL, buffer: 50 mM pH 8.0 KP$_i$, 900 rpm, T = 25°C, t = 24 h.
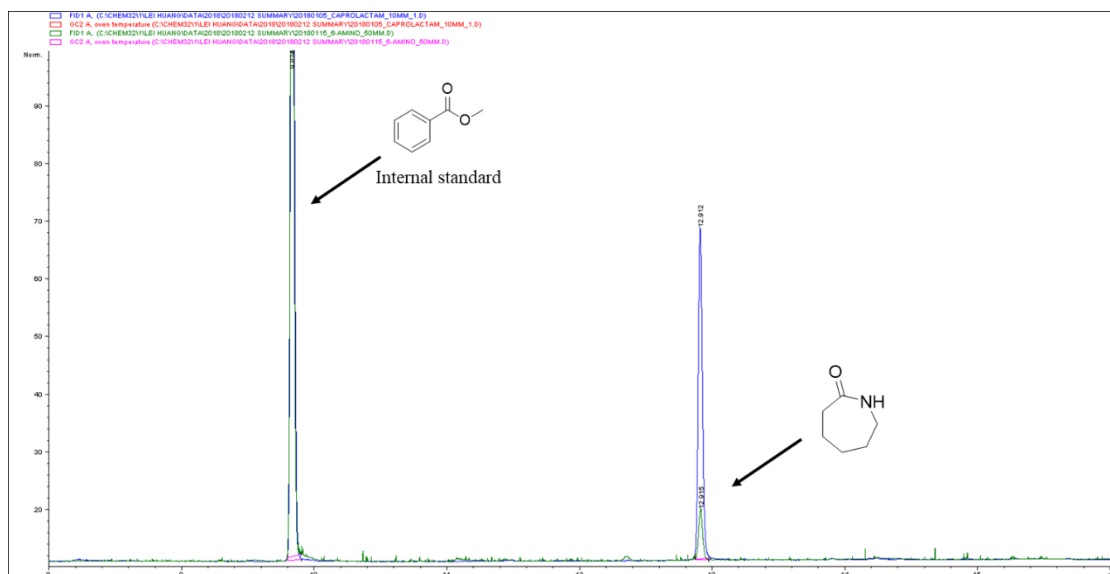
Figure B7. The chromatograms of reference ε-caprolactam and reaction sample (blue/green= 10 mM ε-caprolactam/sample of 24 h). Reaction conditions: c(6-amino-1-hexanol) = 10 mM, c(NAD$^+$) = 1 mM, c(HLADH) = 1.0 mg/mL, c(SmNOX) = 1.0 mg/mL, buffer: 50 mM KP$_i$ (pH 8.0), 900 rpm, 25°C, 24 h.
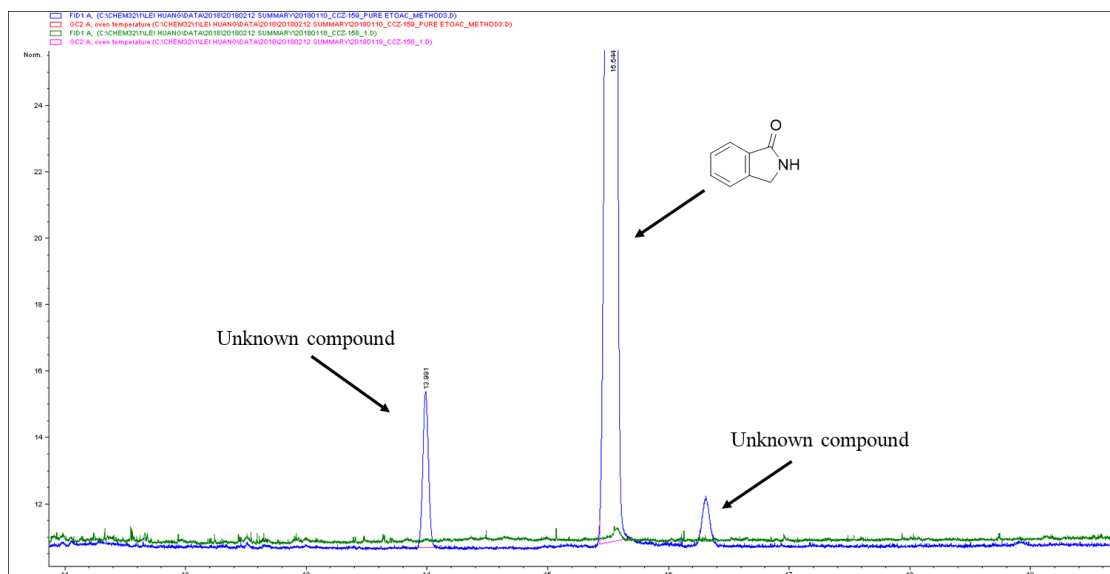
Figure B8. The chromatograms of reference 1-isoindolinone and reaction sample (blue/green= 10 mM 1-isoindolinone/sample of 24 h). Reaction conditions: c((2-(2-aminoethyl)phenyl)-methanol) = 10 mM, c(NAD$^+$) = 1 mM, c(HLADH) = 1.0 mg/mL, c(SmNOX) = 1.0 mg/mL, buffer: 50 mM KP$_i$ (pH 8.0), 900 rpm, 25°C, 24 h.
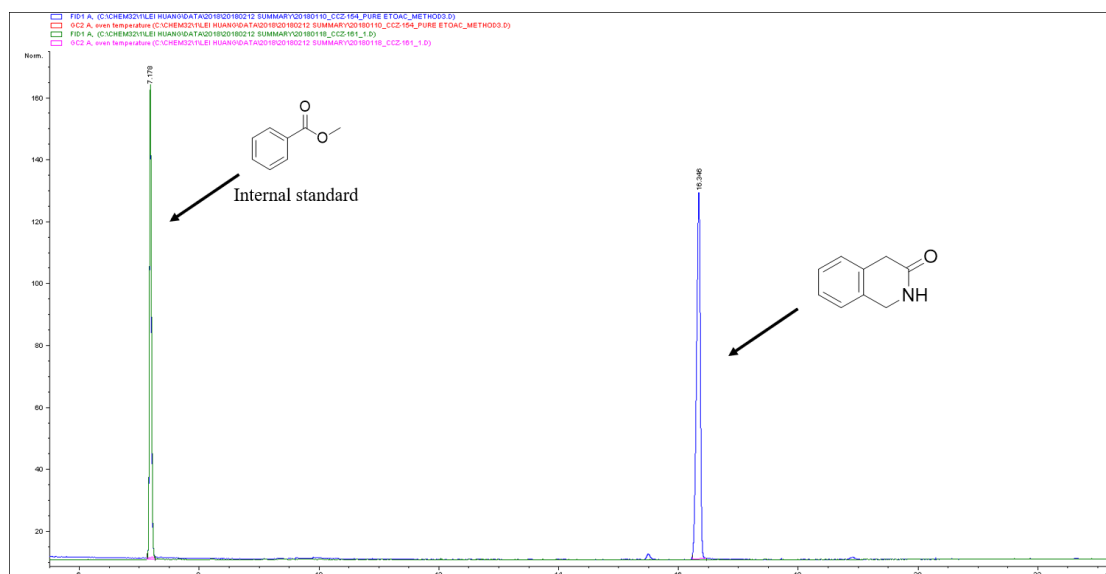
Figure B9. The chromatograms of reference 3,4-dihydro-2H-isoquinolin-1-one and reaction sample (blue/green= 10 mM 3,4-dihydro-2H-isoquinolin-1-one/sample of 24 h). Reaction conditions: c((2-(aminomethyl)phenyl)methanol) = 10 mM, c(NAD$^+$) = 1 mM, c(HLADH) = 1.0 mg/mL, c(*Sm*NOX) = 1.0 mg/mL, buffer: 50 mM KP$_i$ (pH 8.0), 900 rpm, 25°C, 24 h.

B 3   NMR spectra
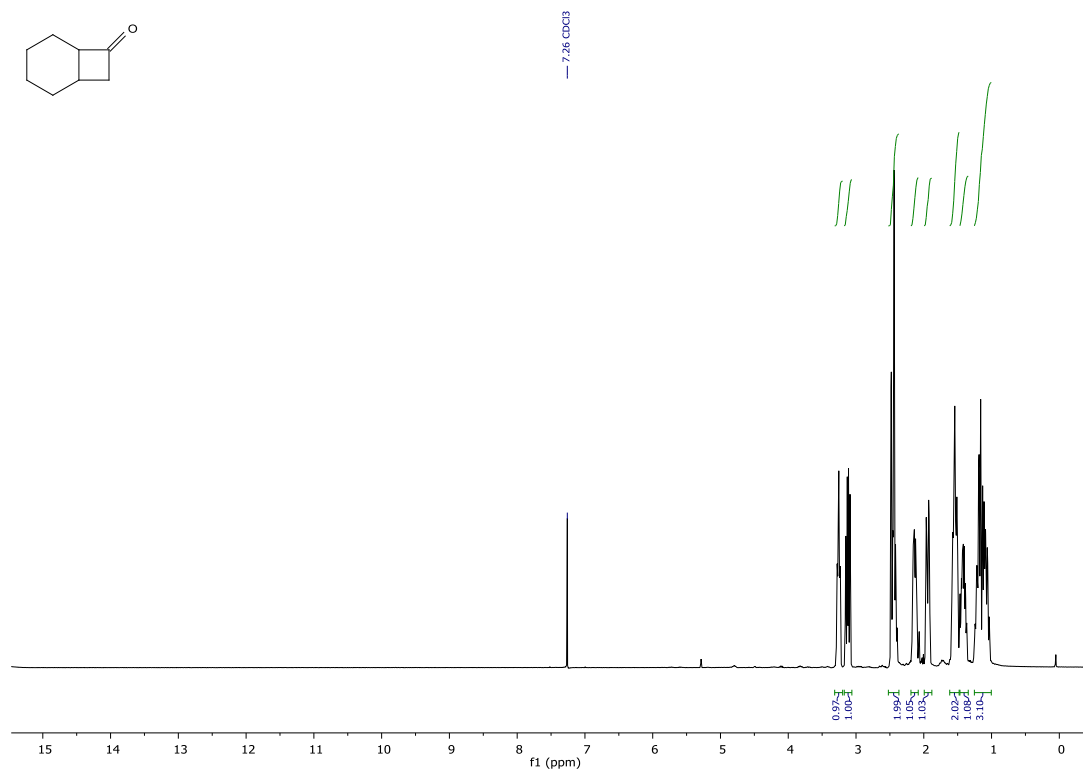
Figure B10. ^{1}H NMR of synthesized bicyclo[4.2.0]octan-7-one. The NMR measurement was done by TU Wien.
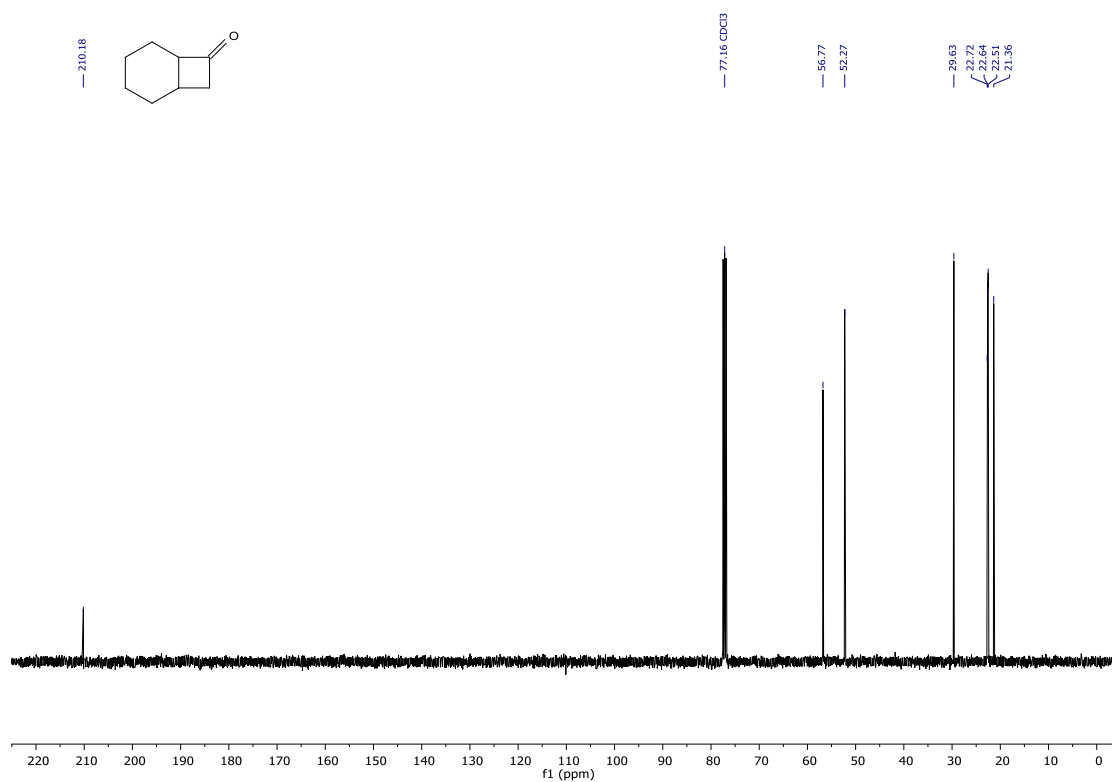
Figure B11. ^{13}C NMR of synthesized bicyclo[4.2.0]octan-7-one. The NMR measurement was done by TU Wien.
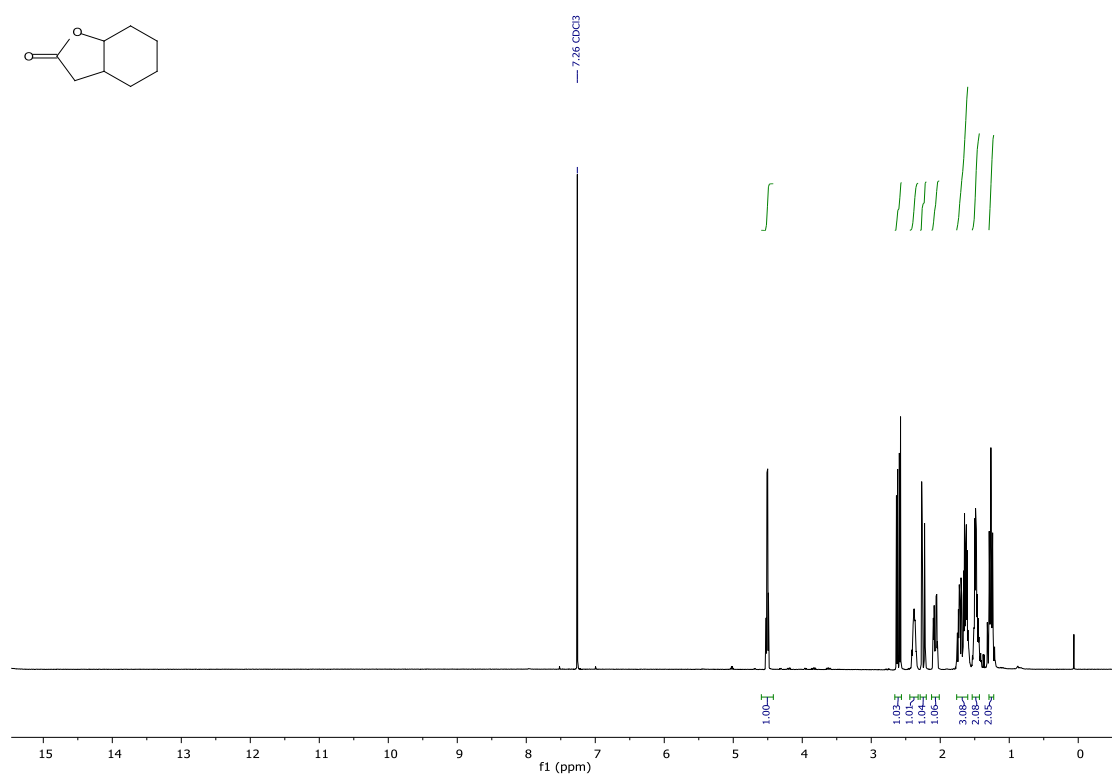
Figure B12. ^{1}H NMR of synthesized lactone. The NMR measurement was done by TU Wien.
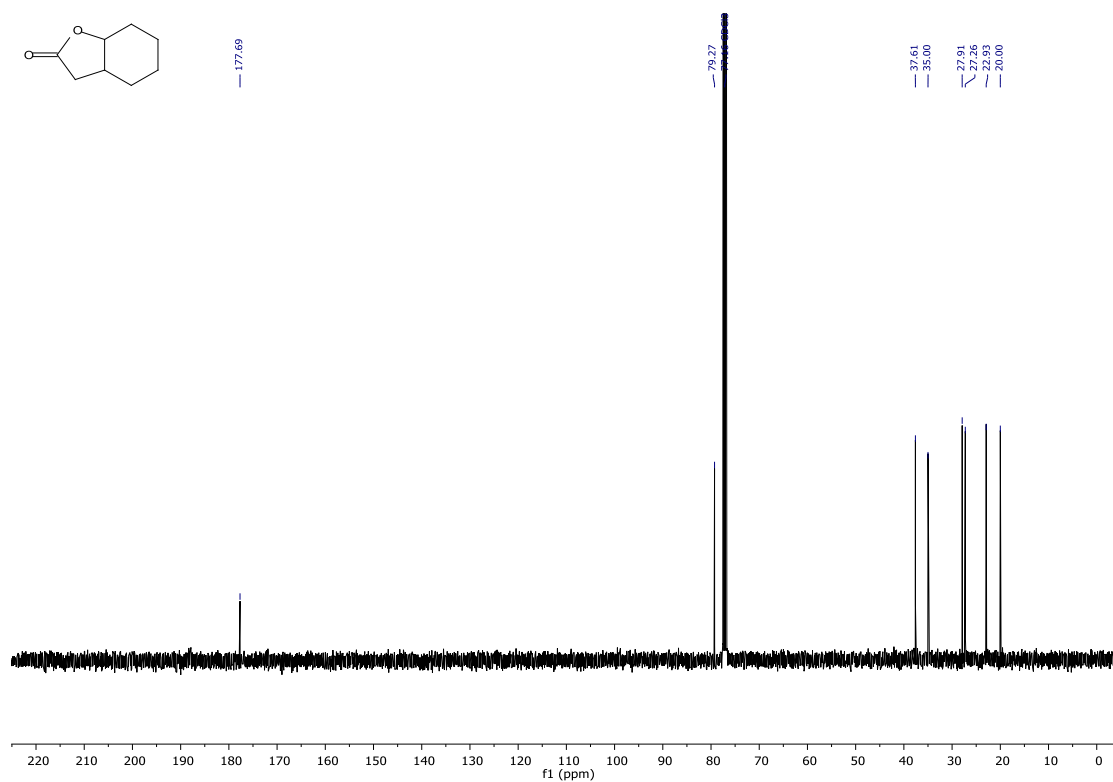
Figure B13. ^{13}C NMR of synthesized lactone. The NMR measurement was done by TU Wien.
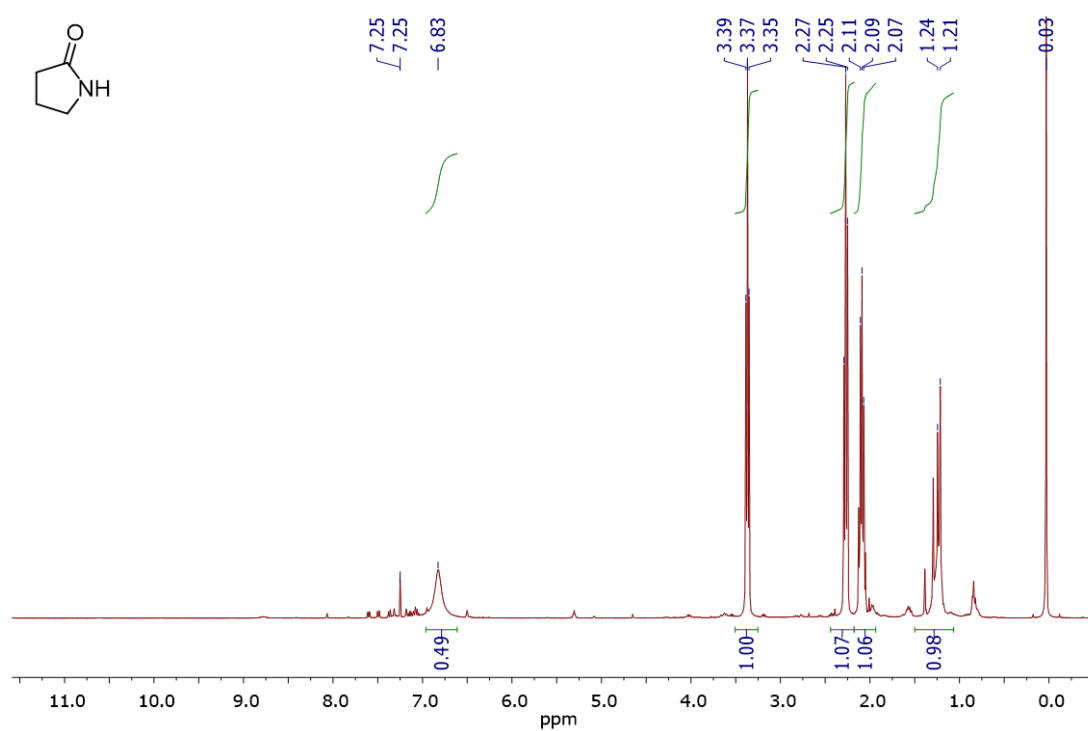
Figure B14. ^{1}H NMR of synthesized γ-butyrolactam. The NMR measurement was done by TU Delft.

106
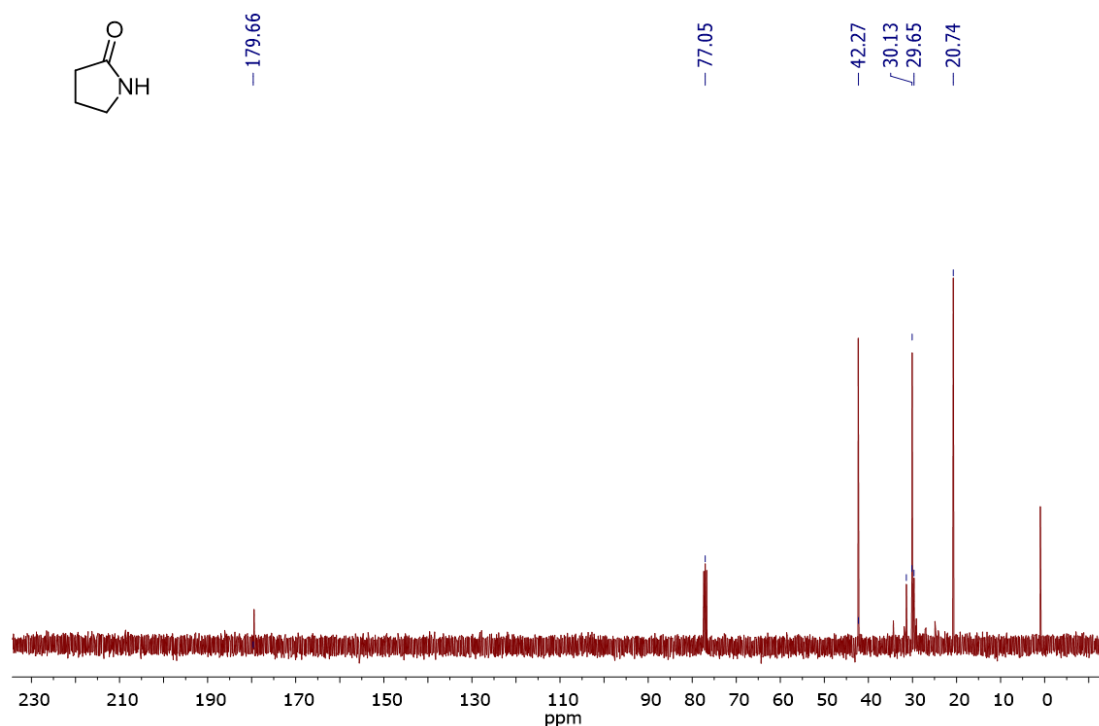
Figure B15. ^{13}C NMR of synthesized γ-butyrolactam. The NMR measurement was done by TU Delft.

B 4   Matlab script

FMO-E kinetic assay with Michaelis-Menten double-substrate equation Matlab program 1

```
clc
Dir = 'C:\Users\clh1750\Desktop\2016-05-31 Kinetics\';
File = 'MMKineticFMO.xlsx';

% Loading rates and concentrations

c_Sub = xlsread(File, 'Sheet2', 'G68:G85');  % Substrate
c_NADH = xlsread(File, 'Sheet2', 'H68:H85');  % NADH

conc = [c_Sub c_NADH];
rate = xlsread(File, 'Sheet2', 'I68:I85');  % Reaction rate

% Startparameters

vmax = 3;    % U/mg
km_Sub = 3;   % µM
km_NADH = 0.02;   % mM
k_0 = [vmax; km_Sub; km_NADH];

% nonlinear least square data fitting
```

107

```matlab
[par, Res, Jac, Sigma, MSE] = nlinfit(conc, rate, @eq_Kinetik_FMO, k_0);

disp('Determined parameters:');
disp(par);
disp('Variation:')
CInt = nlparci(par, Res, 'covar', Sigma);
CInt = abs((CInt(:,1)-CInt(:,2))/2);
disp(CInt);
%save([Dir 'Par_GDH'], 'par');

% Setting the parameter

vmax = par(1);
km_Sub = par(2);
km_NADH = par(3);

% Calculation of a smooth curve
Max = [20 0.5 0.2]; % up to which concentrations the simulation should be
done: SUB first - NADH last values
Std = [10 0.1 10];
Pts = 5000;
FConc = zeros(3*Pts,3);
for i = 1:3
    for j = 1:Pts
        FConc((i-1)*Pts+j,:) = Std;
        FConc((i-1)*Pts+j,i) = Max(i)/Pts*(j-1);
    end
end
c_Subfit = FConc(:,1);
c_NADHfit = FConc(:,2);

v_fit =  vmax*c_Subfit.*c_NADHfit./((km_Sub + c_Subfit).*(km_NADH +
c_NADHfit));

% Visualization

f1 = figure(1);
plot(c_NADH(1:9), rate(1:9), 'bd', 'MarkerFaceColor','b', 'MarkerSize', 8);
hold on
plot(FConc(Pts+1:Pts*2,2), v_fit(Pts+1:Pts*2), 'b-', 'LineWidth', 0.8);
hold off
title('FMO-E Kinetics', 'FontSize', 16, 'FontName', 'Arial');
xlabel('NADH [mM]', 'FontSize', 16, 'FontName', 'Arial');
```

```matlab
ylabel('Activity [U mg^{-1}]', 'FontSize', 16, 'FontName', 'Arial');
leg = legend('with 10 mM SUB');
set(leg, 'Location', 'NorthEast');
axis([0 0.2 0 2]);
set(gca, 'xtick', 0:0.04:0.2, 'ytick', 0:0.5:2, 'FontSize', 16, 'FontName',
'Arial');
set(f1, 'PaperPositionMode', 'manual', 'PaperUnits', 'centimeter',
'PaperPosition', [0,0,12,7]);

%saveas(f1, [Dir 'Kinetik GDH1.png'], 'png');
%saveas(f1, [Dir 'Kinetik GDH1.eps'], 'epsc');

f2 = figure(2);
plot(c_Sub(10:18), rate(10:18), 'rs', 'MarkerFaceColor','r', 'MarkerSize',
8);
hold on
plot(FConc(1:Pts,1), v_fit(1:Pts), 'r-', 'LineWidth', 0.8);
hold off
title('FMO-E Kinetics', 'FontSize', 16, 'FontName', 'Arial');
xlabel('bicyclo[3.2.0]hept-2-en-6one [mM]', 'FontSize', 16, 'FontName',
'Arial');
ylabel('Activity [U mg^{-1}]', 'FontSize', 16, 'FontName', 'Arial');
leg = legend('with 0.1 mM NADH');
set(leg, 'Location', 'NorthEast');
axis([0 20 0 2]);
set(gca, 'xtick', 0:2:20, 'ytick', 0:0.5:2, 'FontSize', 16, 'FontName',
'Arial');
set(f2, 'PaperPositionMode', 'manual', 'PaperUnits', 'centimeter',
'PaperPosition', [0,0,12,7]);
```

FMO-E kinetic assay with Michaelis-Menten double-substrate equation Matlab program 2

```matlab
function rate = eq_Kinetik_FMO(k0, xdata)

c_SUB = xdata(:,1);

vmax = k0(1);
km_SUB = k0(2);

rate =  vmax*c_SUB/((km_SUB + c_SUB).*(km_NADH + c_NADH));

end
```

REFERENCES

1.   Labet, M.; Thielemans, W., Synthesis of polycaprolactone: a review. *Chemical Society Reviews* **2009,** *38* (12), 3484-3504.

2.   Woodruff, M. A.; Hutmacher, D. W., The return of a forgotten polymer—polycaprolactone in the 21st century. *Progress in Polymer Science* **2010,** *35* (10), 1217-1256.

3.   Hutmacher, D. W.; Schantz, T.; Zein, I.; Ng, K. W.; Teoh, S. H.; Tan, K. C., Mechanical properties and cell cultural response of polycaprolactone scaffolds designed and fabricated via fused deposition modeling. *Journal of Biomedical Materials Research: An Official Journal of The Society for Biomaterials, The Japanese Society for Biomaterials, and The Australian Society for Biomaterials and the Korean Society for Biomaterials* **2001,** *55* (2), 203-216.

4.   Jenkins, M.; Harrison, K.; Silva, M.; Whitaker, M.; Shakesheff, K.; Howdle, S., Characterisation of microcellular foams produced from semi-crystalline PCL using supercritical carbon dioxide. *European Polymer Journal* **2006,** *42* (11), 3145-3151.

5.   Pena, J.; Corrales, T.; Izquierdo-Barba, I.; Doadrio, A. L.; Vallet-Regí, M., Long term degradation of poly (ε-caprolactone) films in biologically related fluids. *Polymer Degradation and Stability* **2006,** *91* (7), 1424-1432.

6.   Lam, C. X.; Teoh, S. H.; Hutmacher, D. W., Comparison of the degradation of polycaprolactone and polycaprolactone–(β-tricalcium phosphate) scaffolds in alkaline medium. *Polymer international* **2007,** *56* (6), 718-728.

7.   Chen, D.; Bei, J.; Wang, S., Polycaprolactone microparticles and their biodegradation. *Polymer Degradation and Stability* **2000,** *67* (3), 455-459.

8.   Sinha, V.; Bansal, K.; Kaushik, R.; Kumria, R.; Trehan, A., Poly-ϵ-caprolactone microspheres and nanospheres: an overview. *International journal of pharmaceutics* **2004,** *278* (1), 1-23.

9.   Ikada, Y.; Tsuji, H., Biodegradable polyesters for medical and ecological applications. *Macromolecular rapid communications* **2000,** *21* (3), 117-132.

10.   Joshi, P.; Madras, G., Degradation of polycaprolactone in supercritical fluids. *Polymer Degradation and Stability* **2008,** *93* (10), 1901-1908.

11.   Horváth, I. T.; Mehdi, H.; Fábos, V.; Boda, L.; Mika, L. T., γ-Valerolactone—a sustainable liquid for energy and carbon-based chemicals. *Green Chemistry* **2008,** *10* (2), 238-242.

12.   Bond, J. Q.; Alonso, D. M.; Wang, D.; West, R. M.; Dumesic, J. A., Integrated catalytic conversion of γ-valerolactone to liquid alkenes for transportation fuels. *Science* **2010,** *327* (5969), 1110-1114.

13.   Alonso, D. M.; Wettstein, S. G.; Dumesic, J. A., Gamma-valerolactone, a sustainable platform molecule derived from lignocellulosic biomass. *Green Chemistry* **2013,** *15* (3), 584-595.

14.   Serra, S.; Fuganti, C.; Brenna, E., Biocatalytic preparation of natural flavours and fragrances. *TRENDS in Biotechnology* **2005,** *23* (4), 193-198.

15.   Waché, Y.; Aguedo, M.; Nicaud, J.-M.; Belin, J.-M., Catabolism of hydroxyacids and biotechnological production of lactones by *Yarrowia lipolytica*. *Applied microbiology and biotechnology*

2003, *61* (5-6), 393-404.

16. Berger, R. G., *Flavours and fragrances: chemistry, bioprocessing and sustainability*. Springer Science & Business Media: 2007.

17. http://vietnampolybag.com/biodegradable-plastics-better-environment.html. (accessed August 25, 2018).

18. http://www.renewablegreenenergypower.com/biofuel-101/. (accessed August 25, 2018).

19. http://www.solvents.org.uk/forms-of-solvent/. (accessed August 25, 2018).

20. https://thefreenewsman.com/flavor-and-fragrance-market-production-and-consumption-analysis-forecast-2018-to-2025/159876/. (accessed August 25, 2018).

21. Palmer, R. J., Polyamides, Plastics. In *Encyclopedia of Polymer Science and Technology*, John Wiley & Sons, Inc.: 2002.

22. Zhang, C. L.; Feng, L. F.; Hu, G. H., Anionic polymerization of lactams: A comparative study on various methods of measuring the conversion of ε-caprolactam to polyamide 6. *Journal of applied polymer science* **2006,** *101* (3), 1972-1981.

23. Harreus, A. L.; Backes, R.; Eichler, J. O.; Feuerhake, R.; Jäkel, C.; Mahn, U.; Pinkos, R.; Vogelsang, R., 2-Pyrrolidone. In *Ullmann's Encyclopedia of Industrial Chemistry*, Wiley-VCH Verlag GmbH & Co. KGaA: 2000.

24. Willey, A. D.; Burns, M. E.; Tsunetsugu, S., Bleaching compounds comprising acyl valerolactam bleach activators. Google Patents: 1995.

25. Penicillins, O., Appropriate prescribing of oral beta-lactam antibiotics. *Am Fam Physician* **2000,** *62*, 611-620.

26. https://www.centerwatch.com/news-online/2014/03/24/antibacterial-drugs-market-to-top-45b-globally-in-2019/. (accessed August 25, 2018).

27. https://www.indiamart.com/proddetail/mixed-colors-nylon-dori-14825981448.html. (accessed August 25, 2018).

28. https://publicpolicy.wharton.upenn.edu/live/news/2390-preventing-price-gouging-in-the-pharmaceutical/for-students/blog/news.php. (accessed August 25, 2018).

29. https://www.kmart.com/en_us/international-landing.html. (accessed August 25, 2018).

30. https://dir.indiamart.com/vadodara/chemical-solvent.html. (accessed August 25, 2018).

31. Baeyer, A.; Villiger, V., Einwirkung des caro'schen reagens auf ketone. *Berichte der deutschen chemischen Gesellschaft* **1899,** *32* (3), 3625-3633.

32. Wolfe, J. F.; Ogliaruso, M. A., The synthesis of lactones and lactams. *Acid Derivatives (1979) Supplement B: Part 2* **1979,** *2*, 1063-1330.

33. Mukaiyama, T., New synthetic reactions based on the onium salts of aza-arenes [New synthetic methods (29)]. *Angewandte Chemie International Edition in English* **1979,** *18* (10), 707-721.

34. Bassetti, M.; D'Annibale, A., Metathetic synthesis of common and medium-sized lactones: the state of the art. In *Synthesis of Heterocycles by Metathesis Reactions*, Springer: 2015; pp 57-110.

35.   Mitsudome, T.; Noujima, A.; Mizugaki, T.; Jitsukawa, K.; Kaneda, K., Supported gold nanoparticles as a reusable catalyst for synthesis of lactones from diols using molecular oxygen as an oxidant under mild conditions. *Green Chemistry* **2009,** *11* (6), 793-797.

36.   Endo, Y.; Bäckvall, J. E., Aerobic lactonization of diols by biomimetic oxidation. *Chemistry–A European Journal* **2011,** *17* (45), 12596-12601.

37.   Suzuki, T.; Morita, K.; Tsuchida, M.; Hiroi, K., Mild and chemoselective synthesis of lactones from diols using a novel metal−ligand bifunctional catalyst. *Organic letters* **2002,** *4* (14), 2361-2363.

38.   Ito, M.; Osaku, A.; Shiibashi, A.; Ikariya, T., An efficient oxidative lactonization of 1, 4-diols catalyzed by Cp* Ru (PN) complexes. *Organic letters* **2007,** *9* (9), 1821-1824.

39.   Murahashi, S.; Naota, T.; Ito, K.; Maeda, Y.; Taki, H., Ruthenium-catalyzed oxidative transformation of alcohols and aldehydes to esters and lactones. *The Journal of organic chemistry* **1987,** *52* (19), 4319-4327.

40.   Zhu, Q.-J.; Dai, W.-L.; Fan, K.-N., A green process for the oxidative lactonization of 1, 2-benzenedimethanol by tungstic acid with aqueous H_2O_2. *Green Chemistry* **2010,** *12* (2), 205-208.

41.   Zhao, J.; Hartwig, J. F., Acceptorless, neat, ruthenium-catalyzed dehydrogenative cyclization of diols to lactones. *Organometallics* **2005,** *24* (10), 2441-2446.

42.   Musa, S.; Shaposhnikov, I.; Cohen, S.; Gelman, D., Ligand–metal cooperation in PCP pincer complexes: rational design and catalytic activity in acceptorless dehydrogenation of alcohols. *Angewandte Chemie International Edition* **2011,** *50* (15), 3533-3537.

43.   Zhang, J.; Balaraman, E.; Leitus, G.; Milstein, D., Electron-rich PNP-and PNN-type ruthenium (II) hydrido borohydride pincer complexes. Synthesis, structure, and catalytic dehydrogenation of alcohols and hydrogenation of esters. *Organometallics* **2011,** *30* (21), 5716-5724.

44.   Fujita, K. i.; Ito, W.; Yamaguchi, R., Dehydrogenative lactonization of diols in aqueous media catalyzed by a water-soluble iridium complex bearing a functional bipyridine ligand. *ChemCatChem* **2014,** *6* (1), 109-112.

45.   Peña-López, M.; Neumann, H.; Beller, M., Iron(II) Pincer-catalyzed synthesis of lactones and lactams through a versatile dehydrogenative domino sequence. *ChemCatChem* **2015,** *7* (5), 865-871.

46.   Tinge, J.; Groothaert, M.; op het Veld, H.; Ritz, J.; Fuchs, H.; Kieczka, H.; Moran, W. C., Caprolactam. *Ullmann's Encyclopedia of Industrial Chemistry* **2018**, 1-31.

47.   Rico, I.; Halvorsen, K.; Dubrule, C.; Lattes, A., Effect of micelles on cyclization reactions: the use of N-hexadecyl-2-chloropyridinium iodide as an amphiphilic carboxyl-activating agent in lactonization and lactamization. *The Journal of Organic Chemistry* **1994,** *59* (2), 415-420.

48.   Huang, W.; Kalivretenos, A. G., Synthesis of medium ring lactams via cyclization reactions using polymer bound HOBT as catalyst. *Tetrahedron letters* **1995,** *36* (50), 9113-9116.

49.   Murahashi, S.-I.; Kondo, K.; Hakata, T., Ruthenium catalyzed synthesis of secondary or tertiary amines from amines and alcohols. *Tetrahedron Letters* **1982,** *23* (2), 229-232.

50.   Naota, T.; Murahashi, S.-I., Ruthenium-catalyzed transformations of amino alcohols to lactams. *ChemInform* **1991,** *23* (17).

51.   Pingen, D.; Vogt, D., Amino-alcohol cyclization: selective synthesis of lactams and cyclic amines from amino-alcohols. *Catalysis Science & Technology* **2014,** *4* (1), 47-52.

52.   Lane, E. M.; Uttley, K. B.; Hazari, N.; Bernskoetter, W., Iron-catalyzed amide formation from the dehydrogenative coupling of alcohols and secondary amines. *Organometallics* **2017,** *36* (10), 2020-2025.

53.   Cheng, H.; Xiong, M.-Q.; Cheng, C.-X.; Wang, H.-J.; Lu, Q.; Liu, H.-F.; Yao, F.-B.; Verpoort, F.; Chen, C., *In situ* generated ruthenium catalytic systems bearing diverse *N*-heterocyclic carbene precursors for the atom-economic amide synthesis from alcohols and amines. *Chemistry–An Asian Journal* **2018**.

54.   Leisch, H.; Morley, K.; Lau, P. C., Baeyer-Villiger monooxygenases: more than just green chemistry. *Chemical reviews* **2011,** *111* (7), 4165-4222.

55.   Stewart, J. D., Cyclohexanone monooxygenase: a useful asymmetric Baeyer-Villiger reactions. *Curr Org Chem* **1998,** *2*, 195-216.

56.   de Gonzalo, G.; Mihovilovic, M. D.; Fraaije, M. W., Recent developments in the application of Baeyer–Villiger monooxygenases as biocatalysts. *ChemBioChem* **2010,** *11* (16), 2208-2231.

57.   Doig, S. D.; Avenell, P. J.; Bird, P. A.; Gallati, P.; Lander, K. S.; Lye, G. J.; Wohlgemuth, R.; Woodley, J. M., Reactor operation and scale-up of whole cell Baeyer-Villiger catalyzed lactone synthesis. *Biotechnology progress* **2002,** *18* (5), 1039-1046.

58.   Baldwin, C. V.; Wohlgemuth, R.; Woodley, J. M., The first 200-L scale asymmetric Baeyer− Villiger oxidation using a whole-cell biocatalyst. *Organic Process Research & Development* **2008,** *12* (4), 660-665.

59.   Gutman, A. L.; Zuobi, K.; Bravdo, T., Lipase-catalyzed preparation of optically active. gamma.-butyrolactones in organic solvents. *The Journal of Organic Chemistry* **1990,** *55* (11), 3546-3552.

60.   Sharma, A.; Chattopadhyay, S., Enzymatic lactonization stategy for enantioselective synthesis of a tetrahydrolipstatin synthon. *The Journal of organic chemistry* **1999,** *64* (22), 8059-8062.

61.   Efe, C.; Straathof, A. J.; van der Wielen, L. A., Options for biochemical production of 4-hydroxybutyrate and its lactone as a substitute for petrochemical production. *Biotechnology and bioengineering* **2008,** *99* (6), 1392-1406.

62.   Korpak, M.; Pietruszka, J., Chemoenzymatic one-pot synthesis of γ-butyrolactones. *Advanced Synthesis & Catalysis* **2011,** *353* (9), 1420-1424.

63.   Gatfield, I., The enzymatic synthesis of esters in nonaqueous systems. *Annals of the New York Academy of Sciences* **1984,** *434* (1), 569-572.

64.   Antczak, U.; Gora, J.; Antczak, T.; Galas, E., Enzymatic lactonization of 15-hydroxypentadecanoic and 16-hydroxyhexadecanoic acids to macrocyclic lactones. *Enzyme and microbial Technology* **1991,** *13* (7), 589-593.

65.   Robinson, G. K.; Alston, M. J.; Knowles, C. J.; Cheetham, P.; Motion, K., An investigation into the factors influencing lipase-catalyzed intramolecular lactonization in microaqueous systems. *Enzyme and microbial technology* **1994,** *16* (10), 855-863.

66.   Götz, K.; Liese, A.; Ansorge-Schumacher, M.; Hilterhaus, L., A chemo-enzymatic route to synthesize (*S*)-γ-valerolactone from levulinic acid. *Applied microbiology and biotechnology* **2013,** *97* (9),

3865-3873.

67.   Irwin, A. J.; Jones, J. B., Asymmetric syntheses *via* enantiotopically selective horse liver alcohol dehydrogenase catalyzed oxidations of diols containing a prochiral center. *Journal of the American Chemical Society* **1977,** *99* (2), 556-561.

68.   Irwin, A. J.; Jones, J. B., Regiospecific and enantioselective horse liver alcohol dehydrogenase catalyzed oxidations of some hydroxycyclopentanes. *Journal of the American Chemical Society* **1977,** *99* (5), 1625-1630.

69.   Jakovac, I. J.; Goodbrand, H. B.; Lok, K. P.; Jones, J. B., Enzymes in organic synthesis. 24. Preparations of enantiomerically pure chiral lactones *via* stereospecific horse liver alcohol dehydrogenase catalyzed oxidations of monocyclic meso diols. *Journal of the American Chemical Society* **1982,** *104* (17), 4659-4665.

70.   Lok, K. P.; Jakovac, I. J.; Jones, J. B., Enzymes in organic synthesis. 34. Preparations of enantiomerically pure exo- and endo-bridged bicyclic [2.2.1] and [2.2.2] chiral lactones via stereospecific horse liver alcohol dehydrogenase catalyzed oxidations of meso diols. *Journal of the American Chemical Society* **1985,** *107* (8), 2521-2526.

71.   Patel, R. N.; Liu, M.; Banerjee, A.; Thottathil, J. K.; Kloss, J.; Szarka, L. J., Stereoselective microbial/enzymatic oxidation of (exo, exo)-7-oxabicyclo [2.2. 1] heptane-2, 3-dimethanol to the corresponding chiral lactol and lactone. *Enzyme and microbial technology* **1992,** *14* (10), 778-784.

72.   Osa, T.; Kashiwagi, Y.; Yanagisawa, Y., Electroenzymatic oxidation of alcohols on a poly (acrylic acid)-coated graphite felt electrode terimmobilizing ferrocene, diaphorase and alcohol dehydrogenase. *Chemistry letters* **1994,** *23* (2), 367-370.

73.   Schröder, I.; Steckhan, E.; Liese, A., *In situ* NAD$^+$ regeneration using 2, 2′-azinobis (3-ethylbenzothiazoline-6-sulfonate) as an electron transfer mediator. *Journal of Electroanalytical Chemistry* **2003,** *541*, 109-115.

74.   Gargiulo, S.; Arends, I. W.; Hollmann, F., A photoenzymatic system for alcohol oxidation. *ChemCatChem* **2011,** *3* (2), 338-342.

75.   Kara, S.; Spickermann, D.; Schrittwieser, J. H.; Weckbecker, A.; Leggewie, C.; Arends, I. W. C. E.; Hollmann, F., Access to lactone building blocks *via* Horse Liver Alcohol Dehydrogenase-catalyzed oxidative lactonization. *Acs Catalysis* **2013,** *3* (11), 2436-2439.

76.   Díaz-Rodríguez, A.; Lavandera, I.; Kanbak-Aksu, S.; Sheldon, R. A.; Gotor, V.; Gotor-Fernández, V., From diols to lactones under aerobic conditions using a laccase/TEMPO catalytic system in aqueous medium. *Advanced Synthesis & Catalysis* **2012,** *354* (18), 3405-3408.

77.   Díaz-Rodríguez, A.; Martínez-Montero, L.; Lavandera, I.; Gotor, V.; Gotor-Fernández, V., Laccase/2,2,6,6-Tetramethylpiperidinoxyl Radical (TEMPO): An efficient catalytic system for selective oxidations of primary hydroxy and amino groups in aqueous and biphasic media. *Advanced Synthesis & Catalysis* **2014,** *356* (10), 2321-2329.

78.   Vivienne Barker, C.; I. Page, M.; R. Korn, S.; Monteith, M., Esterase catalysed enantioselective ring closure. *Chemical Communications* **1999,**   (8), 721-722.

79.   Ladkau, N.; Hermann, I.; Buhler, B.; Schmid, A., Enzyme-catalyzed laurolactam synthesis *via*

intramolecular amide bond formation in aqueous solution. *Advanced Synthesis & Catalysis* **2011,** *353* (13), 2501-2510.

80. Gutman, A. L.; Meyer, E.; Yue, X.; Abell, C., Enzymatic formation of lactams in organic solvents. *Tetrahedron letters* **1992,** *33* (27), 3943-3946.

81. Stavila, E.; Loos, K., Synthesis of lactams using enzyme-catalyzed aminolysis. *Tetrahedron Letters* **2013,** *54* (5), 370-372.

82. Herter, S.; McKenna, S. M.; Frazer, A. R.; Leimkuhler, S.; Carnell, A. J.; Turner, N. J., Galactose oxidase variants for the oxidation of amino alcohols in enzyme cascade synthesis. *Chemcatchem* **2015,** *7* (15), 2313-2317.

83. Zajkoska, P.; Cárdenas-Fernández, M.; Lye, G. J.; Rosenberg, M.; Turner, N. J.; Rebroš, M., Chemo-biocatalytic one-pot two-step conversion of cyclic amine to lactam using whole cell monoamine oxidase. *Journal of Chemical Technology & Biotechnology* **2017,** *92* (7), 1558-1565.

84. Zheng, D.; Zhou, X.; Cui, B.; Han, W.; Wan, N.; Chen, Y., Biocatalytic α-Oxidation of cyclic amines and *N*-methylanilines for the synthesis of lactams and formamides. *ChemCatChem* **2017,** *9* (6), 937-940.

85. Hollmann, F.; Arends, I. W. C. E.; Buehler, K.; Schallmey, A.; Buhler, B., Enzyme-mediated oxidations for the chemist. *Green Chemistry* **2011,** *13* (2), 226-265.

86. Punniyamurthy, T.; Velusamy, S.; Iqbal, J., Recent advances in transition metal catalyzed oxidation of organic substrates with molecular oxygen. *Chemical Reviews* **2005,** *105* (6), 2329-2364.

87. Anastas, P. T.; Warner, J. C., *Green chemistry: theory and practice*. Oxford university press Oxford: 2000; Vol. 30.

88. Turfitt, G., The microbiological degradation of steroids: 4. Fission of the steroid molecule. *Biochemical Journal* **1948,** *42* (3), 376.

89. Donoghue, N. A.; Norris, D. B.; Trudgill, P. W., The purification and properties of cyclohexanone oxygenase from *Nocardia globerula* CL1 and *Acinetobacter* NCIB 9871. *European Journal of Biochemistry* **1976,** *63* (1), 175-192.

90. Mihovilovic, M. D.; Muller, B.; Stanetty, P., Monooxygenase-mediated Baeyer-Villiger oxidations. *European Journal of Organic Chemistry* **2002,** (22), 3711-3730.

91. Colonna, S.; Gaggero, N.; Pasta, P.; Ottolina, G., Enantioselective oxidation of sulfides to sulfoxides catalysed by bacterial cyclohexanone monooxygenases. *Chemical Communications* **1996,** (20), 2303-2307.

92. Ottolina, G.; Bianchi, S.; Belloni, B.; Carrea, G.; Danieli, B., First asymmetric oxidation of tertiary amines by cyclohexanone monooxygenase. *Tetrahedron letters* **1999,** *40* (48), 8483-8486.

93. Riebel, A.; Fink, M. J.; Mihovilovic, M. D.; Fraaije, M. W., Type II flavin-containing monooxygenases: a new class of biocatalysts that harbors Baeyer–Villiger monooxygenases with a relaxed coenzyme specificity. *ChemCatChem* **2014,** *6* (4), 1112-1117.

94. Ziegler, D. M., Flavin-containing monooxygenases: enzymes adapted for multisubstrate specificity. *Trends in pharmacological sciences* **1990,** *11* (8), 321-324.

95. Jensen, C. N.; Cartwright, J.; Ward, J.; Hart, S.; Turkenburg, J. P.; Ali, S. T.; Allen, M. J.; Grogan,

G., A flavoprotein monooxygenase that catalyses a Baeyer–Villiger reaction and thioether oxidation using NADH as the nicotinamide cofactor. *ChemBioChem* **2012,** *13* (6), 872-878.

96. Riebel, A.; de Gonzalo, G.; Fraaije, M. W., Expanding the biocatalytic toolbox of flavoprotein monooxygenases from Rhodococcus jostii RHA1. *Journal of Molecular Catalysis B-Enzymatic* **2013,** *88*, 20-25.

97. Van Berkel, W.; Kamerbeek, N.; Fraaije, M., Flavoprotein monooxygenases, a diverse class of oxidative biocatalysts. *Journal of biotechnology* **2006,** *124* (4), 670-689.

98. Ghisla, S.; Massey, V., Mechanisms of flavoprotein-catalyzed reactions. In *EJB Reviews 1989*, Springer: 1989; pp 29-45.

99. Walsh, C. T.; Chen, Y. C. J., Enzymic Baeyer–Villiger oxidations by flavin-dependent monooxygenases. *Angewandte Chemie International Edition in English* **1988,** *27* (3), 333-343.

100. Entsch, B.; Van Berkel, W., Structure and mechanism of para-hydroxybenzoate hydroxylase. *The FASEB journal* **1995,** *9* (7), 476-483.

101. Massey, V., Activation of molecular oxygen by flavins and flavoproteins. *Journal of Biological Chemistry* **1994,** *269* (36), 22459-22462.

102. Ceccoli, R. D.; Bianchi, D. A.; Rial, D. V., Flavoprotein monooxygenases for oxidative biocatalysis: recombinant expression in microbial hosts and applications. *Frontiers in microbiology* **2014,** *5*.

103. Mihovilovic, M. D., Enzyme mediated Baeyer-Villiger oxidations. *Current Organic Chemistry* **2006,** *10* (11), 1265-1287.

104. Mihovilovic, M. D.; Kapitán, P.; Kapitánová, P., Regiodivergent Baeyer–Villiger oxidation of fused ketones by recombinant whole-cell biocatalysts. *ChemSusChem* **2008,** *1* (1-2), 143-148.

105. Rodríguez-Mata, M.; Lavandera, I.; Gotor-Fernández, V.; Gotor, V.; García-Cerrada, S.; Mendiola, J.; de Frutos, Ó.; Collado, I., Baeyer–Villiger monooxygenase-catalyzed desymmetrizations of cyclobutanones. Application to the synthesis of valuable spirolactones. *Tetrahedron* **2015**.

106. Dong, J.; Fernández-Fueyo, E.; Hollmann, F.; Paul, C.; Pasic, M.; Schmidt, S.; Wang, Y.; Younes, S.; Zhang, W., Biocatalytic oxidation reactions-a Chemist's perspective. *Angewandte Chemie (International ed. in English)* **2018**.

107. Gruber, C. C.; Lavandera, I.; Faber, K.; Kroutil, W., From a racemate to a single enantiomer: deracemization by stereoinversion. *Advanced Synthesis & Catalysis* **2006,** *348* (14), 1789-1805.

108. Könst, P.; Merkens, H.; Kara, S.; Kochius, S.; Vogel, A.; Zuhse, R.; Holtmann, D.; Arends, I. W. C. E.; Hollmann, F., Enantioselective oxidation of aldehydes catalyzed by alcohol dehydrogenase. *Angewandte Chemie International Edition* **2012,** *51* (39), 9914-9917.

109. Gargiulo, S., *Novel approaches for using dehydrogenases and ene-reductases for organic synthesis*. TU Delft, Delft University of Technology: 2015.

110. LEI HUANG, P. D. D. M., SELIN KARA, The 'water challenge': Opportunities and challenges of using oxidoreductases in non-conventional media. *Chimica Oggi - Chemistry Today* **2018**.

111. Kara, S.; Schrittwieser, J. H.; Hollmann, F.; Ansorge-Schumacher, M. B., Recent trends and novel concepts in cofactor-dependent biotransformations. *Applied Microbiology and Biotechnology* **2014,** *98*

(4), 1517-1529.

112. Paul, C. E.; Arends, I. W. C. E.; Hollmann, F., Is simpler better? Synthetic nicotinamide cofactor analogues for redox chemistry. *ACS Catalysis* **2014,** *4* (3), 788-797.

113. García-Junceda, E.; Lavandera, I.; Rother, D.; Schrittwieser, J. H., (Chemo)enzymatic cascades—Nature's synthetic strategy transferred to the laboratory. *Journal of Molecular Catalysis B: Enzymatic* **2015,** *114*, 1-6.

114. Ricca, E.; Brucher, B.; Schrittwieser, J. H., Multi-enzymatic cascade reactions: overview and perspectives. *Advanced Synthesis & Catalysis* **2011,** *353* (13), 2239-2262.

115. Abu, R.; Woodley, J. M., Application of enzyme coupling reactions to shift thermodynamically limited biocatalytic reactions. *ChemCatChem* **2015,** *7* (19), 3094-3105.

116. Hummel, W.; Gröger, H., Strategies for regeneration of nicotinamide coenzymes emphasizing self-sufficient closed-loop recycling systems. *Journal of biotechnology* **2014,** *191*, 22-31.

117. Schrittwieser, J. H.; Sattler, J.; Resch, V.; Mutti, F. G.; Kroutil, W., Recent biocatalytic oxidation–reduction cascades. *Current Opinion in Chemical Biology* **2011,** *15* (2), 249-256.

118. Bornadel, A.; Hatti-Kaul, R.; Hollmann, F.; Kara, S., A bi-enzymatic convergent cascade for ε-caprolactone synthesis employing 1, 6-hexanediol as a 'double-smart cosubstrate'. *ChemCatChem* **2015,** *7* (16), 2442-2445.

119. Huang, L.; Romero, E.; Ressmann, A. K.; Rudroff, F.; Hollmann, F.; Fraaije, M. W.; Kara, S., Nicotinamide adenine dinucleotide-dependent redox-neutral convergent cascade for lactonizations with type II llavin-containing monooxygenase. *Advanced Synthesis & Catalysis* **2017,** *359* (12), 2142-2148.

120. Wandrey, C.; Fiolitakis, E.; Wichmann, U.; Kula, M. R., l-Amino acids from a racemic mixture of α-hydroxy acids. *Annals of the New York Academy of Sciences* **1984,** *434* (1), 091-094.

121. Mutti, F. G.; Knaus, T.; Scrutton, N. S.; Breuer, M.; Turner, N. J., Conversion of alcohols to enantiopure amines through dual-enzyme hydrogen-borrowing cascades. *Science* **2015,** *349* (6255), 1525-1529.

122. Knaus, T.; Mutti, F. G., Biocatalytic hydrogen-borrowing cascades. *Chimica oggi* **2017,** *35* (5).

123. Gröger, H.; Borchert, S.; Krauẞer, M.; Hummel, W., Enzyme-Catalyzed Asymmetric Reduction of Ketones. *Encyclopedia of Industrial Biotechnology: Bioprocess, Bioseparation, and Cell Technology* **2009**, 1-16.

124. Bornadel, A.; Hatti-Kaul, R.; Hollmann, F.; Kara, S., Enhancing the productivity of the bi-enzymatic convergent cascade for ε-caprolactone synthesis through design of experiments and a biphasic system. *Tetrahedron* **2015**.

125. Kamerbeek, N. M.; Janssen, D. B.; van Berkel, W. J.; Fraaije, M. W., Baeyer–Villiger monooxygenases, an emerging family of flavin-dependent biocatalysts. *Advanced Synthesis & Catalysis* **2003,** *345* (6-7), 667-678.

126. Pazmino, D. T.; Winkler, M.; Glieder, A.; Fraaije, M., Monooxygenases as biocatalysts: classification, mechanistic aspects and biotechnological applications. *Journal of Biotechnology* **2010,** *146* (1-2), 9-24.

127. Huijbers, M. M. E.; Montersino, S.; Westphal, A. H.; Tischler, D.; van Berkel, W. J. H., Flavin dependent monooxygenases. *Archives of Biochemistry and Biophysics* **2014,** *544*, 2-17.

128. Bučko, M.; Gemeiner, P.; Schenkmayerová, A.; Krajčovič, T.; Rudroff, F.; Mihovilovič, M. D., Baeyer-Villiger oxidations: biotechnological approach. *Applied microbiology and biotechnology* **2016,** *100* (15), 6585-6599.

129. Wu, J. T.; Wu, L. H.; Knight, J. A., Stability of NADPH: effect of various factors on the kinetics of degradation. *Clinical chemistry* **1986,** *32* (2), 314-319.

130. Lundquist, R.; Olivera, B. M., Pyridine nucleotide metabolism in Escherichia coli I. Exponential growth. *Journal of Biological Chemistry* **1971,** *246* (4), 1107-1116.

131. Weckbecker, A.; Gröger, H.; Hummel, W., Regeneration of nicotinamide coenzymes: principles and applications for the synthesis of chiral compounds. In *Biosystems Engineering I*, Springer: 2010; pp 195-242.

132. Hollmann, S. K. J. H. S. F., Strategies for cofactor regeneration in biocatalyzed reductions. In *Synthetic Methods for Biologically Active Molecules*, 2013.

133. Hollmann, F.; Arends, I. W. C. E.; Holtmann, D., Enzymatic reductions for the chemist. *Green Chemistry* **2011,** *13* (9), 2285-2314.

134. Kamerbeek, N. M.; Fraaije, M. W.; Janssen, D. B., Identifying determinants of NADPH specificity in Baeyer-Villiger monooxygenases. *European Journal of Biochemistry* **2004,** *271* (11), 2107-2116.

135. Popelkova, H.; Fraaije, M. W.; Novak, O.; Frebortova, J.; Bilyeu, K. D.; Frebort, I., Kinetic and chemical analyses of the cytokinin dehydrogenase-catalysed reaction: correlations with the crystal structure. *Biochemical Journal* **2006,** *398*, 113-124.

136. Dudek, H. M.; Pazmino, D. E. T.; Rodriguez, C.; de Gonzalo, G.; Gotor, V.; Fraaije, M. W., Investigating the coenzyme specificity of phenylacetone monooxygenase from Thermobifida fusca. *Applied Microbiology and Biotechnology* **2010,** *88* (5), 1135-1143.

137. Beier, A.; Bordewick, S.; Genz, M.; Schmidt, S.; Van Den Bergh, T.; Peters, C.; Joosten, H.-J.; Bornscheuer, U., Switch in cofactor specificity of a Baeyer-Villiger monooxygenase. *ChemBioChem* **2016**, n/a-n/a.

138. Riebel, A.; de Gonzalo, G.; Fraaije, M. W., Expanding the biocatalytic toolbox of flavoprotein monooxygenases from *Rhodococcus jostii* RHA1. *Journal of Molecular Catalysis B: Enzymatic* **2013,** *88*, 20-25.

139. Fraaije, M. W.; Wu, J.; Heuts, D.; van Hellemond, E. W.; Spelberg, J. H. L.; Janssen, D. B., Discovery of a thermostable Baeyer-Villiger monooxygenase by genome mining. *Applied Microbiology and Biotechnology* **2005,** *66* (4), 393-400.

140. Sheng, D.; Ballou, D. P.; Massey, V., Mechanistic studies of cyclohexanone monooxygenase: Chemical properties of intermediates involved in catalysis. *Biochemistry* **2001,** *40* (37), 11156-11167.

141. Bisswanger, H., Enzyme Kinetics: Section 2.6–2.12. In *Enzyme Kinetics*, 2008.

142. Bisswanger, H., Enzyme assays. *Perspectives in Science* **2014,** *1* (1), 41-55.

143. Choi, J.-H.; Kim, T.-K.; Kim, Y.-M.; Kim, W.-C.; Park, K.; Rhee, I.-K., Cloning and

characterization of a gene cluster for cyclohexanone oxidation in *Rhodococcus sp.* TK6. *Journal of microbiology and biotechnology* **2006,** *16* (4), 511-518.

144. GRIFFIN, M.; TRUDGILL, P. W., Purification and properties of cyclopentanone oxygenase of Pseudomonas NCIB 9872. *The FEBS Journal* **1976,** *63* (1), 199-209.

145. Opperman , D. J.; Reetz, M. T., Towards practical Baeyer–Villiger monooxygenases: Design of cyclohexanone monooxygenase mutants with enhanced oxidative stability. *ChemBioChem* **2010,** *11* (18), 2589-2596.

146. Olofsson, L.; Nicholls, I. A.; Wikman, S., TBADH activity in water-miscible organic solvents: correlations between enzyme performance, enantioselectivity and protein structure through spectroscopic studies. *Organic & biomolecular chemistry* **2005,** *3* (5), 750-755.

147. Öztürk, D. C.; Kazan, D.; Denizci, A. A.; Grimoldi, D.; Secundo, F.; Erarslan, A., Water miscible mono alcohols effect on the structural conformation of *Bacillus clausii* GMBAE 42 serine alkaline protease. *Journal of Molecular Catalysis B: Enzymatic* **2010,** *64* (3-4), 184-188.

148. Goncalves, L.; Kracher, D.; Milker, S.; Rudroff, F.; Fink, M. J.; Ludwig, R.; Bommarius, A.; Mihovilovic, M., Mutagenesis-independent, stabilization of class B flavin monooxygenases in operation. *Advanced Synthesis & Catalysis* **2017**.

149. van den Heuvel, R. H. H.; Tahallah, N.; Kamerbeek, N. M.; Fraaije, M. W.; van Berkel, W. J. H.; Janssen, D. B.; Heck, A. J. R., Coenzyme binding during catalysis is beneficial for the stability of 4-hydroxyacetophenone monooxygenase. *Journal of Biological Chemistry* **2005,** *280* (37), 32115-32121.

150. Jörnvall, H.; Harris, J. I., Horse liver alcohol dehydrogenase. *European Journal of Biochemistry* **1970,** *13* (3), 565-576.

151. Park, D. H.; Plapp, B. V., Isoenzymes of horse liver alcohol dehydrogenase active on ethanol and steroids. cDNA cloning, expression, and comparison of active sites. *Journal of Biological Chemistry* **1991,** *266* (20), 13296-13302.

152. Al-Karadaghi, S.; Cedergren-Zeppezauer, E. S.; Hovmöller, S.; Petratos, K.; Terry, H.; Wilson, K., Refined crystal structure of liver alcohol dehydrogenase–NADH complex at 1.8 Å resolution. *Acta Crystallographica Section D: Biological Crystallography* **1994,** *50* (6), 793-807.

153. Quaglia, D.; Irwin, J. A.; Paradisi, F., Horse liver alcohol dehydrogenase: New perspectives for an old enzyme. *Molecular Biotechnology* **2012,** *52* (3), 244-250.

154. Plapp, B. V.; Savarimuthu, B. R.; Ferraro, D. J.; Rubach, J. K.; Brown, E. N.; Ramaswamy, S., Horse liver alcohol dehydrogenase: zinc coordination and catalysis. *Biochemistry* **2017,** *56* (28), 3632-3646.

155. Boratyński, F.; Kiełbowicz, G.; Wawrzeńczyk, C., Lactones 34 [1]. Application of alcohol dehydrogenase from horse liver (HLADH) in enantioselective synthesis of δ-and ε-lactones. *Journal of Molecular Catalysis B: Enzymatic* **2010,** *65* (1), 30-36.

156. Díaz-Rodríguez, A.; Iglesias-Fernández, J.; Rovira, C.; Gotor-Fernández, V., Enantioselective Preparation of δ-valerolactones with lorse liver alcohol dehydrogenase. *ChemCatChem* **2014,** *6* (4), 977-980.

157. Kara, S.; Spickermann, D.; Schrittwieser, J. H.; Leggewie, C.; van Berkel, W. J. H.; Arends, I. W.

C. E.; Hollmann, F., More efficient redox biocatalysis by utilising 1,4-butanediol as a 'smart cosubstrate'. *Green Chemistry* **2013,** *15* (2), 330-335.

158. Burgard, A.; Burk, M. J.; Osterhout, R.; Van Dien, S.; Yim, H., Development of a commercial scale process for production of 1, 4-butanediol from sugar. *Current opinion in biotechnology* **2016,** *42*, 118-125.

159. Andreozzi, S.; Chakrabarti, A.; Soh, K. C.; Burgard, A.; Yang, T. H.; Van Dien, S.; Miskovic, L.; Hatzimanikatis, V., Identification of metabolic engineering targets for the enhancement of 1, 4-butanediol production in recombinant *E. coli* using large-scale kinetic models. *Metabolic engineering* **2016,** *35*, 148-159.

160. Selwyn, M., A simple test for inactivation of an enzyme during assay. *Biochimica et Biophysica Acta (BBA)-Enzymology and Biological Oxidation* **1965,** *105* (1), 193-195.

161. Mihovilovic, M. D.; Rudroff, F.; Grotzl, B.; Kapitan, P.; Snajdrova, R.; Rydz, J.; Mach, R., Family clustering of Baeyer-Villiger monooxygenases based on protein sequence and stereopreference. *Angewandte Chemie-International Edition* **2005,** *44* (23), 3609-3613.

162. Mihovilovic, M. D.; Kapitan, P.; Kapitanova, P., Regiodivergent Baeyer-Villiger oxidation of fused ketones by recombinant whole-cell biocatalysts. *Chemsuschem* **2008,** *1* (1-2), 143-148.

163. Ceccoli, R. D.; Bianchi, D. A.; Fink, M. J.; Mihovilovic, M. D.; Rial, D. V., Cloning and characterization of the Type I Baeyer–Villiger monooxygenase from *Leptospira biflexa. AMB Express* **2017,** *7* (1), 87.

164. Dong, J.; Fernández-Fueyo, E.; Hollmann, F.; Paul, C.; Pasic, M.; Schmidt, S.; Wang, Y.; Younes, S.; Zhang, W., Biocatalytic oxidation reactions-a Chemist's perspective. *Angewandte Chemie* **2018**.

165. Liu, J.; Wu, S.; Li, Z., Recent advances in enzymatic oxidation of alcohols. *Current Opinion in Chemical Biology* **2018,** *43*, 77-86.

166. Patel, R. N.; Liu, M.; Banerjee, A.; Thottathil, J. K.; Kloss, J.; Szarka, L. J., Stereoselective microbial/enzymatic oxidation of (exo, exo)-7-oxabicyclo [2.2.1] heptane-2,3-dimethanol to the corresponding chiral lactol and lactone. *Enzyme and Microbial Technology* **1992,** *14* (10), 778-784.

167. Moreno-Horn, M.; Martinez-Rojas, E.; Görisch, H.; Tressl, R.; Garbe, L. A., Oxidation of 1, 4-alkanediols into γ-lactones via γ-lactols using *Rhodococcus erythropolis* as biocatalyst. *Journal of Molecular Catalysis B: Enzymatic* **2007,** *49* (1), 24-27.

168. Boratyński, F.; Smuga, M.; Wawrzeńczyk, C., Lactones 42. Stereoselective enzymatic/microbial synthesis of optically active isomers of whisky lactone. *Food chemistry* **2013,** *141* (1), 419-427.

169. Boratyński, F.; Szczepańska, E.; Pannek, J.; Olejniczak, T., Microbial Stereoselective one-step conversion of diols to chiral lactones in yeast cultures. *Catalysts* **2015,** *5* (4), 2068-2084.

170. Edegger, K.; Gruber, C. C.; Faber, K.; Hafner, A.; Kroutil, W., Optimization of reaction parameters and cultivation conditions for biocatalytic hydrogen transfer employing overexpressed ADH-'A' from *Rhodococcus ruber* DSM 44541 in *E. coli. Engineering in Life Sciences* **2006,** *6* (2), 149-154.

171. Hollmann, F.; Kleeb, A.; Otto, K.; Schmid, A., Coupled chemoenzymatic transfer hydrogenation catalysis for enantioselective reduction and oxidation reactions. *Tetrahedron: Asymmetry* **2005,** *16* (21), 3512-3519.

172. Heiss, C.; Laivenieks, M.; Zeikus, J. G.; Phillips, R. S., Mutation of cysteine-295 to alanine in secondary alcohol dehydrogenase from *Thermoanaerobacter ethanolicus* affects the enantioselectivity and substrate specificity of ketone reductions. *Bioorganic & medicinal chemistry* **2001,** *9* (7), 1659-1666.

173. Reed, M. C.; Lieb, A.; Nijhout, H. F., The biological significance of substrate inhibition: a mechanism with diverse functions. *Bioessays* **2010,** *32* (5), 422-429.

174. Weidig, C. F.; Halvorson, H. R.; Shore, J. D., Evidence for site equivalence in the reaction mechanism of horse liver alcohol dehydrogenase with aromatic substrates at alkaline pH. *Biochemistry* **1977,** *16* (13), 2916-2922.

175. KVASSMAN, J.; PETTERSSON, G., Unified mechanism for proton-transfer reactions affecting the catalytic activity of liver alcohol dehydrogenase. *The FEBS Journal* **1980,** *103* (3), 565-575.

176. Dalziel, K.; Dickinson, F., The kinetics and mechanism of liver alcohol dehydrogenase with primary and secondary alcohols as substrates. *Biochemical Journal* **1966,** *100* (1), 34.

177. Shore, J. D.; Theorell, H., Substrate inhibition effects in the liver alcohol dehydrogenase reaction. *Archives of biochemistry and biophysics* **1966,** *117* (2), 375-380.

178. Ainslie, G.; Cleland, W., Isotope exchange studies on liver alcohol dehydrogenase with cyclohexanol and cyclohexanone as reactants. *Journal of Biological Chemistry* **1972,** *247* (3), 946-951.

179. Pocker, Y.; Raymond, K., Liver alcohol dehydrogenase: substrate inhibition and competition between substrates. *Alcohol* **1985,** *2* (1), 3-8.

180. Dixon, M., The effect of pH on the affinities of enzymes for substrates and inhibitors. *Biochemical Journal* **1953,** *55* (1), 161.

181. Paul, C. E.; Arends, I. W.; Hollmann, F., Is simpler better? Synthetic nicotinamide cofactor analogues for redox chemistry. *Acs Catalysis* **2014,** *4* (3), 788-797.

182. Bommarius, A. S.; Schwarm, M.; Stingl, K.; Kottenhahn, M.; Huthmacher, K.; Drauz, K., Synthesis and use of enantiomerically pure tert-leucine. *Tetrahedron: Asymmetry* **1995,** *6* (12), 2851-2888.

183. Hollmann, F.; Arends, I. W.; Buehler, K., Biocatalytic redox reactions for organic synthesis: nonconventional regeneration methods. *ChemCatChem* **2010,** *2* (7), 762-782.

184. Rehn, G.; Pedersen, A. T.; Woodley, J. M., Application of NAD (P) H oxidase for cofactor regeneration in dehydrogenase catalyzed oxidations. *Journal of Molecular Catalysis B: Enzymatic* **2016,** *134*, 331-339.

185. Higuchi, M.; Shimada, M.; Yamamoto, Y.; Hayashi, T.; Koga, T.; Kamio, Y., Identification of two distinct NADH oxidases corresponding to H_2O_2-forming oxidase and H_2O-forming oxidase induced in *Streptococcus mutans*. *Microbiology* **1993,** *139* (10), 2343-2351.

186. Matsumoto, J.; Higuchi, M.; Shimada, M.; Yamamoto, Y.; Kamio, Y., Molecular cloning and sequence analysis of the gene encoding the H_2O-forming NADH oxidase from *Streptococcus mutans*. *Bioscience, biotechnology, and biochemistry* **1996,** *60* (1), 39-43.

187. Petschacher, B.; Staunig, N.; Müller, M.; Schürmann, M.; Mink, D.; De Wildeman, S.; Gruber, K.; Glieder, A., Cofactor specificity engineering of *Streptococcus mutans* NADH oxidase 2 for NAD (P)$^+$ regeneration in biocatalytic oxidations. *Computational and structural biotechnology journal* **2014,** *9* (14), 1-11.

188. Malito, E.; Alfieri, A.; Fraaije, M. W.; Mattevi, A., Crystal structure of a Baeyer-Villiger monooxygenase. *Proceedings of the National Academy of Sciences of the United States of America* **2004,** *101* (36), 13157-13162.

189. Alfieri, A.; Malito, E.; Orru, R.; Fraaije, M. W.; Mattevi, A., Revealing the moonlighting role of NADP in the structure of a flavin-containing monooxygenase. *Proceedings of the National Academy of Sciences of the United States of America* **2008,** *105* (18), 6572-6577.

190. Altschul, S. F.; Wootton, J. C.; Gertz, E. M.; Agarwala, R.; Morgulis, A.; Schäffer, A. A.; Yu, Y. K., Protein database searches using compositionally adjusted substitution matrices. *The FEBS journal* **2005,** *272* (20), 5101-5109.

191. Bong, Y. K.; Clay, M. D.; Collier, S. J.; Mijts, B.; Vogel, M.; Zhang, X.; Zhu, J.; Nazor, J.; Smith, D.; Song, S., Synthesis of prazole compounds. Google Patents: 2011.

192. Schmidt, S.; Scherkus, C.; Muschiol, J.; Menyes, U.; Winkler, T.; Hummel, W.; Gröger, H.; Liese, A.; Herz, H. G.; Bornscheuer, U. T., An enzyme cascade synthesis of ε-caprolactone and its oligomers. *Angewandte Chemie International Edition* **2015,** *54* (9), 2784-2787.

193. Scherkus, C.; Schmidt, S.; Bornscheuer, U. T.; Gröger, H.; Kara, S.; Liese, A., A fed-batch synthetic strategy for a three-step enzymatic synthesis of poly-ε-caprolactone. *ChemCatChem* **2016**.

194. Wedde, S.; Rommelmann, P.; Scherkus, C.; Schmidt, S.; Bornscheuer, U. T.; Liese, A.; Gröger, H., An alternative approach towards poly-ε-caprolactone through a chemoenzymatic synthesis: combined hydrogenation, bio-oxidations and polymerization without the isolation of intermediates. *Green Chemistry* **2017,** *19* (5), 1286-1290.

195. Rudroff, F.; Rydz, J.; Ogink, F. H.; Fink, M.; Mihovilovic, M. D., Comparing the stereoselective biooxidation of cyclobutanones by recombinant strains expressing bacterial Baeyer-Villiger monooxygenases. *Advanced Synthesis & Catalysis* **2007,** *349* (8-9), 1436-1444.

196. Beneventi, E.; Ottolina, G.; Carrea, G.; Panzeri, W.; Fronza, G.; Lau, P. C., Enzymatic Baeyer–Villiger oxidation of steroids with cyclopentadecanone monooxygenase. *Journal of Molecular Catalysis B: Enzymatic* **2009,** *58* (1-4), 164-168.

197. Walsh, C. T.; Chen, Y. C. J., Enzymatische Baeyer-Villiger-Oxidationen durch flavinabhängige Monooxygenasen. *Angewandte Chemie* **1988,** *100* (3), 342-352.

198. Schwab, J. M.; Li, W.; Thomas, L. P., Cyclohexanone oxygenase: stereochemistry, enantioselectivity, and regioselectivity of an enzyme-catalyzed Baeyer-Villiger reaction. *Journal of the American Chemical Society* **1983,** *105* (14), 4800-4808.

199. Sheng, D.; Ballou, D. P.; Massey, V., Mechanistic studies of cyclohexanone monooxygenase: chemical properties of intermediates involved in catalysis. *Biochemistry* **2001,** *40* (37), 11156-11167.

200. Ju, S.-S.; Lin, L.-L.; Chien, H. R.; Hsu, W.-H., Substitution of the critical methionine residues in Trigonopsis variabilis D-amino acid oxidase with leucine enhances its resistance to hydrogen peroxide. *FEMS microbiology letters* **2000,** *186* (2), 215-219.

201. Yang, Y.; Jiang, L.; Zhu, L.; Wu, Y.; Yang, S., Thermal stable and oxidation-resistant variant of subtilisin E. *Journal of biotechnology* **2000,** *81* (2-3), 113-118.

202. Morawski, B.; Quan, S.; Arnold, F. H., Functional expression and stabilization of horseradish

peroxidase by directed evolution in Saccharomyces cerevisiae. *Biotechnology and bioengineering* **2001,** *76* (2), 99-107.

203. Lin, L.-L.; Lo, H.-F.; Chiang, W.-Y.; Hu, H.-Y.; Hsu, W.-H.; Chang, C.-T., Replacement of methionine 208 in a truncated Bacillus sp. TS-23 α-amylase with oxidation-resistant leucine enhances its resistance to hydrogen peroxide. *Current microbiology* **2003,** *46* (3), 0211-0216.

204. Miyazaki-Imamura, C.; Oohira, K.; Kitagawa, R.; Nakano, H.; Yamane, T.; Takahashi, H., Improvement of H_2O_2 stability of manganese peroxidase by combinatorial mutagenesis and high-throughput screening using in vitro expression with protein disulfide isomerase. *Protein engineering* **2003,** *16* (6), 423-428.

205. Kim, Y. H.; Berry, A. H.; Spencer, D. S.; Stites, W. E., Comparing the effect on protein stability of methionine oxidation versus mutagenesis: steps toward engineering oxidative resistance in proteins. *Protein engineering* **2001,** *14* (5), 343-347.

206. Perry, L.; Wetzel, R., The role of cysteine oxidation in the thermal inactivation of T4 lysozyme. *Protein Engineering, Design and Selection* **1987,** *1* (2), 101-105.

207. Slavica, A.; Dib, I.; Nidetzky, B., Single-site oxidation, cysteine 108 to cysteine sulfinic acid, in d-amino acid oxidase from *Trigonopsis variabilis* and its structural and functional consequences. *Applied and environmental microbiology* **2005,** *71* (12), 8061-8068.

208. Imlay, J. A., The molecular mechanisms and physiological consequences of oxidative stress: lessons from a model bacterium. *Nature Reviews Microbiology* **2013,** *11* (7), 443.

209. Bučko, M.; Gemeiner, P.; Schenkmayerová, A.; Krajčovič, T.; Rudroff, F.; Mihovilovič, M. D., Baeyer-Villiger oxidations: biotechnological approach. *Applied Microbiology and Biotechnology* **2016**, 1-15.

210. Baldwin, C. V.; Woodley, J. M., On oxygen limitation in a whole cell biocatalytic Baeyer–Villiger oxidation process. *Biotechnology and bioengineering* **2006,** *95* (3), 362-369.

211. Rebroš, M.; Lipták, L.; Rosenberg, M.; Bučko, M.; Gemeiner, P., Biocatalysis with *E scherichia coli*-overexpressing cyclopentanone monooxygenase immobilized in polyvinyl alcohol gel. *Letters in applied microbiology* **2014,** *58* (6), 556-563.

212. Brummund, J.; Sonke, T.; Müller, M., Process Development for biocatalytic oxidations applying alcohol dehydrogenases. *Organic Process Research & Development* **2014,** *19* (11), 1590-1595.

213. Tufvesson, P. r.; Lima-Ramos, J.; Nordblad, M.; Woodley, J. M., Guidelines and cost analysis for catalyst production in biocatalytic processes. *Organic Process Research & Development* **2010,** *15* (1), 266-274.

214. Faber, K., Biotransformations in Organic Chemistry, 2000. Springer, Berlin.

215. Jensen, C. N.; Ali, S. T.; Allen, M. J.; Grogan, G., Exploring nicotinamide cofactor promiscuity in NAD (P) H-dependent flavin containing monooxygenases (FMOs) using natural variation within the phosphate binding loop. Structure and activity of FMOs from *Cellvibrio sp.* BR and *Pseudomonas stutzeri* NF13. *Journal of Molecular Catalysis B: Enzymatic* **2014,** *109*, 191-198.

216. Mirza, I. A.; Yachnin, B. J.; Wang, S.; Grosse, S.; Bergeron, H.; Imura, A.; Iwaki, H.; Hasegawa, Y.; Lau, P. C.; Berghuis, A. M., Crystal structures of cyclohexanone monooxygenase reveal complex

domain movements and a sliding cofactor. *Journal of the American Chemical Society* **2009,** *131* (25), 8848-8854.

217. Yachnin, B. J.; Sprules, T.; McEvoy, M. B.; Lau, P. C.; Berghuis, A. M., The substrate-bound crystal structure of a Baeyer–Villiger monooxygenase exhibits a Criegee-like conformation. *Journal of the American Chemical Society* **2012,** *134* (18), 7788-7795.

218. Yachnin, B. J.; McEvoy, M. B.; MacCuish, R. J.; Morley, K. L.; Lau, P. C.; Berghuis, A. M., Lactone-bound structures of cyclohexanone monooxygenase provide insight into the stereochemistry of catalysis. *ACS chemical biology* **2014,** *9* (12), 2843-2851.

219. Bornscheuer, U.; Kazlauskas, R. J., Survey of protein engineering strategies. *Current protocols in protein science* **2011,** *66* (1), 26.7. 1-26.7. 14.

220. Bocola, M.; Schulz, F.; Leca, F.; Vogel, A.; Fraaije, M. W.; Reetz, M. T., Converting phenylacetone monooxygenase into phenylcyclohexanone monooxygenase by rational design: towards practical Baeyer–Villiger monooxygenases. *Advanced Synthesis & Catalysis* **2005,** *347* (7-8), 979-986.

221. Reetz, M. T.; Wu, S., Greatly reduced amino acid alphabets in directed evolution: making the right choice for saturation mutagenesis at homologous enzyme positions. *Chemical Communications* **2008,** (43), 5499-5501.

222. Reetz, M. T.; Wu, S., Laboratory evolution of robust and enantioselective Baeyer− Villiger monooxygenases for asymmetric catalysis. *Journal of the American Chemical Society* **2009,** *131* (42), 15424-15432.

223. Wu, S.; Acevedo, J. P.; Reetz, M. T., Induced allostery in the directed evolution of an enantioselective Baeyer–Villiger monooxygenase. *Proceedings of the National Academy of Sciences* **2010,** *107* (7), 2775-2780.

224. Schmidt, S.; Genz, M.; Balke, K.; Bornscheuer, U. T., The effect of disulfide bond introduction and related Cys/Ser mutations on the stability of a cyclohexanone monooxygenase. *Journal of biotechnology* **2015,** *214*, 199-211.

225. Yang, H.; Liu, L.; Xu, F., The promises and challenges of fusion constructs in protein biochemistry and enzymology. *Applied microbiology and biotechnology* **2016,** *100* (19), 8273-8281.

226. Chen, X.; Zaro, J. L.; Shen, W.-C., Fusion protein linkers: property, design and functionality. *Advanced drug delivery reviews* **2013,** *65* (10), 1357-1369.

227. Iturrate, L.; Sánchez-Moreno, I.; Oroz-Guinea, I.; Pérez-Gil, J.; García-Junceda, E., Preparation and characterization of a bifunctional aldolase/kinase enzyme: A more efficient biocatalyst for C-C bond formation. *Chemistry–A European Journal* **2010,** *16* (13), 4018-4030.

228. Aalbers, F. S.; Fraaije, M. W., Coupled reactions by coupled enzymes: alcohol to lactone cascade with alcohol dehydrogenase–cyclohexanone monooxygenase fusions. *Applied Microbiology and Biotechnology* **2017**, 1-9.

229. Kohl, A.; Srinivasamurthy, V.; Böttcher, D.; Kabisch, J.; Bornscheuer, U. T., Co-expression of an alcohol dehydrogenase and a cyclohexanone monooxygenase for cascade reactions facilitates the regeneration of the NADPH cofactor. *Enzyme and microbial technology* **2018,** *108*, 53-58.

230. Lee-Ruff, E.; Wells, D., Bicyclic mucleoside synthesis—a photochemical approach. *Nucleosides,*

Nucleotides and Nucleic Acids **2008,** *27* (5), 484-494.

231. Peña-López, M.; Neumann, H.; Beller, M., Ruthenium pincer-catalyzed synthesis of substituted γ-butyrolactones using hydrogen autotransfer methodology. *Chemical Communications* **2015,** *51* (66), 13082-13085.

Lebenslauf

Name	Huang
Vorname	Lei
Staatsangehörigkeit	Chinese
Geburtsdatum	28.10.1988
Geburtsort, -land	Jiangxi, China

09.1996 - 06.2001	Grundschule in Gaoan, Jiangxi/China
09.2001 - 06.2004	Mittelschule in Gaoan, Jiangxi/China
09.2004 - 06.2007	Oberschule in Gaoan, Jiangxi/China
08.2007 - 06.2011	Studium Biotechnik an der Universität Nordwestchinas in Xi'an/China Abschluss: Bachelor
09.2011 - 06.2014	Studium Bioverfahrenstechnik an der Technische Universität Ostchinas in Shanghai/China Abschluss: Master
10.2014 - heute	Wissenschaftlicher Mitarbeiter am Institut für Technische Biokatalyse